TIDAL HEIGHT RETRIEVAL USING GLOBALLY CORRECTED GPS IN THE AMUNDSEN GULF REGION OF THE CANADIAN ARCTIC

By

Travis D. Wert

B.Eng., Royal Military College of Canada, 1996

A Thesis Submitted in Partial Fulfilment of the Requirements for the Degree of

Master of Science in Engineering

In the Graduate Academic Unit of Geodesy and Geomatics Engineering

Supervisors: Dr. Peter Dare, B.Sc. (North East London Polytechnic); M.A.Sc. (Toronto); Ph.D. (East London)

Examining Board: Dr. Sue Nichols, B.Sc. (Acadia); M.Eng., Ph.D. (UNB)

Dr. Richard B. Langley, B.Sc. (Waterloo); Ph.D. (York)

Dr. John Hughes Clarke, B.A. (Oxford); M.Sc. (Southampton); Ph.D. (Dalhousie)

Dr. Karl E. Butler, B.Sc. (Queen's); M.Sc., Ph.D. (UBC)

This thesis is accepted by the Dean of Graduate Studies

THE UNIVERSITY OF NEW BRUNSWICK

September 2004

Abstract

The recent evolution of global Wide Area Differential GPS (WADGPS) networks has greatly increased the already high level of interest in GPS technologies by the hydrographic community. This thesis evaluates one of these WADGPS receivers, the C&C Technologies Globally Corrected GPS (GcGPS) C-Nav receiver, as an instrument for tidal height retrieval in the Canadian Arctic. The C-Nav was mounted aboard the Canadian Coast Guard Ship (CCGS) Amundsen for her 14 month over-wintering expedition in the Northwest Passage. C-Nav height data were collected in Franklin Bay, NWT, over February to April, 2004. Knudsen K320 sub-bottom profiling sonar depth data was collected as a true vertical reference. The 1 Hz C-Nav data were processed and decimated down to 6 minute epochs, thus speeding the filter processing to obtain real-time data latency. The standard deviation of the residuals between the C-Nav and K320 tidal signals was 4.3 cm. This level of positioning is commensurate with International Hydrographic Organization (IHO) Special Order surveys.

In addition, the filtered C-Nav height signal was processed using Least Squares Spectral Analysis (LSSA) to define the tidal constituents in terms of amplitude and phase. The C-Nav derived constituent amplitudes are within centimetres of the K320 determined values, and the historical constituent data for Franklin Bay.

Table of Contents

List of Abbreviations and Acronyms

C/A	Coarse Acquisition Code
CASES	Canadian Arctic Shelf Exchange Study
CCGS	Canadian Coast Guard Ship
CHS	Canadian Hydrographic Service
DFO	Department of Fisheries and Oceans (Canada)
DGPS	Differential GPS
DoD	Department of Defense (U.S.)
DOP	Dilution of Precision
DOY	Day of Year
GBAS	Ground Based Augmentation System
GcGPS	Globally corrected GPS
GGE	Geodesy and Geomatics Engineering (UNB)
GLOSS	Global Sea Level Observing System
GNSS	Global Navigation Satellite System
GPS	Global Positioning System
GQI	GPS Quality Indicator
GRL	Geodetic Research Laboratory (UNB)
GSD	Geodetic Survey Division (Canada)
HAE	Height Above Ellipsoid
IHO	International Hydrographic Organisation
LSSA	Least Squares Spectral Analysis
MSL	Mean Sea Level
NGWLMS	Next Generation Water Level Measuring System
NMEA	National Marine Electronics Association
NOAA	National Oceanic and Atmospheric Administration (U.S.)
NRCan	Natural Resources Canada
OMG	Ocean Mapping Group (UNB)
RINEX	Receiver Independent Exchange Format
RTCM	Radio Technical Commission for Maritime Services
RTG	Real-time Gipsy
RTK-GPS	Real-time Kinematic GPS
SA	Selective Availability
SBAS	Satellite Based Augmentation System
SV	Satellite Vehicle
UNB	University of New Brunswick
WAAS	Wide Area Augmentation System
WADGPS	Wide Area Differential GPS
WCT	Wide Area Correction Transform
WGS84	World Geodetic System 1984
WVR	Water Vapour Radiometer

List of Figures

List of Tables

Acknowledgements

I would like to take the time to thank the people without whom this research could not have been completed. For the insight on technical matters during the research, as well as gracious reminders of the Queen's English during the writing of this thesis, many thanks to my supervisor, Dr. Peter Dare. Dr. John Hughes Clarke was also instrumental in the completion of the project with generous donations of resources, knowledge, and time. For the equipment and technical support, I would like to extend my appreciation to Jim Chance, Art Kleiner, and Tim Patro at C&C Technologies, Inc.

Chapter 1 Introduction

Hydrographers have, over the last two decades, utilized the benefits of global navigation satellite systems (GNSS) such as the Navstar Global Positioning System (GPS) for horizontal positioning. As GPS technologies and procedures have improved, hydrographers have come to realize the full benefits of new GNSS measurement methods, such as real time kinematic GPS (RTK GPS), in providing accurate, high frequency vertical positioning solutions for inshore hydrographic surveys. This has reduced the requirement for the hydrographer to base their vertical solutions on the measurement and collection of raw tidal data, which, when coupled with predictions for propagated amplitude and phase in coastal regions, would become the uneven datum upon which they would measure their soundings.

An offshoot of this advantage is the possible ability to collect these tidal data using GPS heights as an observable for water level estimation in any hydrographic, oceanographic, or similar scenario. Due to the baseline limitations inherent in RTK positioning, it is not a suitable choice for offshore or otherwise remote operations. New, globally reaching technologies have come to the forefront in this question. These systems are known as satellite based augmentation systems (SBAS). This thesis evaluates a new positioning method know as Global Corrected GPS (GcGPS) for tidal height retrieval in an area of small tidal influence, the Amundsen Gulf of the Canadian Arctic. As well, the GcGPS data will be used with Least Squares Spectral Analysis (LSSA) software for harmonic analysis of the tidal signal.

1.1 Purpose

The purpose of this research is to determine the suitability of the C&C Technologies C-Nav Globally Corrected GPS (GcGPS) receiver as an instrument in tidal height retrieval in an area of micro-tidal influence, the Canadian Arctic. GcGPS is a relatively new tool in the GPS field and although there have been numerous 'in house' studies on its static performance conducted by members of the various companies offering a GcGPS service, there has been little independent research on the performance of the GcGPS vertical solution, which may be its greatest benefit. Can the kinematic solution be used as a stand alone instrument for hydrographic positioning, or as a sampling device for tidal data? The answer to these two questions lay in the fulfilment of the following operational capability statements:

1. The vertical positioning precision possible using raw National Marine Electronics Association (NMEA) data string outputs is of an order commensurate with IHO 1st Order survey standards.
2. Simple processing methods exist that enable a smoothed vertical solution to be delivered in real or near-real time, and this smoothed solution can provide accuracies commensurate with IHO Special Order survey standards.
3. The smoothed vertical solution provides a tidal time series signal that can be decomposed with LSSA techniques for harmonic tidal analysis.
4. GcGPS is capable of surmounting the obstacles normally inherent to Arctic operations.

1.2 Experimental Design

The experiment design for this research is as follows; collect NMEA GcGPS data (both static and kinematic type) and evaluate the GcGPS performance as it pertains to the vertical solution in a hydrographic or oceanographic environment. The straightforward approach of the experimental design is accompanied by a variety of data manipulation and processing techniques throughout the various stages of the analysis to reach significant conclusions. The evaluation of the C-Nav was carried out in two stages; static testing in the fall of 2003 at the Department of Geodesy and Geomatics Engineering's Geodetic Research Laboratory (GGE GRL) at the University of New Brunswick campus in Fredericton, and kinematic testing aboard the Canadian Coast Guard Ship (CCGS) Amundsen during February and March of 2004.

Most hydrographic devices, such as sonars and heave sensors, use the NMEA GPGGA format for GPS positioning, therefore the decision was made to limit GPS data to this format. Static tests were used to corroborate previously published conclusions on performance, as well as a means to develop data handling strategies for the kinematic phase. Data were logged at various periods during the fall of 2003 and analysed accordingly. This battery of tests was used for filter evaluation and optimization, and code debugging.

During the kinematic phase of the evaluation, both NMEA and C-Nav binary data were logged. However, all filter analysis and tidal harmonic analysis was carried out with the NMEA strings. For the purposes of post-processing, the binary data files were recorded and then converted to GPS standard Receiver Independent Exchange Format

(RINEX) files. This format enables processing with numerous commercial and scientific software suites.

Several options are presented as a means to improving the raw heights available through the NMEA format. The improved heights are then presented as a means of real-time vertical solutions, capable of satisfying Special Order survey requirements. The smoothed C-Nav tidal signature is compared statistically to one obtained using single beam sonar, and the harmonic constituents resulting from each are discussed. As well, comparisons are made with regards to the two version of LSSA software used, and recommendations of further updates to both put forth.

The final comments of this thesis address the conclusions as pertaining to the statements of capabilities offered in Section 1.1. Portions of those statements not fulfilled are addressed with recommendations for further study.

1.3 Report Structure

As this thesis is rooted in both GPS and tidal theory, there is a requirement to give some explanation to each. Chapter 2 assumes a base level understanding of satellite navigation and therefore avoids a full explanation of GPS theory. However, a fairly full commentary is given on GPS error sources and how they affect different positioning situations. This knowledge is important to understanding why GPS is vulnerable in the vertical dimension, especially in the Arctic, and how GcGPS compensates for this fact.

In Chapter 3, a discussion on the theory behind tidal forces and motions is presented in moderate detail. This is given as in any attempt to resolve and predict something as dynamic and involved as tidal heights, background knowledge is imperative when seeking new and untested methods. Chapter 4 highlights portions of the literary review and preliminary investigation period of the research. The previously written papers on the subject of C-Nav give indication of possible advantages or deficiencies pertaining to this research.

A thorough outline of the preliminary C-Nav evaluations is presented as Chapter 5. This chapter describes in detail the various processing steps that were taken at each stage. Justification is given to choices made at every level of the experiment, from data logging to program selection, so that the clear line of thought can be unveiled. Chapter 6 describes the field research portion of the thesis; including the research platform, acquisition period, and processing steps. The experimental results are contained within Chapter 7. Both the hydrographic and oceanographic analysis is given alongside. By revisiting Section 1.1, Chapter 8 ascertains the conclusions as a function of those operational capability statements, and makes recommendations on possible avenues for future work.

Chapter 2 GPS Background

As stated, the intent of this research was to develop and analyze a new approach to GPS positioning; one that purports to overcome the weaknesses of preceding stand-alone systems. The critical components in achieving this goal are a full understanding of GPS error sources, and a complete appreciation of the evolution in both technology and technique in attempts to minimize these limitations. However, a full and thorough explanation of the GPS service will not be given here. An extensive description of basic GPS architecture and methodologies can be found in publications such as Leick [1995], Misra and Enge [2001], or Wells et al. [1986], to name a few. A list of GPS related publications can be found in the reference section at the end of this report.

2.1 GPS Measurements

To fully appreciate the limitations of GPS, it is imperative to understand how the measurement processes are affected by the different error sources. There are two distinct modes of GPS ranging, pseudo-random code (PRC) ranging, and carrier phase measurements. For PRC measurements, either C/A code or P code modulation is used to determine the distance from each satellite to the receiver. Carrier phase observations solve for the range value by estimating the number of completed and partial cycles of the carrier frequency along the signal path from satellite to receiver. These two methods are

susceptible to the same sources of error; however, some of the sources affect each of these ranging methods differently. For PRC measurements, the observation equation, shown as Equation 2.1, is given as:

$$\boxed{\rho = r + c(\partial T - \partial t) + I_\rho + T_\rho + \varepsilon_\rho} \tag{2.1}$$

where:
ρ = pseudo-range
r = true geometric range
c = speed of light
∂T = receiver clock error
∂t = satellite clock error
I_ρ = ionospheric delay
T_ρ = tropospheric Delay
ε_ρ = unmodeled error sources.

For carrier-phase measurements, this equation becomes:

$$\boxed{\Phi = r + c(\partial T - \partial t) - I_\Phi + T_\Phi + \lambda N + \varepsilon_\Phi} \tag{2.2}$$

where:
Φ = distance measured in units of cycles
r = true geometric range
c = speed of light
∂T = receiver clock error
∂t = satellite clock error
I_Φ = ionospheric delay
T_Φ = tropospheric delay
λN = integer ambiguity
ε_Φ = unmodeled error sources.

2.2 GPS Error Sources

The errors that plague GPS measurements can be grouped into 3 sets, based on their nature; satellite-based, propagation-based, and receiver- or user-based [Leick, 1995]. Mitigation of each of these errors is largely dependent on the access and control a user has at each level. Receiver based errors can be handled directly by the user, with site selection and receiver design. Propagation-based errors can also be limited with receiver design and atmospheric modeling. Mitigation of satellite-based errors is the most elusive for the average user, although we will see how the C&C Technologies C-Nav system aims to overcome this obstacle.

2.2.1 Satellite-based Errors

Satellite-based errors consist mainly of ephemeris and clock errors. The ephemeris errors manifest themselves in equations (2.1) and (2.2) in the true range component, *r*. Each range that has been observed must be measured from some origin, and this origin is each satellite's position (*Xs, Ys, Zs*) as given by the ephemeris broadcast within the navigation message. The receiver coordinates (*Xr, Yr, Zr*) are involved in the range measurement as per Equation 2.3:

$$\boxed{r = \sqrt{(Xs - Xr)^2 + (Ys - Yr)^2 + (Zs - Zr)^2}} \qquad (2.3)$$

The propagation of satellite vehicle (SV) coordinate error into the receiver solution is obvious. Ephemeris errors are broken into 3 orthogonal components; radial, along track, and across track. Within these, the radial error tends to be the smallest which is fortunate given the nature of the ranging system. Initially the root mean square (rms) contribution of clock and ephemeris errors to the ranging error was limited to 6 m as per specification, but usually < 3 m was obtained. Recently this specification has been officially tightened by the Navstar Consortium to 3 m for the Block IIF constellation [Misra and Enge, 2001].

Until 2 May 2000, the largest clock error was due to the intentional dither of the satellite clocks and possible degradation of broadcast ephemeris, known as selective availability (SA), by the US Department of Defense (DoD). This resulted in an rms error of 25 m. A US Presidential Directive turned off SA, marking the single largest performance increase available to the civilian user. The current contribution of the clock error to the 3 m ephemeris/clock tolerance is limited to 1.5 m with once-a-day data uploads. Newer generation SV's have the added capability known as Autonav, which allows Block IIR and IIF satellites to cross-link data so that any small variations in clock or ephemeris corrections can be quickly uploaded to the entire constellation regardless of each SV's position with respect to the uplink stations. The system is designed so that clock and ephemeris errors shall not exceed 3 m for up to 60 days out of contact with the control segment [Misra and Enge, 2001].

2.2.2 Propagation-based Errors

The propagation-based errors are a result of the GPS signals traveling through a non-homogeneous medium from satellite to receiver. The range and phase equations are based on the vacuum speed of light, c = 299,792,458 m/s. Throughout the 20,000 km signal path, all but the final 1000 km can be assumed to be vacuum space. In this last 1000 km, however, the atmosphere begins to refract, or delay, the signals within its uppermost, electrically charged portion, know as the ionosphere. Closer to the earth's surface, from an altitude of approximately 40 km, the signals are refracted again throughout the neutral portions of the atmosphere known as the troposphere and stratosphere. Since most of the refraction in the neutral atmosphere occurs in the troposphere, this neutral refraction is labelled tropospheric delay.

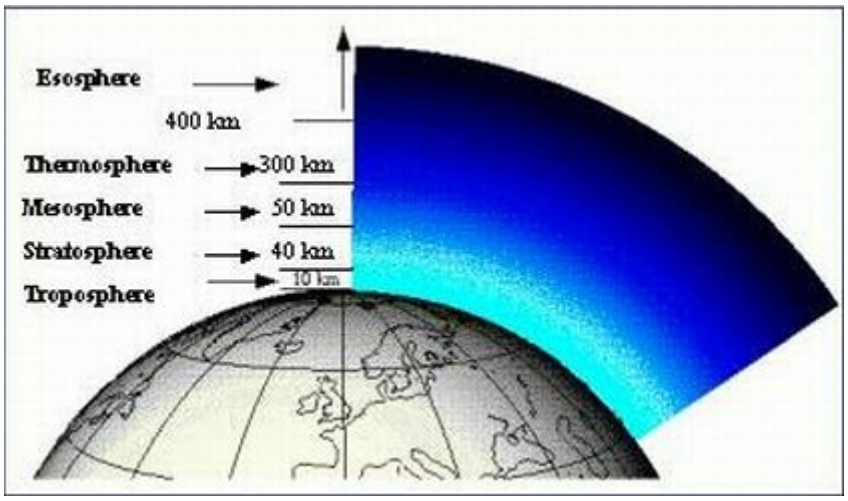

Figure 2.1: Atmospheric Layers [from http://geodaf.mt.asi.it/html/GPSAtmo/atmo.jpg, 2003]

Figure 2.1 illustrates the involved sections of the earth's atmosphere, including the lower portion of the ionosphere.

The greater portion of this atmospheric delay occurs in the ionosphere, where particles energized by the sun increase the refractive index along the signal path. This effect is not homogeneous and the refractive index can vary greatly along the path. This delay can be quantified and is largely based on the Total Electron Content (TEC) of the medium, and can therefore be modeled somewhat. However, due to the dispersive nature of the ionosphere, this error can be eliminated when dual frequency architecture is employed. It can be shown that the ionosphere-free range can be given as:

$$\rho^* = \frac{f_{L1}^2}{(f_{L1}^2 - f_{L2}^2)}\rho_{L1} - \frac{f_{L2}^2}{(f_{L1}^2 - f_{L2}^2)}\rho_{L2} \tag{2.4}$$

where: ρ^* = ionosphere-free range

f_{L1} = L1 frequency, 1575.42 MHz

f_{L2} = L2 frequency, 1227.60 MHz

ρ_{L1} = L1 observed range

ρ_{L2} = L2 observed range.

The lower portion of the atmosphere, the troposphere, contributes roughly 20% of the propagation ranging error. In this medium, the GPS signals are non-dispersive, and therefore this error cannot be eliminated by the use of two frequencies. The tropospheric delay is broken into two portions; the dry delay, which accounts for roughly 90% of the total tropospheric effect and is due to dry gases such as N_2 and O_2 throughout the lower atmosphere, and the wet delay, which accounts for the remaining 10% and is due to water vapour. The dry gases vary with season, latitude, and altitude, and remain relatively stable. They can be effectively modeled and removed from the solution. Water vapour content however varies considerably with the weather and can change rapidly. If a GPS

receiver is co-located with a meteorological sensor, accurate determinations of temperature, pressure, and relative humidity can be used in conjunction with advanced models and mapping functions to deduce local tropospheric delay effects, thereby improving the GPS solution. This has been the focus of much study in recent years. For a detailed description and analysis of atmospheric effects, see Mendes [1999].

2.2.3 User-based Errors

User-based error sources are also referred to as receiver-based errors. This group of ranging biases includes antennae phase-center offset variation, clock biases, receiver noise, and multipath effects. The antennae's phase center is the point to which the receiver physically measures the GPS signal. It is different for L1 and L2. The phase centre offset is the difference between the referenced geometric centre of the antennae as indicated by the manufacturer, and the receiver's instantaneous phase centre. The phase centre variation is the change in phase centre offset caused by variations in the incidence angle of the incoming satellite signals with respect to the receiver's non-spherical phase response pattern. These two effects are extremely difficult to minimize, and together can be in the order of 1-2 cm.

The use of low-grade timing devices in the receiver is overcome by solving explicitly for receiver time as an unknown while solving for receiver position. Therefore, clock uncertainties are not critical; however, time biases can contribute to the total ranging error. Receiver noise is the ability of the receiver to cleanly extract and measure

the incoming code or phase signal. Generally, receivers are easily able to do so at a noise level of 1% of signal wavelength. This implies varying performance of code and phase observables of 50 cm and 2 mm respectively.

Another large source of ranging error is multipath. This is the phenomenon whereby signals travel are reflected off natural or man-made structures prior to reaching, the antennae, as shown in Figure 2.2.

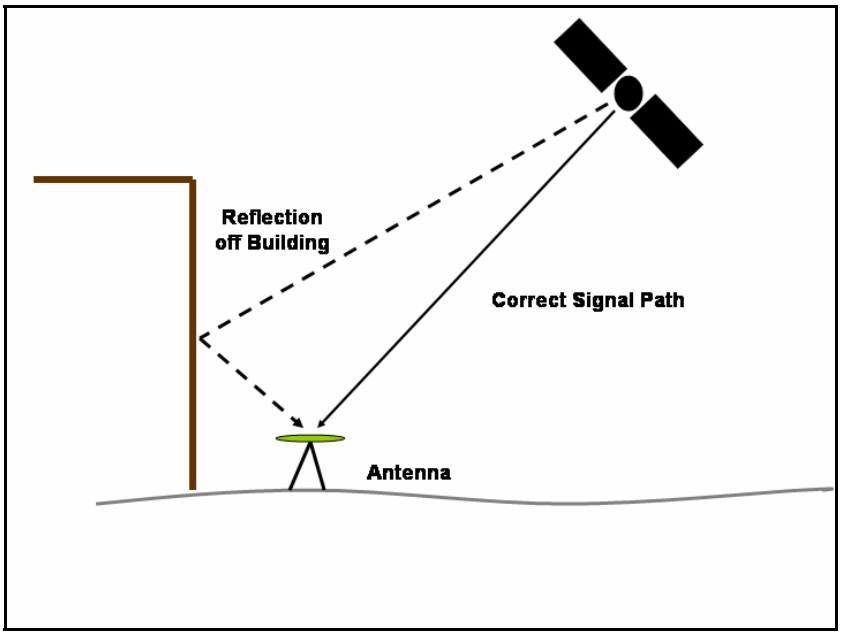

Figure 2.2: Example of Multipath

In this case, the pure solution from the direct signal path will be contaminated by the delayed solution, arriving later, with an apparently increased range. The magnitude of multipath error also varies significantly depending on the observable. Code measurements can be afflicted with multipath errors as high as 5 m in poor placements, though values of 1 m are more common. Phase error due to multipath cannot exceed 25% of a cycle, or roughly < 10 cm (5 cm for L1) while values of 1 cm are more

common. Multipath can be reduced if not eliminated with site selection, keeping the receiver away from reflective structures such as trees, buildings, or vehicles. Elevation angle cut-offs, as well as ground plane and choke ring antennae also prohibit low elevation reflections from contaminating the solution, thereby reducing the effects of multipath. As well, advanced receiver designs such as carrier-based smoothing can greatly limit the effects of multipath.

2.2.4 Arctic Effects on GPS

Optimum GPS performance can only be realized when we efficiently manage all of the GPS error sources described above. Once this is done, we end up with an expected positional uncertainty for a given confidence level. However, before we can state the system's overall performance, we must first consider Dilution of Precision (DOP). DOP is a numerical value that indicates the robustness of the GPS constellation geometry at each epoch. A well dispersed constellation provides a better solution, while closely grouped SV's create a solution with a higher level of uncertainty. A low DOP value indicates favourable geometry, and a better solution. DOP values can be multiplied by the accuracy limits of a receiver to give approximate precision values. DOP can also be expressed in terms of Horizontal DOP (HDOP) and Vertical DOP (VDOP) among others.

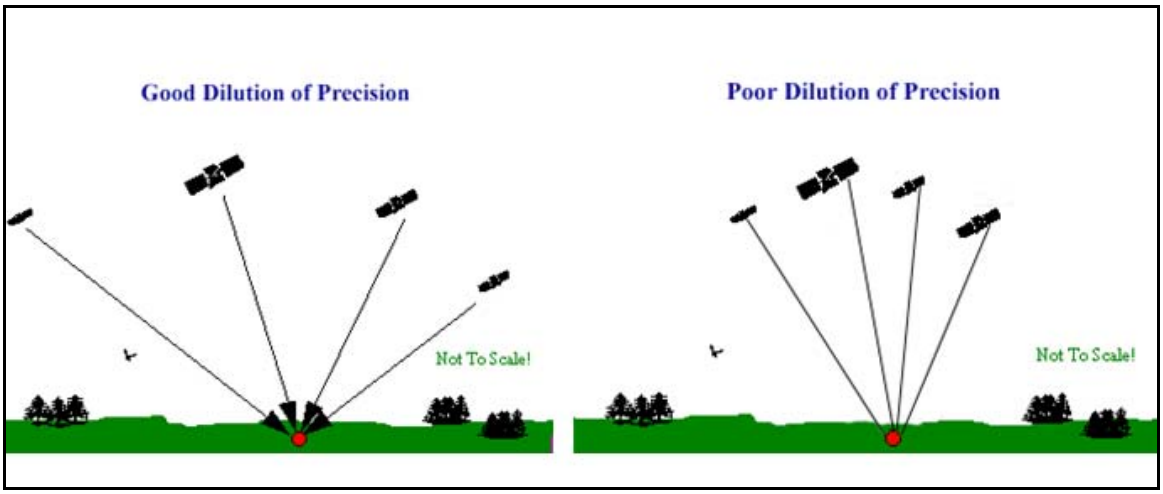

Figure 2.3: Example of Horizontal Dilution of Precision [from www.cmtinc.com/gpsbook, 2004]

Figure 2.3 illustrates a case of good and poor horizontal DOP (HDOP). Good HDOP indicates a situation of good geometry and therefore good VDOP is probable. However, due to the fact that for the vertical solution, all satellites are ranging from some angle above the receiver, much higher VDOP values are experienced compared to HDOP values. Hypothetically, if there were satellites ranging from below the horizon, then we could expect VDOP values similar to HDOP values.

One of the concerns with GPS in the Arctic is the impact of low elevation satellites. The initial requirements for GPS were to provide all-weather positioning to the U.S. military during operations around the globe. Cost and design limitations have reduced the area of quality GPS coverage to that which extends from approximately 80° N to 80° S. At the Polar Regions, this means that SV's rarely rise to a high elevation angle, thus making for a well dispersed, low elevation satellite constellation. This results in good horizontal geometry for the trisection problem. However, because there are no satellites passing through high elevation angles, and certainly none overhead, the vertical trisection is poor.

Another impact of Arctic GPS operations is the highly variable ionosphere. Using single frequency receivers in the Polar Regions is unwise as even the best ionospheric models are unable to handle the rapidly changing upper atmosphere. Although delays may not be as large as they are in the mid latitudes or the equator, they are much more difficult to predict and the residuals are generally larger for this reason. This problem can be mitigated with the use of dual frequency receivers.

2.3 Differential Modes of GPS

Although GPS, in its raw and simplest form of single point positioning, was heralded as one of the greatest leap forwards in positioning and navigation performance, its value as a fine measurement tool through the use of differential techniques has broadened its scope, while simultaneously advancing the accuracy attainable to the current level of sub-centimetre in 3-dimensions. Differential GPS (DGPS) comes in many forms, from code or carrier DGPS and the larger network Wide Area Differential GPS (WADGPS), to common static or kinematic relative positioning techniques. As well, recent differentiations have been made based on the nature of the corrections forming subgroups termed Ground Based Augmentation Systems (GBAS), and Space Based Augmentation Systems (SBAS) [Dixon, 2003]. In this section, beginning with the technique of relative positioning, a brief outline of each method is given along with a summary of strengths and weaknesses.

2.3.1 Relative Positioning

The term *differential* is commonly used to denote any form of GPS positioning using the base station/rover architecture. This group can be further decomposed into range correction, and relative positioning techniques. In this thesis, differential shall be used to refer to the traditional range correction technique using a base receiver, or network, and one or more roving units, and is discussed in the following section. Relative positioning will be used to describe the common post-processing practice of range differencing. Relative positioning can be implemented using code or phase observables; however, since it is usually performed in order to gain the highest orders of accuracy, it is most often performed using the carrier signal. Whereas code measurements are limited at 1 m in terms of resolution, and therefore accuracy, carrier phase observables can be resolved typically to several millimetres [Hofmann-Wellenhof et al., 2001]. It is this characteristic that makes them the preferred observable for high order applications such as relative positioning. Relative positioning usually differences the individual ranging data, at the receiver of interest, from each satellite with respect to the reference receiver to calculate a position relative to the reference receiver. This allows for high order positioning in environments that are considered impossible with stand-alone GPS. The main drawback of this technique is the requirement for a separate base station, and a reliable real-time data link to the supported receiver(s). This can be avoided with post-processing techniques, though at the expense of real-time capabilities. This technique, in all its forms, is well described in most GPS processing or application texts and will not be further explained here.

2.3.2 Ground Based Augmentation Systems

With the initial effects of SA, early C/A-code position accuracies were commonly in the order of 10's of metres. In an effort to improve this standard, while avoiding the costs of higher-end dual frequency receivers, the basic differential concept was developed. Two receivers situated in relative proximity, are affected similarly by random or systematic errors. One receiver, the reference station, is set up over a point of known coordinates, so that its GPS calculated position would reflect the values of all of the separate errors in the solution. These discrepancies would of course be manifested as range errors. These range corrections, relatively constant over a geographic area, are then transmitted to the remote receiver, so that they may be applied to the measured ranges, thus providing a more accurate position. Even this simple system has separate modes of operation. The navigation mode would have all of the corrections transmitted to the remote receiver so that it would calculate its improved position. In surveillance mode, the receiver would transmit its observable back to the base station and all of the calculations would take place at the more robust, stationary receiver. This has the advantage of allowing for a smaller portable receiver in the field. In both modes, it is required that the two receivers are observing the same satellites.

This architecture can be implemented using either code or phase observables. DGPS, using code observables, is capable of metre-level accuracies, while the carrier phase implementation can achieve centimetre precision. The frequency of correction transmission also has a large impact on the network accuracy. Errors commonly eliminated, such as atmospheric delays, are not constant and can change rapidly in some

instances. For this reason, a common setup is to have a base station connected to a radio modem link transmitting the corrective message at 1 Hz. RTK-GPS uses the phase observables in differential mode with a correction data latency near or equal to zero. Another problem that hinders DGPS performance in this design is the spatial de-correlation that occurs as one moves further away from the reference receiver. With single receiver reference networks, the de-correlation accounts for roughly 1 cm of positioning inaccuracy per kilometre of distance from the receiver. [Hofmann-Wellenhof et al., 2001]. This problem is addressed with WADGPS, using multiple reference receiver networks.

2.3.3 Wide Area Differential GPS

In the WADGPS configuration, multiple base receivers are used as a reference network, providing a more robust correction algorithm, as well as the ability to survive single receiver failure. However, due to the nature of the corrective service, a central station is required for processing and distributing the correction to the remote receivers. This additional step also invokes a small period of data latency that may prove prohibitive for some GPS uses. WADGPS corrections are produced through two distinct forms of processing; the domain approach, and the state-space approach. The domain approach is similar to the single receiver DGPS correction algorithm. Each base receiver's errors are calculated and weighted to form a set of corrections for the network area. This approach has the undesired result of correction performance dependent upon

the remote receiver's geographic position within the network matrix. The state-space approach models and evaluates the separate errors within the confines of the network, and will be discussed further in the next section.

The correction format for the above differential methods is normally dependent on the manufacturer of the GPS receiver hardware. GPS receiver distribution companies such as Trimble and Ashtech (now part of Thales Navigation) have each developed their own proprietary differential correction message. Similar to the development of the RINEX format, a standard for differential correction messaging has evolved. This format was proposed by the Radio Technical Commission for Maritime Services (RTCM) Special Committee 104, and has been in use at some levels since its draft version was published in 1985. The format has taken the name RTCM 104, or simply RTCM. This format's newer versions, 2.2 or newer, allow for corrections from code and phase observables from GPS, or its Russian counterpart GLONASS.

Although the most common medium for correction transmission is through radio frequency (RF), there is considerable variance. For small scale operations, users will often work a closed system correction utilizing VHF or UHF frequencies and simple modem communications between the receivers. For larger scale operations, a dedicated radio frequency can be employed to transmit the correction, or it can be modulated onto an existing channel. As is described in the next section, several WADGPS systems are now employing communication satellites, in geostationary orbits, for correction transmission.

2.3.4 Satellite Based Augmentation Systems

A common misconception concerning SBAS services, is that the denotation of 'satellite based' is due to the geostationary satellite communication link used by many for the correction signal transmission. This is erroneous. 'Satellite based' refers simply to the root of the corrections themselves, being those concerned with the clock and ephemeris errors inherent to the satellites [Dixon, 2003]. Previously we discussed the state-space method of corrections when discussing WADGPS networks. SBAS systems are a manifestation of this idea, focusing on the separate errors occurring in the satellite domain. SBAS's use a reference network to compute corrections for each error source individually; atmosphere, satellite clock and orbit. Each of these corrections is transmitted to the user receivers via satellite communications. Although these systems are commonly advertised as stand alone positioning services, they do carry the same reference network requirement as a regular DGPS setup, the difference being that the reference network is operated and maintained independently of the remote receivers. Several regional SBAS networks have already been or are being established. They include Japan's Multifunction Transportation Satellite (MTSAT)-based Satellite Augmentation System (MSAS), Europe's European Geostationary Navigation Overlay Service (EGNOS), the American Federal Aviation Administration's (FAA) Wide Area Augmentation System (WAAS), as well as Canada's own Canada-wide Differential GPS (CDGPS). All of these systems are government initiatives originally intended for other purposes, such as aviation navigation. The advantage is that these services will be available to all users within the correction footprint, although perhaps at an increased

cost. Low cost, recreational grade WAAS capable receivers have been available for some time, offering L1 corrections at a minimally increased cost. Table 2.1 compares the different SBAS services, along with the Initial Operational Capability (IOC) dates for each service [Dixon, 2003].

Table 2.1: SBAS Comparison

SBAS	IOC	Region	Corrections	Ref Sites	1σ Hor.	1σ Vert.
WAAS L1	2003	USA, Puerto Rico	Ion., GPS	25	3 m	7 m
WAAS L1/L2			GPS		.40 m	.60 m
EGNOS	2004	Europe	Ion., GPS, Gal	34	.40 m	.60 m
MSAS	2005	Japan	Ion., GPS	6	4.3 m	7.5 m
CDGPS	2003	Canada	Ion., GPS	n/a	~ 1 m	~ 2 m

Expectedly, several of the leading private sector GPS research and production companies have recently thrown their 'hat in the ring' in the establishment of SBAS services. These commercial ventures include Fugro Chance's Starfix-HP, Thales Geosolutions Group Inc.'s SkyFix XP, and the service used in this research, the NavCom Technologies/C&C Technologies C-Nav GcGPS. A comparison of these three commercial services is given by Bisnath et al. [2003], and therefore will not be covered here. The advantage of the commercial services, at an increased cost, is the greater accuracy (10 cm horizontally, 15 cm vertically, at 1σ), and a global footprint. The limiting factor in the corrective service is not the integrity of the network, but the communication link that relays the correction to the individual receivers. As all of these systems utilize geostationary satellites to transmit the corrections, polar regions (> ~74° lat.) are blacked out as the communication satellites remain below the horizon.

2.4 C-Nav Globally Corrected GPS

In a partnership with NavCom Technology Inc., a subsidiary of John Deere and Co., C&C Technologies has developed a SBAS implemented WADGPS service. This technology is designed to provide decimetre level positioning worldwide, for the hydrographic, offshore oil, construction, and geodetic survey industries [Hudson et al., 2001]. This section contains a brief explanation of the service; to include its evolution, global infrastructure, user equipment, and published specifications. Additional papers describing the service, many of which are also cited in the reference section of this thesis, can be found on the C&C Technologies website, *www.cctechnol.com*.

2.4.1 System Infrastructure

As previously mentioned, C&C Technologies GcGPS is essentially a marine version of NavCom Technology Inc.'s StarFire service. StarFire was developed by NavCom and Ag Management Systems (AMS), both subsidiaries of John Deere and Company, and is operated by NavCom Technology Inc. The system is based on dual frequency architecture and therefore corrects for only satellite orbit and clock errors. Tropospheric effects are modeled using the UNB3 model (also used by WAAS and CDGPS) while multipath is reduced using advanced carrier smoothing techniques.

Initially, StarFire consisted of several regional, independent DGPS networks in the Americas, Europe, and Australia. NavCom's Wide Area Correction Transform

(WCT) technology was used as the algorithm put in place to support the international agricultural operations of John Deere. In terms of infrastructure, little has changed between early versions of StarFire, and the current evolution, although as we will see later, there has been a much larger reference network component added to the system. The initial setup can be decomposed into 7 distinct components:

- Reference stations in the WCT network number 20, with 8 in the US, 5 in Australia, 4 in Europe, and 3 in South America. A full set of observables (C/A and P code pseudoranges, L1 and L2 phase measurements, plus a record of the broadcast ephemeris) to each satellite in view is sent from each reference station to terrestrial network processing hubs.

- Network Processing Hubs (NPH) take the smoothed, refraction corrected pseudoranges and normalize them with respect to clock offsets, and further augment with site modeled tropospheric effects. These ranges are then amalgamated in a weighted average to produce a single, wide area correction for each satellite in the constellation.

- Land Earth Stations (LES) are satellite uplink facilities that upload the correction messages to the geostationary satellites.

- Communication links are required to transmit data from each reference station to the processing hubs, and again from the hubs to the LES's. The data are

sent via a wide and redundant assortment of transmissions, ensuring that there are never any signal stoppages between any of the separate components.

- Geostationary satellites upload the corrections from the LES and transmit them to users via L-Band satellite communication frequencies. Currently, StarFire transmits via Inmarsat, with coverage between 76˚ N and 76˚ S latitude.

- Monitor receivers are distributed throughout the global footprint to continually observe the operation and health of the system.

- StarFire user equipment combines the broadcast corrections with the raw, dual frequency GPS observables through a Kalman filter, giving the precise position solution.

Two important advances were made with WCT to eliminate weaknesses of WADGPS; first a dual frequency system was chosen to eliminate ionospheric effects, and secondly, extended carrier smoothing techniques were developed, thus eliminating multipath effects at the receiver, thereby negating the two largest sources of error in WADGPS solutions. The dual frequency, refraction corrected pseudoranges allow for a differential correction free from the spatial de-correlation existent in ionospheric delays using single frequency observables, thus making the initial StarFire WCT corrections valid over the continental network footprints. This central processing allows for

upgrades or changes to the processing algorithms to be carried out transparent to users, while the single correction over the continental footprint requires much less bandwidth, thereby lowering cost of the service considerably. The one sigma accuracy expected from WCT StarFire is 23 cm horizontal and 32 cm vertical [Hatch et al., 2003].

As with WAAS, the performance of the WCT corrections is dependent on the receiver's location with respect to the reference network. WCT correction performance degrades increasingly as the receiver moves away from the respective continental footprints. Principally, this is due to the inaccuracies in broadcast satellite orbits limiting the differential solution to an extent which makes it inoperable over a global area. Using a state-space approach, satellite errors can be estimated and corrected in the satellite space, irrespective of the user receiver position. Employing this theory, the improved evolution of the system, StarFire RTG, uses satellite clock and orbit error estimates from the Jet Propulsion Laboratory's (JPL) Real Time Gipsy (RTG) software to provide global sub-decimetre accuracy.

The California Institute of Technology's JPL has developed a precise GPS positioning software package, GIPSY-OASIS II. Recently, improvements to the initial GIPSY algorithms were made, enabling the software to perform in real-time, culminating in the RTG correction software. RTG corrects for two significant error sources [Gregorius, 1996]:

- Clock corrections for each GPS satellite. These are computed every few seconds, optimized for dual frequency users.
- Orbit corrections for each GPS satellite. These are computed every few minutes.

In support of NASA space vehicle positioning requirements, a global GPS reference network, known as the Global GPS Network (GGN), was established and maintained by NASA and JPL. This network consists of 60 stations, 23 of which have to date been linked to JPL's RTG algorithm. These sites maximize the observability of the GPS constellation and are therefore concentrated in the mid latitudes. Again, global representation is not a requirement of the network as the corrections computed are rooted in the satellite state-space, not on the earth based receivers, or their local effects.

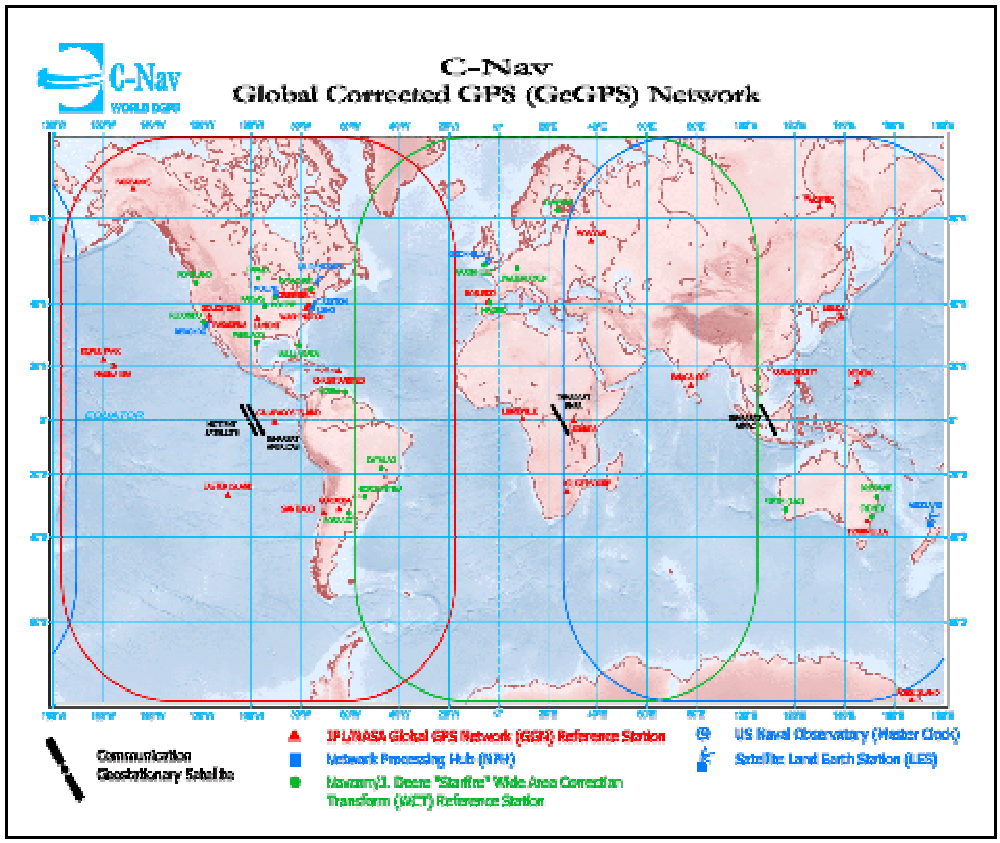

Figure 2.4: C-Nav StarFire Global Network [from www.cctechnol.com, 2003]

Figure 2.4 shows the C-Nav representation of the StarFire Network. The original John Deere WCT reference sites are shown in green, while the JPL/NASA GGN sites are shown in red. The RTG algorithms use the full set of observables from each RTG and

WCT station. The WCT corrections are still offered as a backup set of corrections in the areas where WCT is available. The blue symbols in the figure represent the processing and communication components, such as the NPH's, the satellite uplink LEH's, and the GPS master clock located at the US Naval Observatory. The footprint, and nadir position of each Inmarsat communication satellite is also visible.

2.4.2 C-Nav User Equipment

The C-Nav user equipment is tasked with receiving the broadcast StarFire corrections, applying these values to its own dual frequency, refraction corrected observables, and performing the position and navigation solution. To carry this out, the user equipment consists of:

- A tri-band antennae; GPS L1 and L2, as well as the L-band Inmarsat signal.
- An Inmarsat signal receiver which acquires, tracks, and demodulates the StarFire correction data.
- A high performance dual-frequency GPS engine, the NavCom NCT2000D.

Illustrations of the three separate components as well as a picture of the completely integrated housing are shown in Figure 2.5. A hardhat is placed next to the C-Nav unit to give scale.

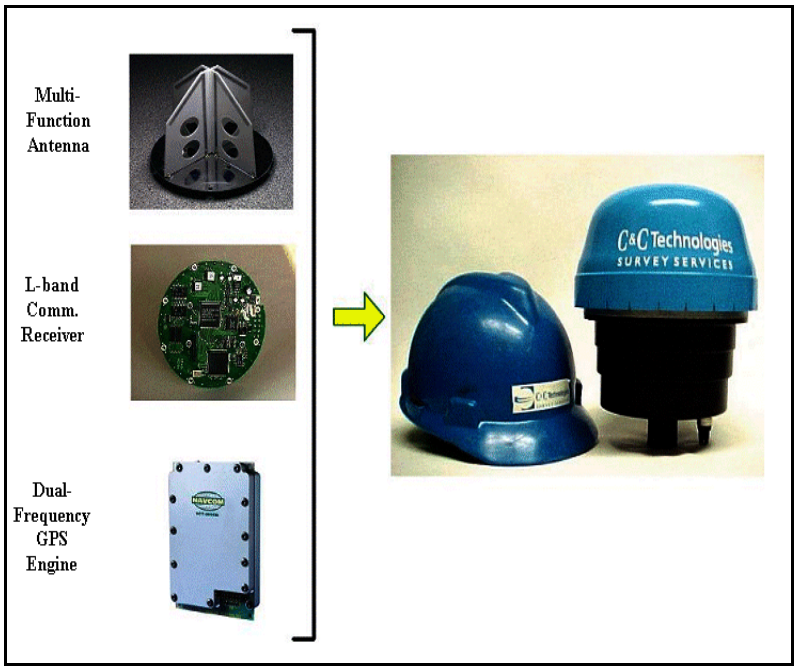

Figure 2.5: C-Nav Antennae/Receiver [from www.cctechnol.com, 2003]

The GPS engine tracks 12 dual frequency channels, 10 for GPS and 2 for the L-band WAAS signal. Multipath mitigation and robust P-code recovery are improved using patented techniques, which further enhance the 10 Hz or 1 Hz solution. Although not a critical component of the system, the CnC D.U. (display unit) can be used for receiver settings and firmware upgrades, or they can be input via serial communications from laptop computer.

2.4.3 C-Nav Specifications

C-Nav's specified 1σ accuracies, as published in the product brochure [C&C, 2003] are 10 cm horizontal, <30 cm vertical. This reference also states a 0.02 m/s velocity determination, and an environmental limit on cold weather operations of -20° C.

Chapter 3 Tidal Measurement and Analysis

The influence of tidal effects on water levels has been studied by humans since they first began settling along the ocean's shores. A thorough understanding of tidal motions is imperative to mariners, fishermen, and hydrographers, who spend their time upon the sea. In addition, oceanographers study the tides to gain a better understanding of the physical properties of the sea in order to predict and monitor its movements upon the shores, and the inherent consequences for those that inhabit those shores. In this dissertation, we view the tides as both signal and noise, in an attempt to utilize GcGPS as an instrument for tidal sampling and dynamic positioning respectively.

We should all be aware of the tides and their effects being due to the gravitational pull of the sun and moon. The earth is orbited by the moon while it simultaneously rotates on its axis and orbits the sun. These motions explain the period, amplitude and phase of the tidal constituents that are observable within the Earth's oceans. To better see the current problem, however, requires a deeper understanding of the tides and tidal mechanics in the region of interest. At risk to those who fully understand the physical oceanography at hand, the following explanation is given as an introduction to the tidal regime in the Canadian Arctic.

3.1 Tidal Mechanics

Although there are many, widely varying definitions of what actually constitutes or defines a 'tide', the definition used within this thesis is taken from the Canadian Tide Manual [Forrester, 1983]. It defines ocean tide as "*the response of the ocean to the periodic fluctuations in the tide-raising forces of the moon and sun."* To fully understand this statement, the definition of the tide-raising force follows.

3.1.1 Tide-raising Forces

Tide-raising forces are the resultant residual when portions of the moon's or the sun's gravitational attraction are left unbalanced by the centripetal acceleration of the earth experienced due to its solar orbit. Figure 3.1 shows the example of the solar tide-raising force.

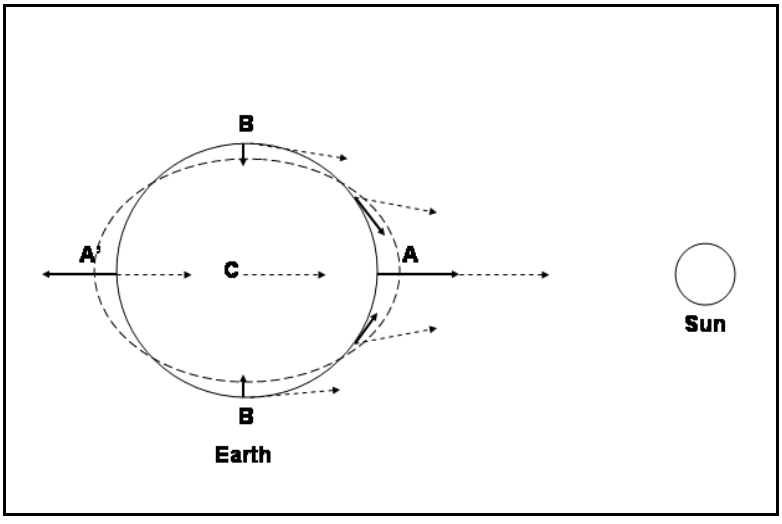

Figure 3.1: Generation of Tide-raising Forces

The dashed arrows indicate both the direction and magnitude of the gravitational force exerted by the sun upon each location, on the surface or within the earth. At each point on earth, the magnitude of the centripetal acceleration away from the sun is the same, and is always directed away from the sun, parallel to the plane of orbit. The solid lines illustrate the resulting tide-raising forces. At the centre of the earth, **C**, the gravitational pull of the sun is equal and opposite to the centripetal acceleration, which is the physical requirement for orbital motion. At the point on the earth's surface nearest the sun, **A**, the gravitational pull is slightly larger than that at **C** due to the smaller distance from the sun, and therefore greater in magnitude than the opposing centripetal force, resulting in a net force towards the sun. Directly opposite at **A'**, the gravitational pull is slightly smaller than at **C**, due to the increased distance from the sun, while the centripetal force remains constant which results in a net force away from the sun. At the two **B** points, the gravitational force is similar to that experienced at **C**, however it is inclined so that the resulting force is directed towards the centre of the earth. At a point midway between **A** and **B,** it can be seen that the resultant force becomes tangential to the surface of the earth. This force is referred to as the tractive force, and is the most important in tide amplification. The dashed ellipse represents the tidal bulge that forms at the points nearest and furthest from the sun. Similarly, it can be seen that that the moon also produces tide-raising forces upon the earth's oceans [Hughes Clarke, 2003].

It would first appear that since the sun has a much greater gravitational pull on the earth, it should have a greater influence on the tides. This, however, is incorrect. It can be shown that the tides are proportional to the inverse cube of the distance between the

two bodies, versus the inverse square; therefore, the proximity of the moon to the earth results in a tide-raising force that is more than 2 times that of the sun.

3.1.2 Harmonic Constituents

There is an obvious relationship between the tidal frequencies, or *harmonic constituents*, and the periodicities of the orbital motions of the earth, sun, and moon. The most important period is perhaps the day, defined in separate terms for both the sun and moon. A day can be defined as the time taken for the earth to present the same terrestrial point, at nadir, to the sun or moon. These periods are not constant and are described in terms of a mean value. A mean solar day (m.s.d.) is equal to 24 solar hours. A mean lunar day is slightly longer, at 24.84 solar hours. The two primary and basic tidal constituents are a product of these two periods. At any time, the tidal bulge illustrated in section 3.1 is present upon the earth both proximal and distal to the sun or moon. This means that over the course of the periods described above, the bulge will pass over a point twice giving rise to tidal frequencies of 2 cycles per solar or lunar day, having periods of 12.00 and 12.42 hours respectively. These two constituents are knows as the basic solar tide, S2, and the basic lunar tide, M2. Termed semi-diurnal constituents, they have periods of roughly 12 hours, giving roughly 2 maxima per day. Conversely, diurnal constituents have a period of approximately 1 day, with a single maximum. The M2 and S2 constituents are also the two strongest in terms of tidal potential.

Tidal potential is the unbalanced gravitational potential of a constituent at a point on the earth's surface, due to the involved bodies and inherent periodicities. Tidal potential can be viewed as 'absolute amplitude' that can be used to compare the magnitude of different constituents under equilibrium conditions. This is never the case, however, as the shape and volume of ocean basins and shorelines play a significant role in the tides experienced at given locations. The concept of tidal potential requires a deep and thorough explanation that will not be given here, but can be found in Godin [1972], or Foreman [1977], for example.

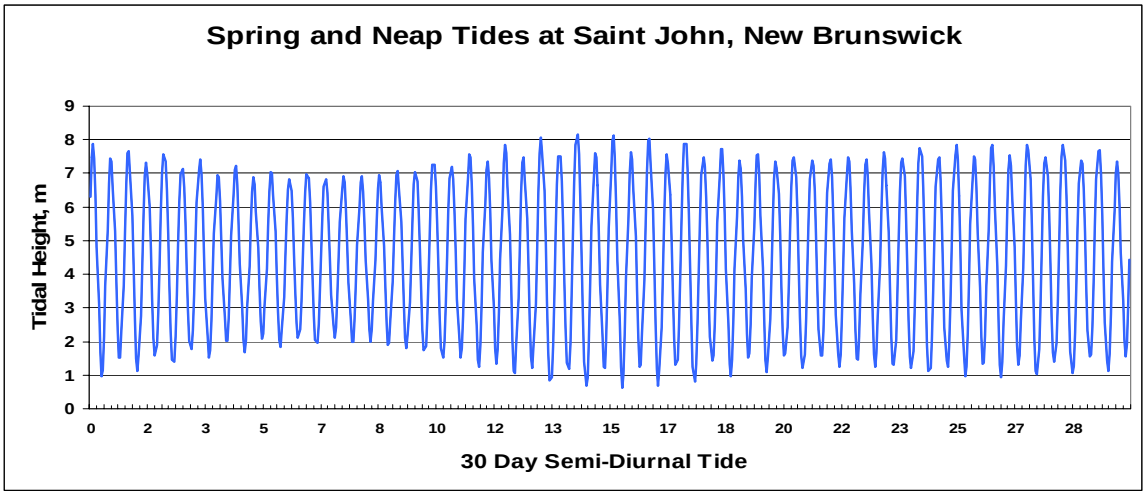

Figure 3.2: 30 day tidal record at Saint John, New Brunswick

Figure 3.2 shows a clear example of an M2 dominated, semi-diurnal tide. It is a 30 day record of tides in the Bay of Fundy. There are 60 tidal maxima, of varying amplitudes, over the 30 days. In addition to the semi-diurnal frequencies caused by the moon and sun, tides are affected by other periodicities of celestial motion.

3.1.3 Spring and Neap Tides

Of all the other celestial periods induced on tidal heights, the most apparent effect is the concept of spring and neap tides, which is the periodic fluctuation in the amplitude of the tidal signal. Over the course of a synodic month (period of the phase of the moon), the position of the moon relative to the sun determines whether the solar tide will enhance or diminish the effects of the lunar tide.

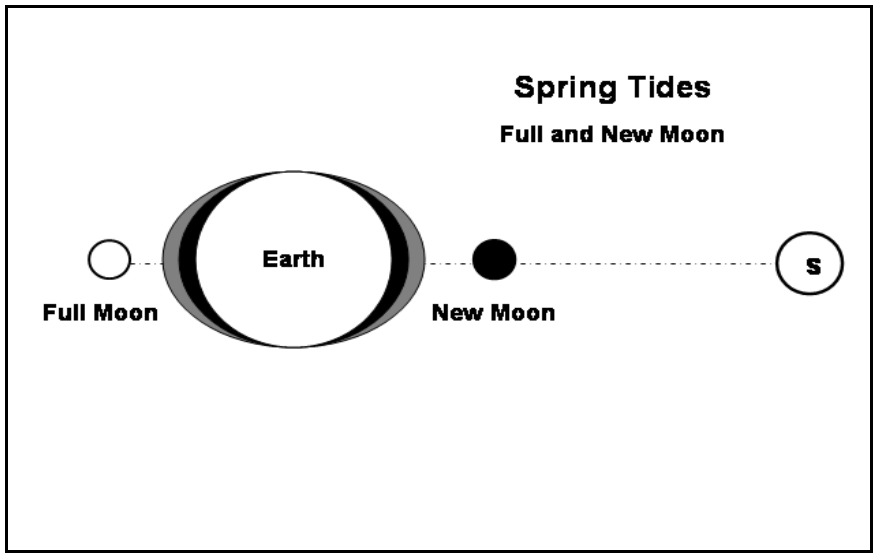

Figure 3.3: Luni-Solar alignment for Spring Tides

Figure 3.3 illustrates the case of spring tides, when the moon is at a new or full position. The lunar (grey) and solar (black) tidal effects are coincident and therefore give an enhanced amplitude.

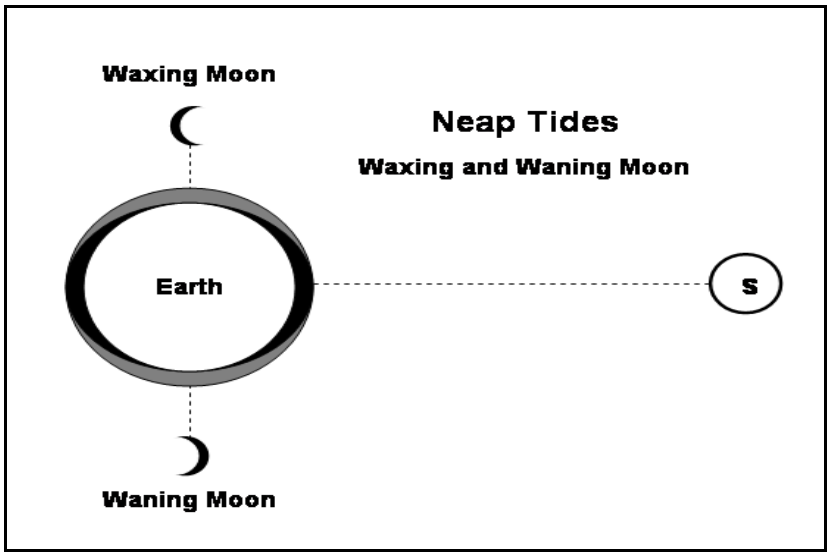

Figure 3.4: Luni-solar alignment for Neap Tides

Figure 3.4 shows the case of neap tides, where the effects of the sun and moon counteract one another thereby producing reduced tidal amplitude.

3.1.4 Tidal Constituent Formation

In addition to the cases explained above, all tidal frequencies can be seen to depend on the location of the earth with respect to the moon and sun, such that they are combinations of the astronomical periods shown in Tables 3.1 and 3.2.

Table 3.1: Periodic Definitions of a Year

Description	Point of Reference	Duration (m.s.d.)
Sidereal	Fixed point on celestial sphere	365.2564
Tropical	Vernal equinoctial point	365.2422
Anomalistic	Perihelion	365.2596
Eclipse	Moon's ascending node	365.6200

Table 3.2: Periodic Definitions of a Month

Description	Point of Reference	Duration (m.s.d.)
Nodical	Moon's ascending node	27.2122
Sidereal	Fixed point on celestial sphere	27.3217
Tropical	Vernal equinoctial point	27.3216
Anomalistic	Moon's perigee	27.5546
Synodic	Phase of moon	29.5306

Using periods from the preceding tables, four main constituent periods will be computed. The period of declination of both the moon in its orbit and the earth in its orbit (tropical month and year respectively) give rise to the periods shown in Table 3.3.

Table 3.3: Diurnal Constituents

Primary Period	Secondary Period	Resultant Period (hrs)	Name
1 cycle / lunar day	+1 cycle / tropical month	23.934	$K1^M$
1 cycle / lunar day	-1 cycle / tropical month	25.819	O1
1 cycle / solar day	+1 cycle / tropical year	23.934	$K1^S$
1 cycle / solar day	-1 cycle / tropical year	24.066	P1

Since the periods for the declinational values $K1^M$ and $K1^S$ are identical, they are thereby indistinguishable and are grouped together as the luni-solar declinational value K1 [Marchuk and Kagan, 1984].

As well, the variable distance of the moon and sun to the earth throughout the orbital cycles varies with the period of the anomalistic month and year respectively. This produces the following semi-diurnal frequencies, based upon the basic solar and lunar constituents, shown in Table 3.4.

Table 3.4: Semi-diurnal Constituents

Primary Period	Secondary Period	Resultant Period (hrs)	Name
2 cycle / lunar day (M2)	+1 cycle / anomalistic month	12.658	N2
2 cycle / lunar day (M2)	-1 cycle / anomalistic month	12.192	L2
2 cycle / solar day (S2)	+1 cycle / anomalistic year	12.016	T2
2 cycle / solar day (S2)	-1 cycle / anomalistic year	11.984	R2

The possible combinations of harmonics to produce tidal constituents evolve *ad infinitum*, though due to the timeframe of this experiment, we shall concentrate on the major resolvable constituents, in the diurnal and semi-diurnal range. For a fuller understanding of the combined harmonics, see Marchuk & Kagan [1984].

As we have shown, constituents are grouped into *species* dependent upon the nature of their periods. Diurnal periods, denoted with the marker '**1**', such as K1, O1, and P1, all share a period close to 24 hours. The semi-diurnal constituents, denoted as '**2**', share similar periods, at or near 12 hours. At any place on earth, the presence of each and every constituent is possible. This depends on latitude and local geographic factors. The shape and topography of different sea basins will allow different harmonics to resonate, thus amplifying some constituents above others. Without prior knowledge, it is difficult to establish, and therefore predict, which constituents will play a significant role at a given location. Only through harmonic analysis of a tide time series can we ascertain the presence or absence of significant harmonics constituents. Prior to looking at the mathematical analysis of the tidal signal, the technique of tidal measurement will be explained.

3.2 Tide Measurement and Analysis

Tidal measurements normally consist of shore based monitoring stations known as tide gauges. There exists an international network of water level observing stations known as the Global Sea Level Observing System (GLOSS). GLOSS was conceived in the mid 1980's as a means of observing global sea level changes as they applied to oceanography, geophysics, and climate change. Within this organization is the Permanent Service for Mean Sea Level (PSMSL). This service groups all the worldwide permanent tide gauge installations into a core network used as a global tidal baseline. Although these stations are numerous, they are shore based, and due to the cost of operation and maintenance, are concentrated in high marine traffic areas of developed nations.

3.2.1 Tide Measurement Techniques

There are numerous methods for measuring the tidal heights. The National Oceanic and Atmospheric Administration (NOAA) in the United States has developed a system termed the Next Generation Water Level Measuring System (NGWLMS) which utilizes an acoustic sounder to accurately measure the water level from a referenced datum. In this elaborate design, the acoustic signal is sent down through a PVC pipe to reflect off the water's surface. Simultaneously, a second signal is sent down a capped pipe of known length thus providing for calibration. The actual tidal height recorder in

the NGWLMS is a small component of the overall infrastructure. Co-located with each acoustic sounder are current and pressure sensors, as well additional data collection devices and network transmission lines. Figure 3.5 shows the overall schematic of a NGWLMS station.

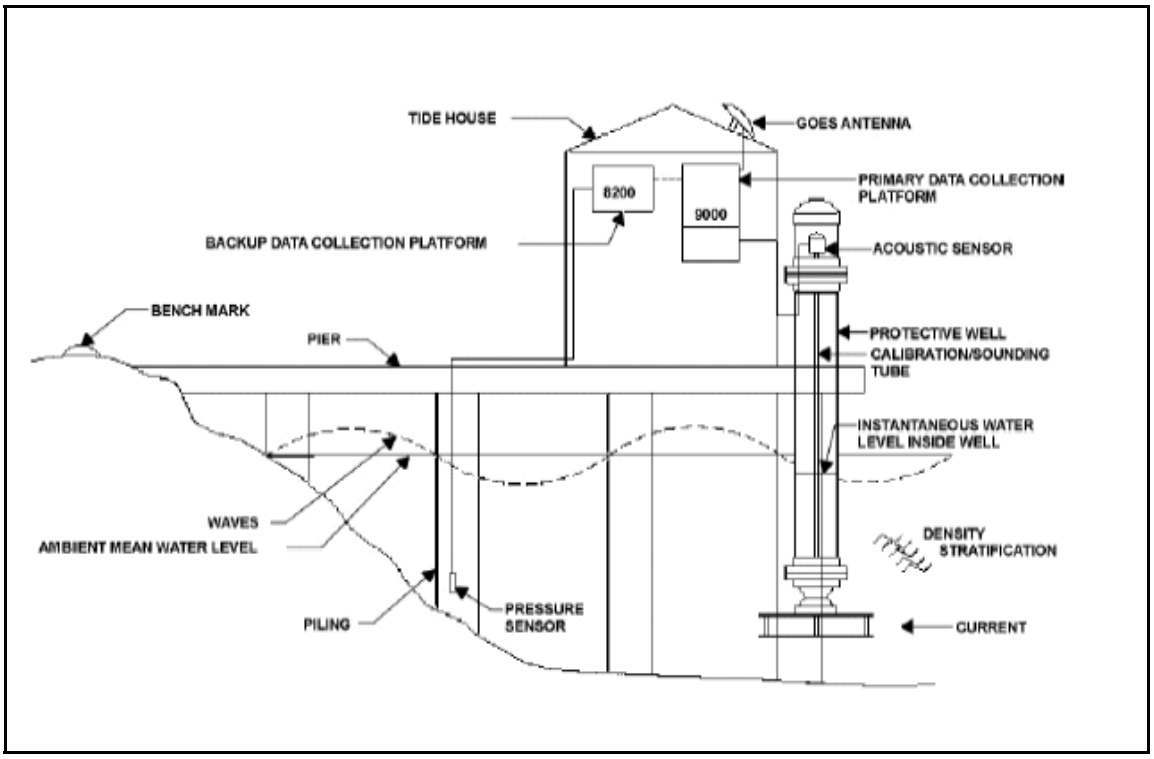

Figure 3.5: NGWLMS Station Schematic [from http://co-ops.nos.noaa.gov, 2003]

Although quite accurate (~ 1 cm at 2σ) and robust, this system of tidal measurement is very expensive compared to the traditional and simple measurements methods of the float gauge described later in this section.

Several countries are also actively employing pressure gauges which translate the pressure sensed at a submerged position as hydraulic head, to the height of the water column. These devices work well in offshore areas, where there is no possibility of mounting a stable tide gauge station. Pressure gauges can be quite inaccurate, as the

calculated depths are a function of sea water density, which is greatly affected by temperature and salinity, and ambient atmospheric pressure. To correct for this, additional measurements of atmospheric pressure, and water column temperature and salinity are required in order to attain a higher level of precision.

One of the simplest and perhaps most common techniques for measuring water levels, is the float gauge. Figure 3.6 depicts a common float gauge as used by the Canadian Hydrographic Service (CHS).

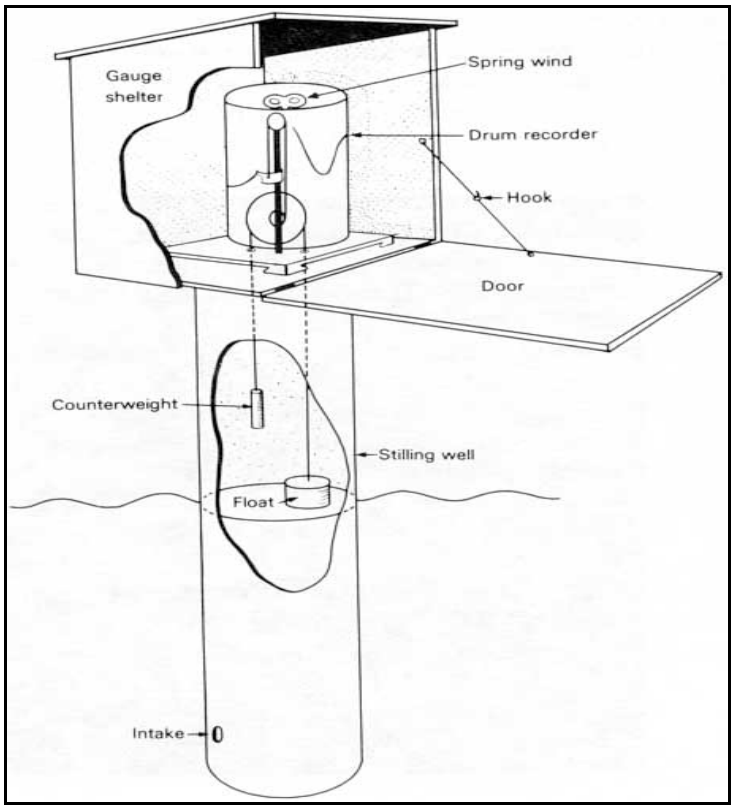

Figure 3.6: Common Float Gauge Installation [from Forrester, 1983]

In these systems, a float is suspended upon the water's surface within the confines of a stilling well used to protect the float and dampen short wavelength motion. As the water level moves up and down, the chain connecting the float to a counterweight rotates

a wheel recorder that translates the angular motion into a vertical heave or drop. This movement is recorded on a digital device which can be either manually downloaded or automatically transmitted to a processing station elsewhere for analysis. One of the biggest advantages of float systems over the other techniques mentioned is that they can be cheaply and easily set up in areas where there is a need for high accuracy tidal observations over a short time (i.e. < 1 year). In these instances, low-cost gauges can be installed in a couple hours and provide dependable height readings with the only maintenance requirement being weekly or monthly data downloads.

3.2.2 Tidal Analysis

In describing the tides, we have seen that at every point where they can be observed, they are a result of separate tidal constituents, summed to give a temporally dynamic signal. Once separated, these harmonic frequencies are defined uniquely at each location by *amplitude* and *Greenwich phase lag*. These two values are known as *harmonic constants*. The amplitude of a tidal signal is governed by the tidal potential, as well as other factors, such as latitude and local basin physical boundary conditions. Tidal potential was defined in Section 3.1.2 and can be viewed as a comparative strength of the tidal constituents. M2 is the strongest constituent, followed by K1 and S2, remembering that K1 is actually a combination of two separate tidal constituents, coincidentally with similar periods. The Greenwich phase lag is used to reduce all measured constituents to a common zone, thus enabling comparisons of tidal records from dissimilar time frames

[Godin, 1972]. This phase lag is relative to the moon's passage across the Greenwich meridian. A full explanation of the mathematical tidal theory, containing derivations explaining these concepts can be found in Forrester [1983], or Foreman [1977], and therefore will not be repeated here. Those wishing to gain a deeper understanding of the mathematics behind the theory of tides and their analysis should consult these two volumes. However, in order to understand some of the basic concepts, some mathematical understanding is required. Equation 3.1 forms the basis of harmonic tidal analysis.

$$h(t) = h_0 + \sum_{n=1}^{i} A_n \cos(\omega_n t - \Phi_n) + h_r(t) \qquad (3.1)$$

where: $h(t)$ = instantaneous water level at time t,

h_0 = mean water level over observation period,

A_n = amplitude of n^{th} constituent,

ω_n = frequency of n^{th} constituent,

Φ_n = Greenwich phase lag of n^{th} constituent,

$h_r(t)$ = residual height from non-tidal forces at time t.

The sum is performed across the total number of resolvable frequencies, *i*. The minimum input into this equation consists of ω_n, the frequency of the n^{th} constituent, calculated in section 3.1, and the time series of observed heights, $h(t)$. Using Least Squares Spectral Analysis (LSSA), algorithms can then be utilized to solve for A_n and Φ_n, the tidal constants for that location. LSSA is a complex but robust technique that requires substantial explanation. The method will be briefly described in Chapter 6 of this thesis,

though a thorough mathematical explanation can be found in Wells et al. [1985]. This research employed two versions of LSSA software, reported in Wells et al. [1985], and Foreman [1992].

Although there are 45 main astronomic constituents, and over twice as many inferred constituents, in many cases the tidal signature can be accurately measured as the sum of only a few main harmonics. Spectral analysis dictates that resolvable frequencies are limited by the sampling rate, and observation time. The Nyquist Theorem limits the highest detectable frequency to one half the sampling rate. The lowest observable frequency is that of equal period to the observation time. As many constituents are near in frequency or are mathematical combinations of one another, resolvable constituents are also limited by the Rayleigh criterion [Godin, 1972]. The Rayleigh criterion between a pair of correlated frequencies has the effect of lengthening the time series required to properly observe and resolve the constituents' harmonic constants. This is mathematically stated as $|F_o - F_1| \, T \leq RAY$, where RAY is commonly given the value of 1. Therefore, T is the observation period required to resolve the harmonics, F_o and F_1, separately. This increases as the frequencies converge. This is shown by Foreman [1977] where the requisite tidal record to resolve the primary semi-diurnal M2 constituent is only 13 hours, but the sample duration required to solve for the similar N2 constituent increases to 662 hours. A common practice to avoid this scenario is to observe only the primary constituent, and use historical relationships to infer the secondary or tertiary components [Foreman, 1977].

3.3 Hydrographic Concerns with Vertical Positioning

For the hydrographer, tides are a nuisance parameter. That is to say, there is not an explicit requirement to solve for their value, only a need to remove their effects from the hydrographic data. It is of course beneficial to the hydrographer to gain a higher understanding of tides and their origins in order to remove them from the data set being processed. Tides are not the only 'noise' in hydrographic sounding values. As a hydrographic vessel steams along its course, the three dimensional position is contaminated by many short period effects as well, such as waves. Short wavelength effects are easily compensated for with the use of a heave sensor and are not important to the content of this thesis. Longer period effects consist of tides, draft, and squat. Draft is the measure of the vessels depth in the water. As a vessel's weight changes, so does its draft. This is not sensed by heave sensors, and is commonly measured pre- and post-survey if a significant change is expected. Squat is the dynamic change in the draught of a vessel as it changes its velocity. Again, this is not well detected by heave sensors and must be otherwise determined.

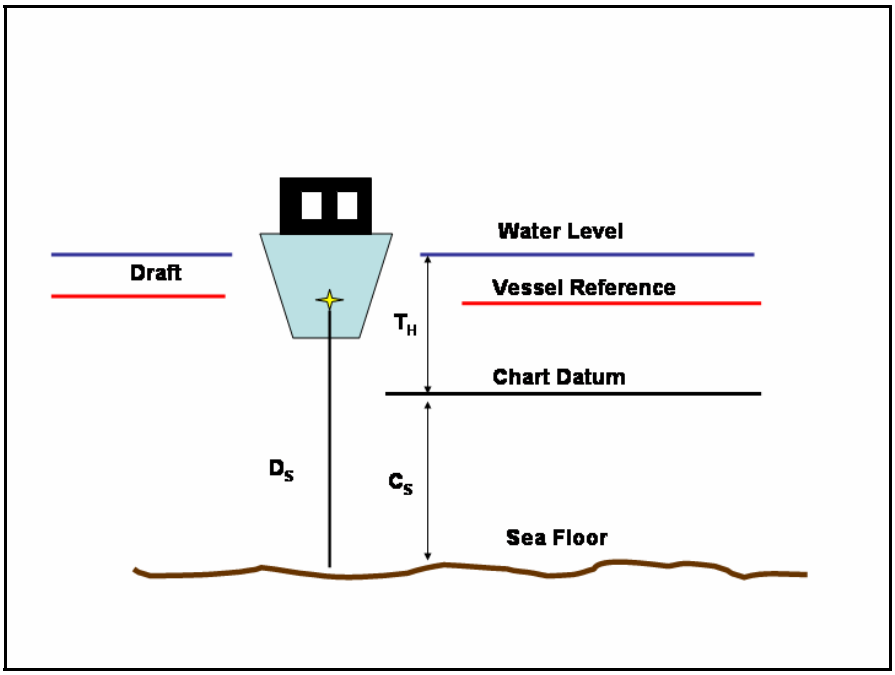

Figure 3.7: Hydrographic Vertical Levels

Figure 3.7 shows the critical measurements in vertical positioning. A displacement must be measured from the water level to sonar's face, or to a vessel origin point. This displacement is essentially the *draft*, affected by squat. The sounding depth, D_S, is measured from the sonar face and can be referenced to the vessel's origin. Instantaneous water level, or tidal height T_H, measurement allows the calculation of chart depth as shown below in equation 3.2:

$$C_S = D_S + Draft - T_H \tag{3.2}$$

Any error in calculating the tidal heights directly contaminates the depth solutions, or chart soundings, C_S. The hydrographer must remove these vertical biases in order to accurately position soundings with respect to chart datum. Long wavelength effects, and specifically tides, can be handled in many ways.

3.3.1 Tide Gauges for Hydrographic Surveys

Hydrographers can use tide gauge data, either from permanent gauge sites or using low cost tide gauges, to establish a tidal datum close to their area of operations that can be applied to their sounding data in post-processing. The International Hydrographic Organization (IHO), in its standard on positioning requirements, Special Publication 44, states that the tides measured at a gauge in the immediate vicinity of the survey area must be measured to a standard deviation not to exceed 5 cm. In areas where immediate co-location of the tide gauge to the site is not possible, the specified 5 cm error at the tide gauge is enlarged as the vessel operates further from the site. To mitigate this factor, techniques employing co-tidal models can be used. Co-tidal models measure the spatial dispersion of both amplitude and phase for a given constituent. This enables tidal signals at a gauge to be transferred closer to the survey area. If co-tidal models are used, then amplitude and phase can be transferred from the gauge to the vessel with minimal loss of precision, but this is a difficult task and is seldom put into practice. The impact of the errors incumbent at the tide gauge or through the modelling practice is clear in Equation 3.2, where $\sigma\mathbf{T_H}$ values directly propagate into $\sigma\mathbf{C_S}$.

3.3.2 Tide Prediction Software

In areas where there are not permanent gauges, and where location makes it undesirable to install one, tidal modeling software can be used. There are several tidal

prediction software suites on the market, as well as some freely available online, such as WXTide, show below. This software can be downloaded at *http://www.wxtide32.com.*

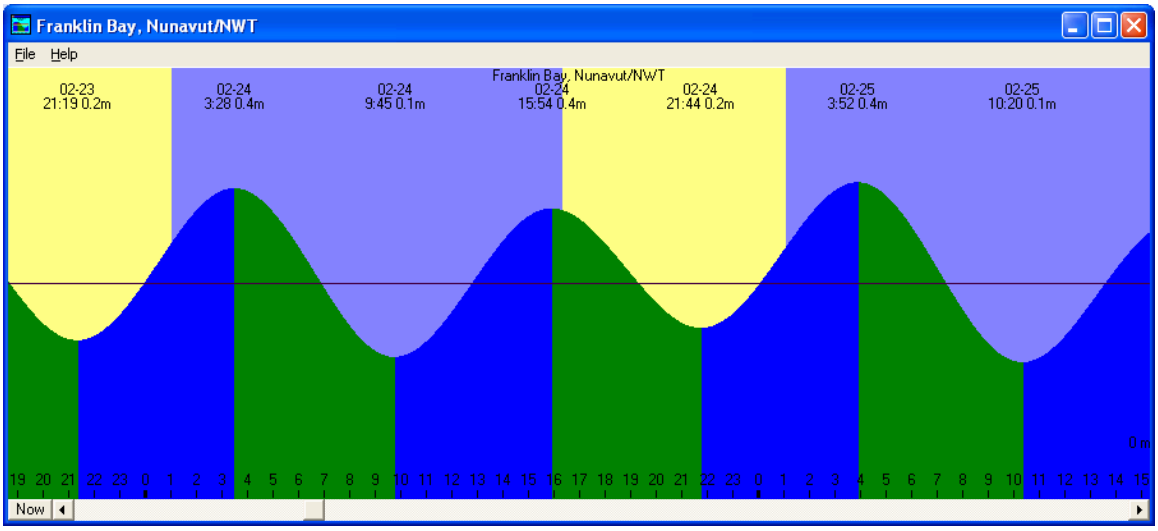

Figure 3.8: WXTide Graphical View

WXTide is a windows application of the UNIX based software XTide. Figure 3.8 shows a late February prediction for tides in Franklin Bay, NWT. Xtide was created by Dave Flater and utilizes all tidal data compiled by the CHS and NOAA at tide gauge sites. It uses a fully developed list of constituents for each separate site and is regarded as one of the best tidal prediction packages available. Canada's Department of Fisheries and Oceans (DFO) also offer a free tidal prediction package online, know as WebTide. An example of WebTide's prediction output for the same time period is shown in Figure 3.9. This software is available through the DFO sciences site which can be found at *http://www.mar.dfo-mpo.gc.ca/science/oceans.*

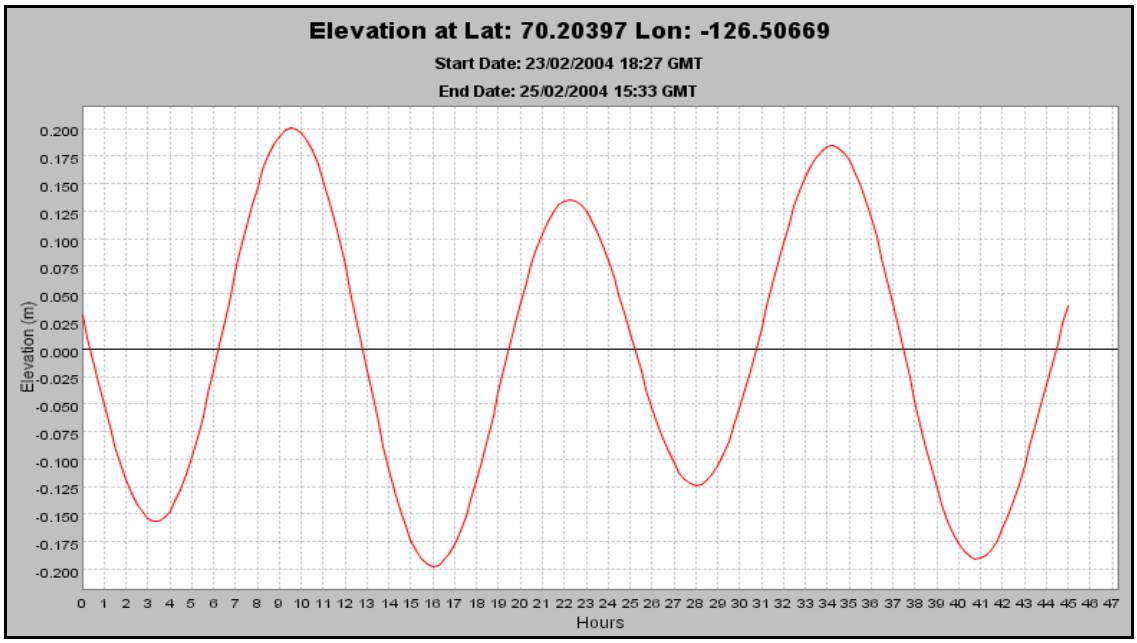

Figure 3.9: WebTide Prediction for Franklin Bay, NWT

WebTide is only for use in Canadian waters but has the added advantage of using interpolation techniques to give tidal predictions for any location, whereas XTide only predicts at shore based locations where constituents are known. One of the drawbacks of WebTide is its limited use of constituents. For instance, for the study area of this thesis, Franklin Bay, NWT, WebTide uses only 5 constituents; diurnal K1 and O1, and semi-diurnal M2, S2, and N2. XTide on the other hand utilizes 24 constituents for its shore based prediction at a historical site in Franklin Bay.

Tidal prediction can be very precise, in the order of centimetres. The quality of the prediction is dependent on the complexity of the tide and perhaps more so, the availability of high quality tidal data, which influences the precision of the derived constituents. This is most common in areas where there is a long and continuous tidal record, at one or more gauge sites. Such an area is the Bay of Fundy that, due to its stature as home to the world's largest tides, has been extensively studied and therefore

has a great deal of archived data, over a great period of time. We will see in Section 3.4 the pitfalls of using common prediction software in the Canadian Arctic.

3.3.3 GPS Height Reference Technique

Differential GPS (DGPS) allows the hydrographer to avoid the whole issue of tides. As mentioned, tides are a nuisance parameter and are not required to be explicitly solved for. With the movement of the IHO to GPS referenced tide gauges, there is now a much clearer understanding of WGS84 to chart datum transfers. These separation values are currently being refined worldwide, producing a separation model similar to the one used by GPS for ellipsoid-geoid height transfers. Using GPS at a vertical positioning accuracy commensurate with the required heighting standard allows the hydrographer to reference their depths directly to the GPS ellipsoid, WGS84, thereby completely avoiding the tidal reduction process. Transfer of these soundings to chart datum then only requires the application of the 1 dimensional shift as described above. This shift however can be cumbersome, and a clear understanding of the vertical datum is required. In areas of marine traffic, benchmarks are positioned near docks and jetties that are measured with respect to chart datum. There are current efforts to annotate each of these benchmarks with GPS ellipsoidal elevations as well. Once this is complete, the practice of mapping GPS heights to chart datum will be a simple scalar addition. For a rigorous explanation of vertical datums, see Deloach [1996], or Lachapelle et al. [1993].

For this method to work, the GPS vertical solution must be of an order that it would satisfy the IHO vertical standards shown below in Table 3.5. This is the common practice put into place with RTK-GPS surveying. Figure 3.10 illustrates the technique, explaining the differences between this method and traditional hydrographic survey height calculations.

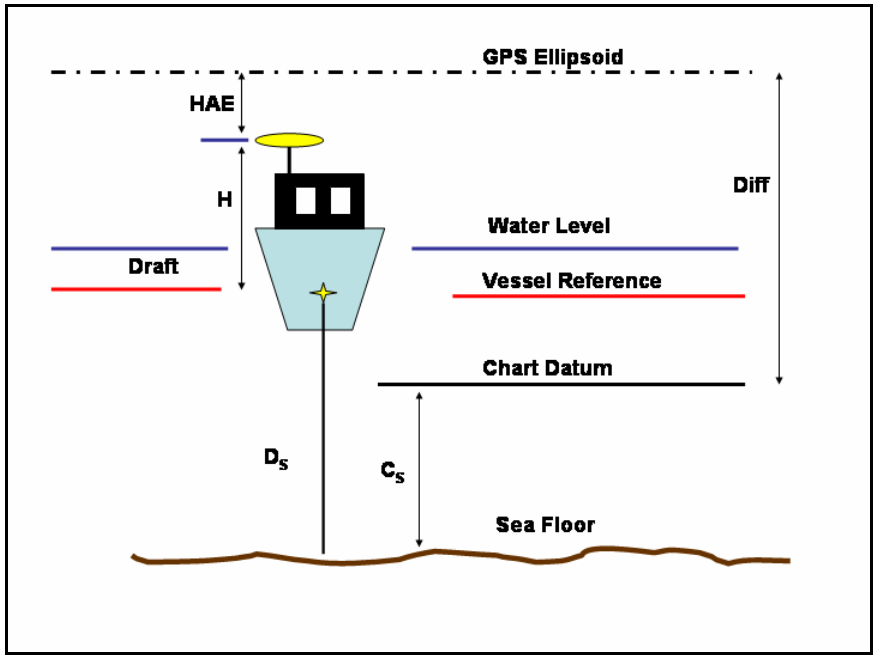

Figure 3.10: Vertical Positioning with GPS

In the case of positioning with GPS, only one measurement is required; GPS height with respect to the ellipsoid, *HAE*. Note that this value can be negative as shown in Figure 3.10. This case measures in essence a GPS height below the ellipsoid. This is generally the case in New Brunswick, where Mean Sea Level (MSL), or its representative geo-potential surface, the geoid, is ~25 m below the WGS84 ellipsoid. The GPS antenna will be surveyed to the vessel coordinate frame once installed, giving the height value, *H*. This measured height value never changes, though we will see later its orientation can.

For each survey area, datum shift values (*Diff* in Figure 3.10) between the WGS84 ellipsoid and chart datum will be established as already mentioned. Therefore, every sounding can be automatically converted into a chart sounding as per equation 3.3.

$$\boxed{C_S = D_S - (HAE - H) - Diff} \tag{3.3}$$

Survey vessels are affected by other motions that may bias these GPS heights. Heave sensors were already mentioned as a requirement for short wavelength vertical motions but they also have another important role. Because the GPS antenna is positioned well away from the centre of gravity of the vessel, normally the centre of the vessel coordinate frame, there is a large lever arm that will reduce GPS antennae's HAE in cases of pitch and roll. Using heave sensor data, these rotations must be applied to the lever arm in order to eliminate the vertical biases caused by these motions.

3.3.4 International Hydrographic Organization Vertical Standards

Although there are numerous country defined designations of allowable tolerances for vertical control during hydrographic surveys, the International Hydrographic Organization has developed a set of standards that have been adopted by many member countries. Table 3.5 from IHO Special Publication 44 [1998] gives the position tolerances as a function of survey order. The depth accuracies include all errors in positioning and propagation. We can roughly equate the fixed '**a**' value for each order to the allowable positioning error.

Table 3.5: IHO Positioning Standards [from IHO Spec. Pub. No. 44, 1998]

Order	Special	First	Second	Third
Area Example	Harbours, berths, critical channels	Harbour approaches, depths to 100m	Areas not yet described up to 200m depth	Offshore areas not classified special, 1st or 2nd order
Horizontal Accuracy, (2σ)	2m	5m + 5% depth	20m + 5%	150m + 5%
Depth Accuracy, (2σ)	a = 0.25m b = 0.0075	a = 0.5m b = 0.013	a = 1.0m b = 0.023	Same as 2nd Order
Where depth accuracy is given as +/- $\sqrt{(a^2 + (b*depth)^2)}$				

Using techniques described in Chapter 2, such as RTK-GPS, centimetre level accuracies are attainable up to distances of 20 km from the base station. This is sufficient for all orders of survey. In addition to the removal of tidal 'noise', GPS also removes the long wavelength effects of dynamic draft.

3.4 The Arctic Tidal Regime

There are numerous concerns when working with oceanographic parameters in the Canadian Arctic. First and foremost is the lack of archived data. While the waters of the Pacific and Atlantic shores have been studied extensively due to their involvement in commercial activities such as fishing and shipping, the Arctic remains largely undiscovered. The fact that a large portion of the archipelago waterways are beset by sea ice for most of the year obviously plays a significant role in this as well. Although ice levels have been shown to be in retreat in recent years, they still affect the passages between the Arctic islands throughout the year. Figure 3.11 illustrates the minimum extent of summer sea ice, which normally occurs in September.

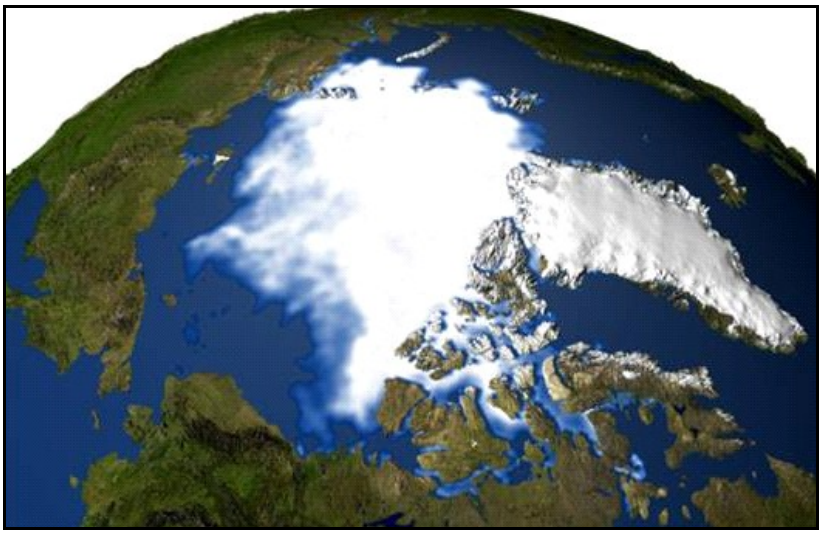

Figure 3.11: Minimum Summer Extent of Sea Ice [from SSMI Composite Data, 2003]

With evidence of diminishing ice levels in the Arctic, research has been initiated to evaluate the possibility of the Northwest Passage becoming a major shipping lane in years to come. The Canadian Arctic Shelf Exchange Study (CASES), and its follow on ArcticNet, have been put in place to investigate this possibility as well as other effects of the reduced ice levels.

3.4.1 Arctic Tidal Measurement and Prediction

As part of the ArcticNet research envelope, the oceanographic parameters of the Arctic must be better determined. In the case of tidal observations, there are currently no permanent tide gauges in the Arctic contributing to GLOSS. Due to the lack of historical data, predicted constituents are poor in quality, and therefore give weak predictions in the assorted software packages previously described. DFO's WebTide states a 35 cm (rms)

error in its Arctic predictions. In some areas of the Arctic such as Franklin Bay, the tidal range is less than 30 cm. In such cases as these, predictions do not suffice. The lack of reliable data is evident in the CHS Bluefile Index (see Figure 3.12), which is a record of all Canadian locations for which tidal constituents are known. Note the concentration of solved shore stations within major shipping areas, and the lack of known stations throughout the Arctic Archipelago.

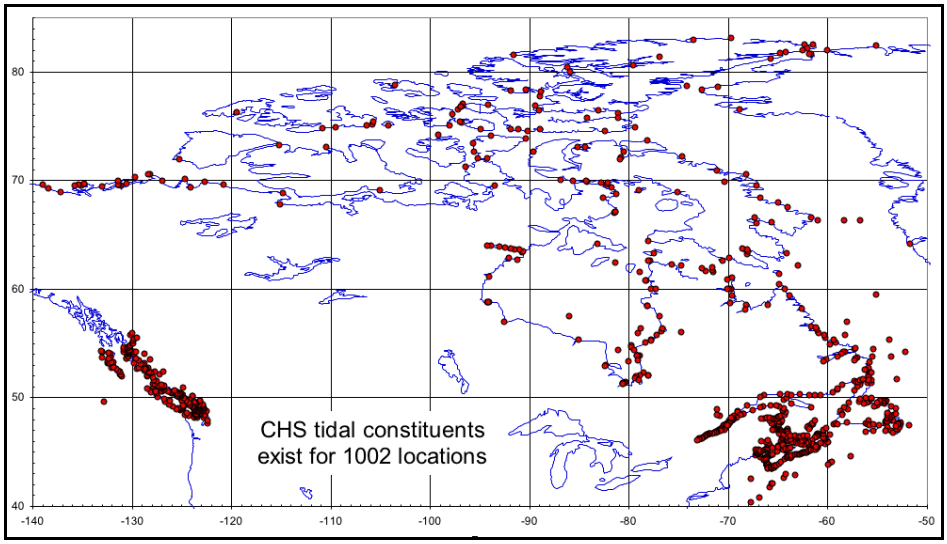

Figure 3.12: CHS Bluefile Sites [Wells, 2003]

3.4.2 GPS Possibilities

If tide gauges are non-existent and prediction software is unreliable, what options are available for water level determinations? RTK-GPS is capable of providing cm level accuracy over 20 km baselines. The problem with RTK in this scenario is the lack of suitable base station sites. A base station needs power, accessibility, and a well

determined reference position. This is difficult to provide along the remote coasts of the Canadian Arctic. As we saw in Chapter 1, there is an alternative, Globally Corrected GPS (GcGPS).

GcGPS, though not as precise as RTK-GPS, is a considerable improvement over regular Wide Area Differential GPS (WADGPS) and may be the key to solving the tidal detection problem for both oceanographers and hydrographers. Preliminary investigations on its suitability will be discussed in Chapter 4.

Chapter 4 Preliminary Investigation

To date, several studies have been carried out investigating the performance of the C-Nav system. In this chapter, findings extracted from these studies are presented with regards to their relevance to this research. Attention is given to those studies focusing explicitly on the performance envelope of C-Nav as a GPS instrument, as well as inquiries into its operational capabilities as a tide measuring device. Notice is made on each conclusion drawn with respect to applicability to this research, given the underlying circumstances of Arctic effects on both tides and GPS.

4.1 C-Nav Positioning Performance

As previously mentioned, C-Nav states impressive accuracies for RTG worldwide operations: 10 cm horizontal and <30 cm vertical at 1σ. Several studies have been performed that corroborate these specifications. Hatch et al. [2001], using 24 hour observation periods in Australia, reported 1σ accuracies of 5.8 cm horizontally and 12.8 cm in the vertical. In a similar test in the U.S. they measured accuracies of 7.7 cm and 11.4 cm respectively. This implies better performance than the specified values.

Roscoe Hudson and Sharp [2001], report similar findings for the RTG service of 7 and 11 cm for the 1σ horizontal and vertical accuracies. This paper also shows the difference between the RTG correction and the lower performance WCT correction. In

this case, the 1σ WCT accuracies were calculated to be 24 cm horizontal, and 41 cm vertical. As well it must be noted that these WCT accuracies are for a stationary point well within the WCT (CONUS) network, and that they would be greatly increased if the receiver was well outside of the continental footprint.

Both of the preceding studies were carried out by members of C&C Technologies. A third and independent study was presented by Bisnath et al. [2003]. This study compared C-Nav with two separate commercial WADGPS service providers. In this study the 1σ horizontal and vertical accuracies were evaluated at 10.4 and 19.4 cm respectively. This is the only published report that does not indicate a better than specified horizontal performance envelope. Although these studies enforce the idea of C-Nav as a valid positioning device, there are no kinematic observations, which are the main focus of this research. A summary of the static findings is presented as Table 4.1.

Table 4.1: Summary of previous RTG evaluations

Paper	Obs. Period (hr)	Horizontal 1σ (cm)	Vertical 1σ (cm)
Hatch et al.	24	5.8	12.8
Roscoe Hudson and Sharp	15	7.8	11.0
Bisnath et al.	24	10.4	19.4

4.2 C-Nav Tidal Measurements

Although there are numerous studies evaluating the positioning performance of C-Nav, there are few that address the true intent of the system, which is the ability to

provide 3-dimensional positions to an accuracy at which the vertical component can be used for water level determination in either a hydrographic or oceanographic sense. Chance et al. [2003] were the first to explicitly investigate this concept. This paper compares the attainable accuracies as seen in previous and independent research, with the values required by the IHO for the various orders of hydrographic survey. A useful derivation of IHO vertical accuracy standards is contained therein, as well as simple comparisons of C-Nav's static vertical accuracies with various instances and requirements of water level determination. However, there is no evaluation of kinematic C-Nav solutions, and therefore no comparison with actual tidal values.

Osbourne and Wing [2004] were the first to evaluate the dynamic vertical positioning performance of C-Nav against an observed tidal signature. Their research consists of several days observations in the Taiwan Strait, where tidal amplitudes are relatively high (~3 m) although unpredictable. In fact, the methodology of Osbourne and Wing's research is quite similar to that carried out in the Arctic. The main principle behind each is the observation and comparison of C-Nav, and tide gauge water levels. Osbourne and Wing used a shore-based tide gauge to compare the observed C-Nav water levels. This method, as we saw in Chapter 3, can add small errors to the 'true' tide values, depending on vessel distance from the gauge. Additionally, there is no compensation for vessel pitch, heave, and roll. Depending on the distance between vessel centre of mass and GPS antenna location, this can introduce significant biases in the data set. However, the study does illustrate that C-Nav could be used for water level determinations in an area of medium to high tidal amplitudes. The paper also concluded that this was dependent on a stable, or fixed, geoid separation value throughout the

survey area. This is currently an issue, but it is one that may soon disappear. As mentioned, given the pervasiveness of GPS in all facets of navigation and positioning, there are movements underway to link every tide gauge to a common surface (the GPS ellipsoid, [Wells, 2003]). Chart datum/ellipsoid separation values would then be local determinations. Current trends in geodesy and geomatics see a move from locally defined reference datums and networks, to those that are global in nature. The same can also be said for the reference ellipsoids upon which geomatic calculations are based. The GPS WGS84 ellipsoid is becoming a widely accepted reference surface in all facets of geomatics. GPS water level determinations are therefore becoming much more practical.

4.3 Arctic Influence on C-Nav Observations

All of the previous analyses share a common thread; the data collection took place at mid-latitudes. This fact ensures that satellite geometry for both the GPS constellation and Inmarsat reception is optimized.

GPS was not designed for polar service. Instances of cycle-slip, or position jumps as SV's cycle in and out of the constellation in view are cumbersome enough at 45° N. At 70º N, these occurrences are more frequent, and due to the generally lower observation angles observed, have a larger impact. We also know that GPS positioning is weaker in the vertical dimension, as opposed to the horizontal. This is due to the geometry of the constellation, providing numerous satellite ranges dispersed radially around the receiver, while always solving for the vertical component from above the

horizontal plane. This effect is magnified in the Arctic regions as lower SV elevation angles mean that the vertical will be solved by numerous shallow incident angle SV's and virtually none overhead. This effect provides for good horizontal geometry, while incurring poor VDOP values.

The correction link of C-Nav is also affected by high latitudes. Inmarsat is intended to relay communication information to the greater part of the inhabited earth. The design envelope is approximately 74 ° N to 74 ° S. Near the limits of the specified envelope, system performance naturally degrades. In regions where the signal is arriving at very low elevation angles, the correction signal itself grows increasingly susceptible to atmospheric effects and other signal contaminants that can trigger correction signal loss. Chapter 5 discusses the static evaluation and algorithm design employed to reduce the aforementioned effects.

Chapter 5 Static Testing and Evaluation

Two C-Nav units were delivered to UNB in spring 2003. This afforded the opportunity to utilise one as a hydrographic positioning device while simultaneously using the other for preliminary evaluation and future experiment design. During the spring and summer periods of 2003, the UNB Ocean Mapping Group (OMG) survey launch CSL Heron, was fitted with a C-Nav (see Figure 5.1) unit while engaged in hydrographic surveys on the Grand Bay-Westfield portion of the St. John River, and in the Shippagan Channel region of Caraquet Harbour, in north eastern New Brunswick.

Figure 5.1: CSL Heron [courtesy Dr. John Hughes Clarke, 2003]

During the Shippagan survey, the C-Nav was used as the primary positioning device, while tide gauge data were used for vertical control. Comparisons of the C-Nav solutions, as available to the hydrographic devices onboard Heron, with the float gauge tidal data are presented later in this chapter. At the conclusion of the summer, the C-Nav unit was transferred from the Heron to the Canadian Coast Guard Ship (CCGS) Amundsen (Figure 5.2) as preparations were made for the field portion of the research.

Figure 5.2: C-Nav and POS/MV Antennae Mounting Aboard Amundsen

Field research was scheduled aboard the Amundsen during Leg 5 of her journey, 17 Feb to 1 Apr, 2004. The intervening time was used analysing the static C-Nav mount at UNB, with goals of establishing standard data handling and processing techniques and procedures.

5.1 Static Data Handling and Evaluation

With a second C-Nav unit to use as a test and evaluation platform while the primary receiver was employed aboard the Amundsen, data handling and processing algorithms designed for the analysis of the Arctic data were developed so that the processing time for the Arctic data was greatly reduced. For this purpose, a unit was mounted atop the UNB Gillin Hall Geodesy Lab as shown in Figure 5.3.

Figure 5.3: Gillin Hall C-Nav Mount

The C-Nav unit was mounted in an area of low multipath influence [Langley, 2004], alongside the UNB2 Suominet GPS station (SA26), and the accompanying Paroscientific Met3A meteorological sensor. In addition to developing processing algorithms, the static C-Nav unit was also used to corroborate results previously published in reports by C&C or NavCom personnel. Another key advantage arising by coincidence was the magnitude

of the earth tide signature apparent in Fredericton. Fortunately, the magnitude of the earth tide signal at the static test location is comparable to the signal magnitude expected from the ocean tides in Franklin Bay. This is presented in Section 5.2.4.

5.1.1 Data Logging

In hydrographic operations the standard GPS position format is the NMEA GPGGA sentence. These data strings are output from GPS receivers to sonars, or other related devices. The GPGGA string is comma delimited and is defined in Table 5.1.

Table 5.1: NMEA GPGGA Field Definitions

$GPGGA,131101.00,4557.00707,N,06638.54116,W,2,7,1.3,45.30,M,-21.01,M,9,108*59	
Field	**Definition**
$GPGGA	- identifies the string as a GPS fix sentence
131101.00	- time displayed as [hhmmss.ss]
4557.00707	- latitude displayed as [ddmm.mm]
N	- north or south latitude
06638.54116	- longitude displayed as [ddmm.mm]
W	- east or west longitude
2	- GPS quality indicator (GQI) [0 = invalid, 1= SPS, 2 = DGPS]
7	- number of satellites used in solution
1.3	- HDOP
45.30,M	- HAE in metres
-21.01,M	- geoid height above ellipsoid in metres
9	- seconds since last DGPS update
108	- DGPS station ID
*59	- checksum, always begins with *

Since all equipment related to hydrographic operations use NMEA as standard input and output, the decision was made to use this data as the sole observable for the hydrographic themed analysis in this thesis. In the processing of data to achieve the best results for

harmonic tidal analysis, some raw GPS data is used in RINEX format. This will be discussed in Chapter 7.

For the static portion of the evaluation, the C-Nav unit was loaded with the most recent firmware version, 12.9. The receiver is capable of outputting data at either 1 or 10 Hz. Higher output rates are ideal for static positioning as they increase the statistical redundancy of observations, thereby improving the accuracy of the solution. However, in this research, the output rate must be at a level appropriate for both statistical optimization and peripheral equipment capacity. The standard RTK-GPS input to hydro systems is 1 Hz. At 1 Hz the sampling rate is significantly high for statistical advantage when working with tidal frequencies, consequently GPGGA data was logged at 1 Hz. For this research, the principle variables in the GPGGA sentence are time and HAE, though the other fields do contain valuable information. For example, inconsistencies in the vertical signature can be attributed to varying numbers of satellite used in the solution, loss of DGPS corrections, or an overall noisy GPS environment.

5.1.2 Data Handling

The GPGGA files were parsed (broken into regular components) to produce text files containing time, HAE, GQI, number of satellites, and HDOP, and arranged for further processing. This was accomplished with *awk* scripts, in the Mandrake Linux 9.3 operating system. Awk, or awk scripting, is a "full-featured text processing language with a syntax reminiscent of **C"** [Linux, 2004]. Awk enables structured text files to be

quickly manipulated using simple shell scripts. As all of the GPGGA sentences are similarly structured, awk is an excellent tool for data handling. In addition, data can be both 'piped' to or from nested awk iterations or other Linux shell commands such as *fgrep*. Information on fgrep and awk scripting can be found in Appendix I of this thesis, at the online reference above, or by referencing the man pages from the Linux shell command line. Once the data had been properly parsed, processing via standard software packages, such as Matlab®, was much easier.

5.1.3 Static Processing

The static evaluation was done on various data sets over November and December of 2003, and January 2004. During the processing, the ellipsoidal heights were smoothed initially using a moving average with a 1 minute window, and then were reduced to zero-mean; giving a clearer statistical connotation to the data. The main focus of the static test was to develop and evaluate data handling and processing scripts for later use, while identifying if the C-Nav vertical solution was as accurate as projected. Long data periods were broken into smaller files of a day or week length. Although the tests are static in nature, as mentioned previously, the expected earth tide at UNB is similar in magnitude to the ocean tides of Franklin Bay. As well, since Fredericton is at a latitude of ~ 45º N, there is little chance of any environmental effects that could possibly degrade Inmarsat signal corrections.

5.1.4 Static Results

The key in this phase was to identify a tidal signal in the noise of the C-Nav altitude solutions, and if possible, build a filter that would extract the tidal signal cleanly. Just over two days of data, beginning in late November 2003, are presented as Figure 5.4.

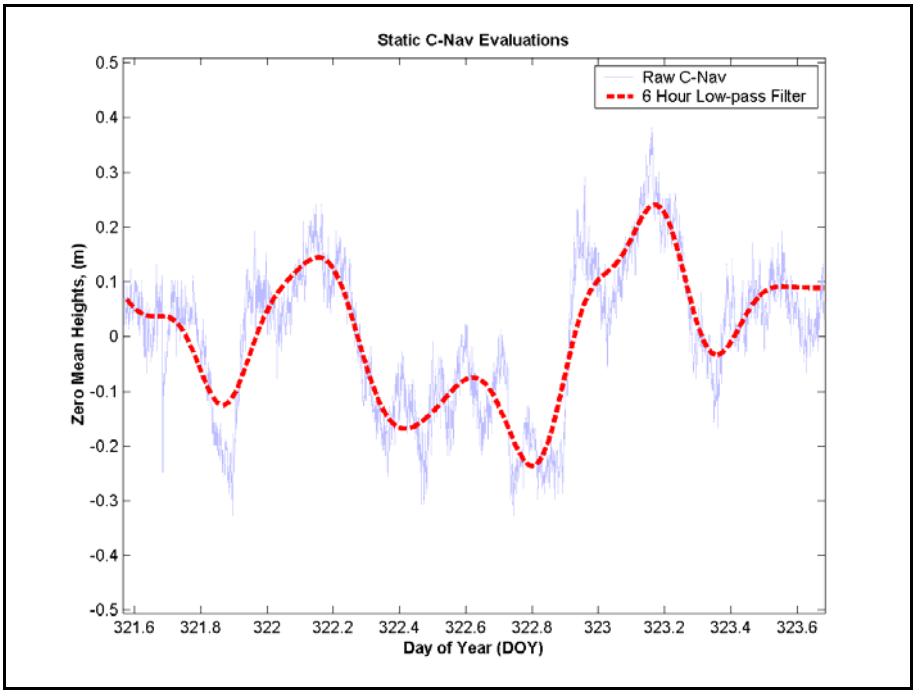

Figure 5.4: Initial Static Evaluation

The lack of noise in the data is impressive. Although there are obvious high frequency trends present (DOY 322.5), the overall noise in the data is very small for a stand alone GPS height solution. Compared to the sub-metre 1σ values exhibited by WAAS [Langley, 2004], the C-Nav solution appears superior. Using simple filtering designs, a six hour low-pass filter was applied in the time domain. The filter is discussed in Appendix II. This removed all harmonic data with periods less than six hours. When

filtering tidal values, especially earth tides, we can assume the highest frequency components to have periods of ~12 hours, so why a six hour low pass filter? Filter performance depends on filter length as a function of total time series length. Even though in this case we are really filtering using spectral values (but in the time domain), the same proves true; too long of a smoothing wavelength in too short of a data series will produce contaminated results. Due to the fact that there are no 'perfect' filter designs, some desired signal is always attenuated, and some noise always bypasses the filter. This can be shown graphically with the 10 hour filter employed in Figure 5.5.

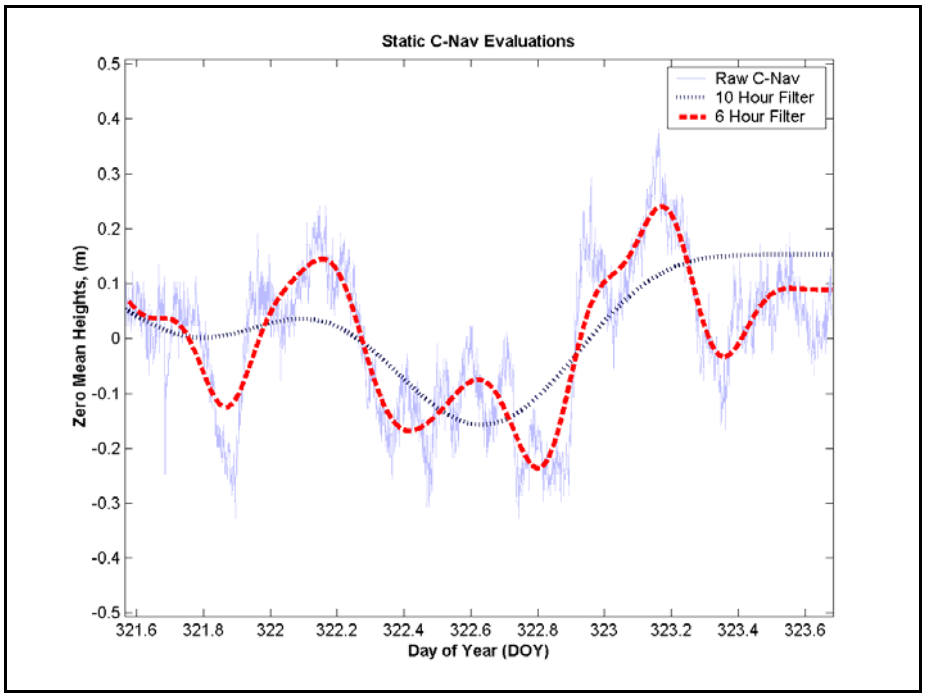

Figure 5.5: Example of Poor Filter Design for Tidal Extraction

The effect of the long period on the short time series is apparent as there is no visible harmonic signature over the two day period. Although higher stop-bands on low-pass filters do allow some unwanted data into the signal, their advantage compared to the great

loss of signal experienced if the cut-off is set too low is obvious. Again, the filter design is outlined in Appendix II.

The biases resulting in the data series are quite interesting and can be well illustrated by extracting the six hour filtered signal from the time series. A short wavelength (~ 3 hour) signal is clearly visible throughout the data set. Figure 5.6 shows a plot of the residuals once the filtered time series has been removed.

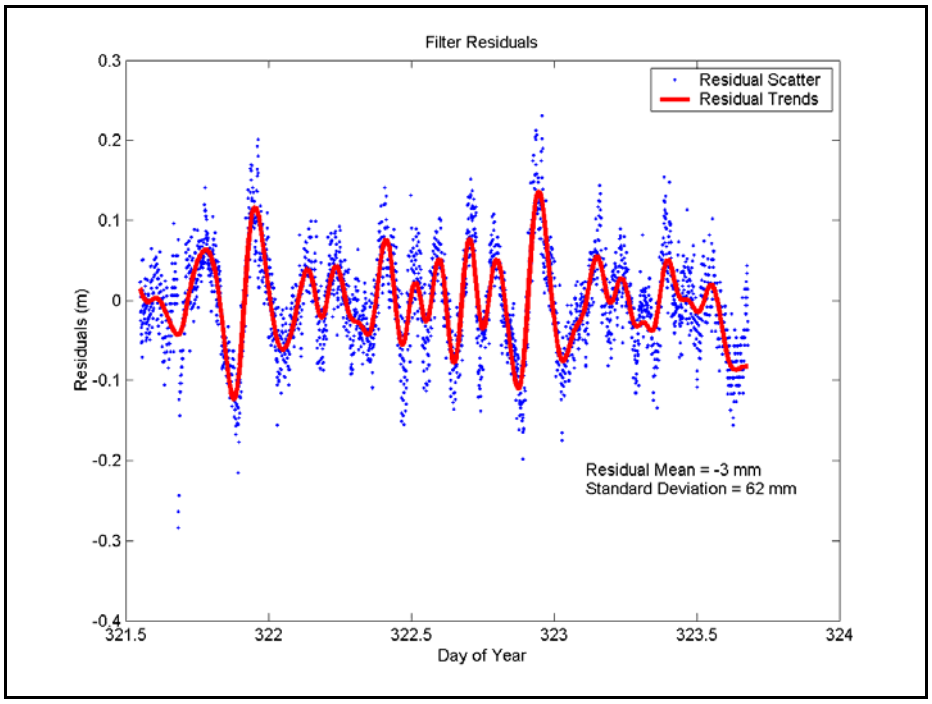

Figure 5.6: Static Evaluation Residuals

There are numerous circumstances that can add biases to a GPS data series, such as multipath or meteorological conditions. C-Nav operates with a patented carrier phase smoothing technique to limit the impact of multipath. In addition, the static test station was in an area expected to be relatively clear of multipath, so this is not suspected of being the cause of the biases. Meteorological effects can certainly contribute several

centimetres of bias, though a systematic contribution such as this would certainly have to be considered a great coincidence. The muted amplitude caused by the filter design may also be involved in this problem, however, where the filter mutes the amplitude only at each peak, the residual time series would only show biases at a similar frequency (i.e. 12 hour wavelength). This phenomenon is not fully understood and merits subsequent study. However, as it was not of immediate concern for this research, only its mention is covered here.

The mean of the residuals is -3 mm, which is insignificant given the C-Nav NMEA elevations are reported at the cm level. The standard deviation of the residuals is 6.2 cm. This is outstanding, assuming the six hour signal is an accurate representation of the earth tides present. A full week of data commencing on 30 December 2003 is shown in Figure 5.7.

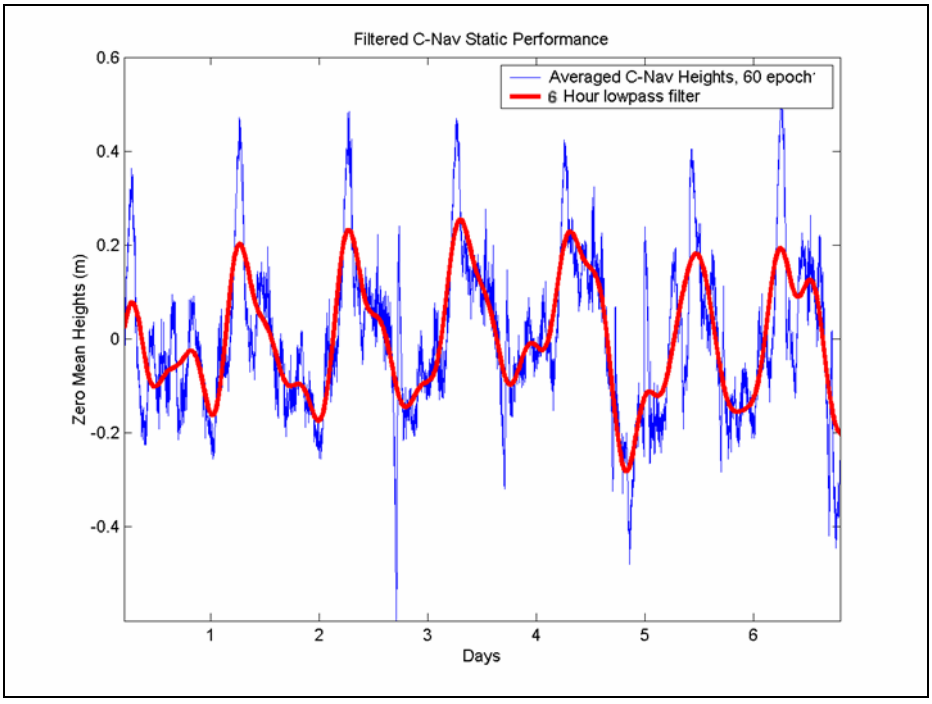

Figure 5.7: 7 Day Static Test

The mixed-mainly diurnal nature of the suspected earth tides is quite apparent in this figure. Earth tides expected in this region are mixed-mainly semi-diurnal. The mixed signature is clear. Also noticeable is an apparent overrun of the altitude at each upper daily peak. The raw signal seems to follow its filtered counterpart closely (<10 cm) for the most part, but at the peaks of the tidal heights, there is a significant short period increase that in some cases exceeds 20 cm.

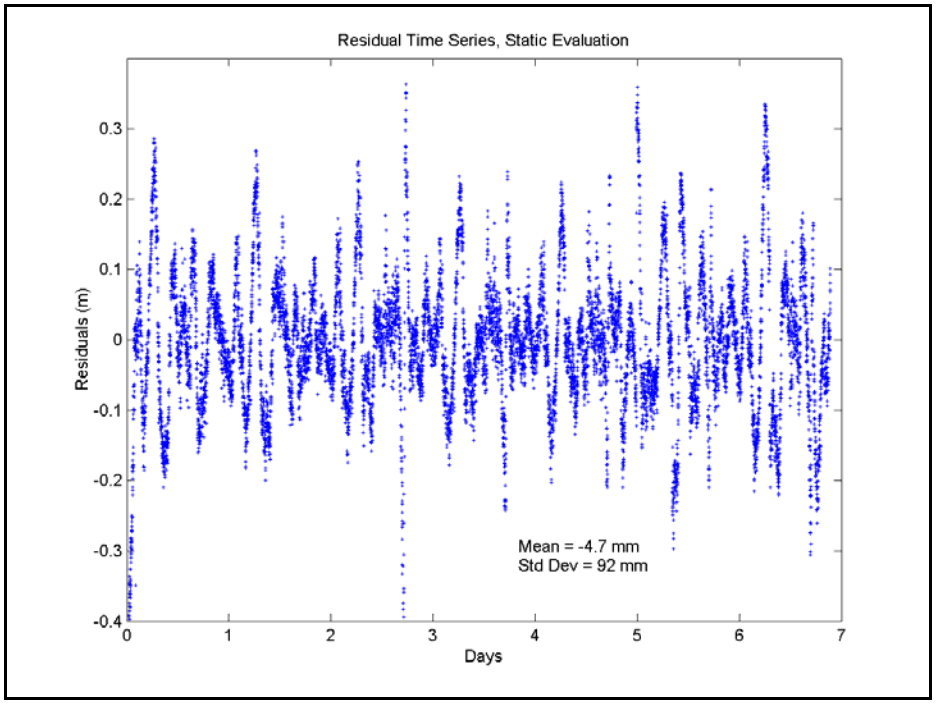

Figure 5.8: 7 Day Static Residuals

The mean of this set of residuals (see Figure 5.8) remained insignificant at -4.7 mm. The standard deviation over the weeklong period was 9.2 cm. Again, this is based on the assumption of the earth tides being accurately determined with the six hour low-pass filtered signal. Although there are still some short period effects present in this data set, the residual signal present in Figure 5.8 is clearly detectable.

5.2 Shippagan Survey Data

Once some data handling techniques were developed, a small evaluation was carried out on a test set of data from the OMG contract survey near Shippagan, New Brunswick. In this instance, tidal values were being sampled with a temporary tide gauge installed at the Government Wharf. Survey operations were carried out for 4-5 hours each day, so there was not a significant continuous period of C-Nav tidal sampling. The survey itself was carried out in an area of greater tide influence (10-15 cm) than the gauge located at the wharf.

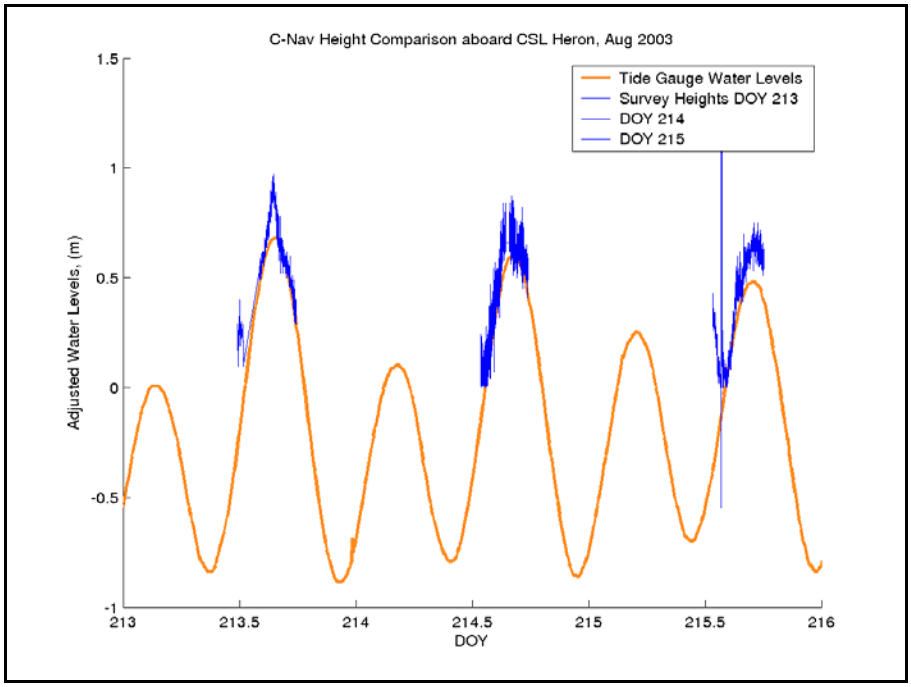

Figure 5.9: Shippagan Tidal Comparisons

In this examination, the C-Nav heights appear to be very close to the gauge values, with separation continuously less than 10 cm. This 10 cm value is a result of the vessel's transit into the area of higher tide.

Chapter 6 Field Research Methodology

As mentioned, the primary role of the preceding analysis was method development. With the data handling techniques trialed and improved, the processing of the field data was completed in a much shorter duration. Several bugs that were discovered late in the initial processing could have set the timeline back immensely if not for the archive of available scripts and algorithms developed during the static processing phase. The first step in the field research was data acquisition aboard CCGS Amundsen.

6.1 CCGS Amundsen

In early 2003, the Canada Foundation for Innovation (CFI), and the Natural Sciences and Engineering Research Council (NSERC), jointly funded the re-fit of the Canadian Coast Guard Ship (CCGS) Franklin, as the newly named CCGS Amundsen. The Amundsen grant is part of an overall increase in funding for Arctic sciences scheduled over the next 20 years [Hughes Clarke, 2003]. The Amundsen is to be a dedicated Arctic research vessel, initially under the control of the Canadian Arctic Shelf Exchange Study (CASES), and then in the continuing program ArcticNet. The Amundsen began her maiden expedition in September 2003, out of Quebec City, and planned for 14 months with an over-wintering destination near Franklin Bay, NWT.

Figure 6.1 shows the Amundsen in the fall of 2003, as she transited north to begin scientific operations.

Figure 6.1: CCGS Amundsen at Sea [Martin Fortier, 2003]

As part of her mission, she is tasked with providing bathymetric and seismic information throughout her time at sea. As a hydrographic platform, she requires precise positioning information and therefore prior to departure was fit with various GPS devices including, an Applanix POS/MV positioning and orientation sensor, as well as the C&C Technologies C-Nav GcGPS receiver. As the POS/MV is capable of passing both position and orientation to the hydrographic sensors onboard, the decision was made to pass the C-Nav Radio Technical Commission for Maritime Services (RTCM) standard corrections to the POS/MV while underway, thus eliminating the requirement for dual inputs to the sonar for differential positioning, while improving the POS/MV positioning performance. The C-Nav and POS/MV antennae are shown atop the Amundsen's aft mast in Figure 5.2.

6.2 Field Data Acquisition

Data were recorded aboard the Amundsen from February 17th until March 31st, 2004. During this period, the Amundsen looked decidedly different (see Figure 6.2) than her portrait in Figure 6.1. The C-Nav receiver is specified to operate to a minimum temperature of -20 °Celsius, and the first test for the unit during the field research was purely environmental. During the 44 days onboard the Amundsen, daytime high temperatures were in the neighbourhood of -30°C to -40°C. The minimum recorded temperature was -53°C. This is considerably lower than the -20°C operating minimum, and colder than the -40°C storage minimum specification. However, these limits seemed conservative as there were no problems encountered due to temperature effects.

Figure 6.2: Author departing Amundsen on Bear Patrol

Figure 6.3 shows the over-wintering site in Franklin Bay, NWT, as well as some of the transects that were run as part of the scientific operations during the fall.

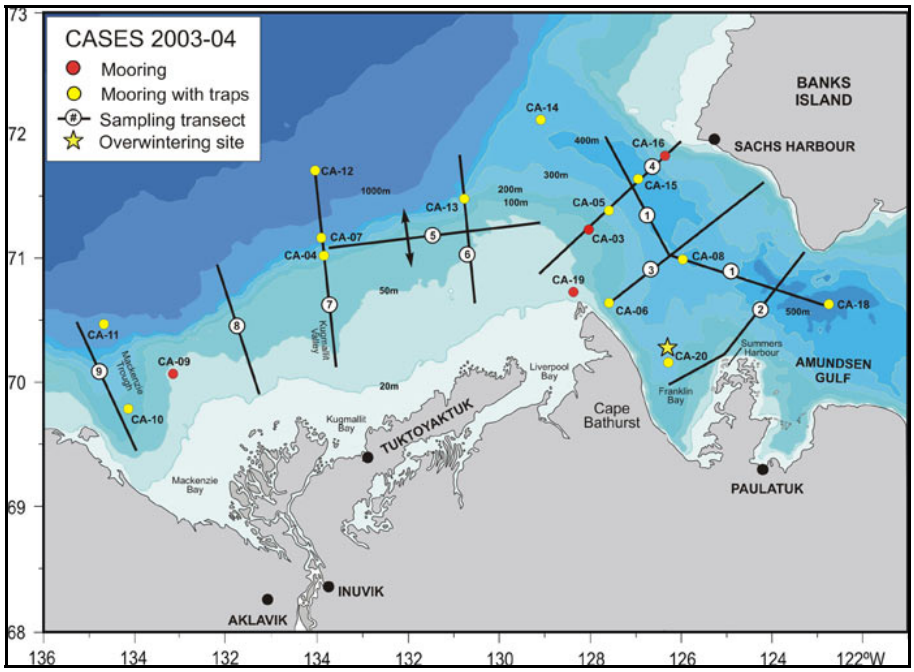

Figure 6.3: Amundsen Over-wintering Site (from cases.quebec-ocean.ulaval.ca, 2003)

6.2.1 C-Nav Data

The C-Nav data were logged aboard the Amundsen in the same manner as during the static evaluations; however, a new version of C-Nav receiver firmware, 13.2, was uploaded upon arrival. A hyper-terminal was established between the C-Nav display unit (CnC D.U.) and the Knudsen K320 controlling PC which copied the streaming NMEA GPGGA sentences to daily files. The display unit was located in the vessel's Auxiliary Generator Room (AGR), along with the POS/MV hardware (see Figure 6.4).

Figure 6.4: C-Nav Display Unit and Applanix POS/MV

As well as logging the NMEA sentences, raw binary data files were logged, using C&C Technologies' StarUtil C-Nav application software package. The binary files were logged via RS232 serial connection between the CnC D.U. and a laptop. In addition to the logging of raw data, the StarUtil software package allows for monitoring of the central GPS receiver engine operation and performance [C-Nav Operations Manual, 2003]. Figure 6.5 illustrates the data logging screen during the logging process.

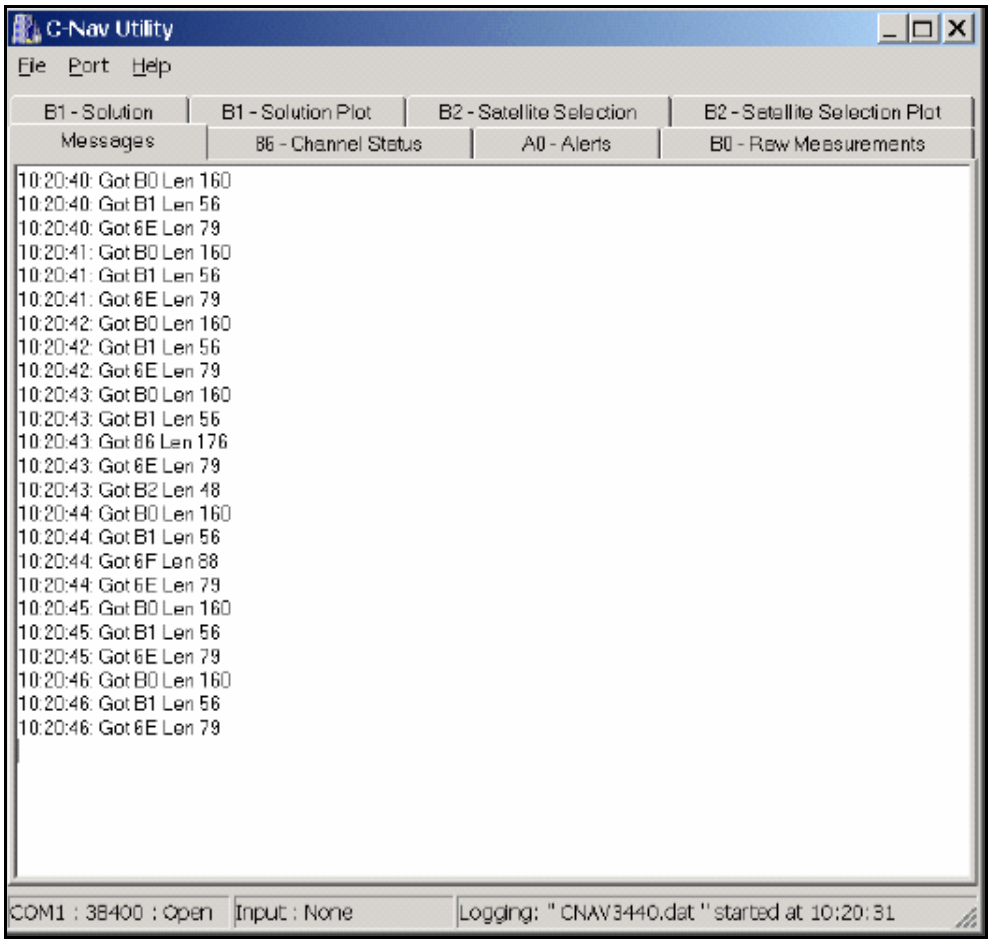

Figure 6.5: StarUtil Binary Data File

6.2.2 Knudsen K320 Sub-bottom Profiler Data

As a vertical reference, Knudsen K320 sub-bottom profiler depths were logged. The K320 depths provided a 'true' tidal signature to which the C-Nav data was compared. The K320 was controlled by a PC in the Data Acquisition Room (DAR). Daily depth files logged on this computer were configured to record only time and depth, as opposed to the fully featured hydrographic output string. During periods of moon-pool

operations by biology scientists onboard, the K320 data were degraded to the point of non-usability. This was caused by the submergence of metallic sampling devices through the ship's hull, interfering with the 30º beam width of the K320. The K320 accuracy was measured to be 2.8 cm at one sigma. Due to the activity from other projects in the first sediment layer, the K320 was setup to track a sub-bottom line that would exhibit no temporal changes during the research. Water column measurements were often taken through the moon-pool, and showed little variability, as was to be expected.

6.2.3 Radiometrics WVR 1100 Data

In addition to the two primary sensors discussed above, Radiometrics WVR 1100 water vapour radiometer observations were also made. A water vapour radiometer (WVR) converts measurements of blackbody temperatures to line of sight (LOS) tropospheric delays. During periods of increased tropospheric activity, we can expect degraded performance of the UNB3 tropospheric delay model used by C-Nav. This translates into greater tropospheric residuals which will contaminate the vertical solutions. The WVR was part of an atmospheric experiment being performed by the University of Manitoba. This version of the WVR 1100 is a simplified model of the WVR 1100 operated by Chaochao Wang of Dr. Peter Dare's Geodesy Lab at the UNB Geodetic Research Lab. This version of the WVR 1100 is designed to measure LOS slant delays at various elevation angles, at a constant azimuth. Due to the high sampling rate, there were sufficient observations made in the zenith direction that no mapping of

slant observations to the zenith was required. Figure 6.6 shows periodic maintenance being performed on the WVR by the author.

Figure 6.6: University of Manitoba WVR 1100

6.3 Field Data Processing

As most of the processing scripts had been written during the static evaluation phase, processing began simultaneously with data acquisition aboard the Amundsen. The

objectives for this thesis can be grouped into two distinct sections: tidal signal removal for hydrographic operations, and tidal signal detection and analysis for oceanographic determinations.

6.3.1 Hydrographic Processing

The hydrographic-themed processing is similar to that carried out during the static evaluation. The data were filtered for incomplete or invalid epochs, and then parsed using the designed awk scripts. Low-pass filters were implemented to eliminate high frequency noise, and the resulting time series were plotted against the K320 depth signatures. Hydrographic operations in the north would normally be performed using predicted tides as the water level datum, so comparisons are also made between these predicted tidal values, and the observed signature of the C-Nav and K320. As the Amundsen was frozen in the sea ice, the combined effects of pitch and roll were expected to be minimal. Given the ~20 m lever arm from the vessel's centre of gravity, a 4º combined inclination would invoke a 5 cm bias into the ellipsoidal heights. Periodic observations of the vessel's pitch and roll were made, but no significant changes (> 1º) were witnessed.

6.3.2 Oceanographic Processing

The intent of the hydrographic processing was to detect and quantify a tidal signal to be removed from the vertical solutions so that a stable horizontal reference surface can be used as a basis for hydrographic soundings. In the oceanographic-themed processing, we are endeavouring to analyze that quantified signal using Least Squares Spectral Analysis (LSSA), in an attempt extract the various harmonic constituents that comprise the tidal signal. Constituent determination is the key to successful prediction, and we will see in the next chapter how prediction programs suffer from poor constituent data.

There is less importance on data latency for oceanographic investigations. Therefore, raw RINEX files were logged from the C-Nav as well. These files were processed using the NRCan Canadian Spatial Reference System (CSRS) Precise Point Positioning (PPP) service. These improved solutions were then filtered in the same manner as the raw NMEA sentences to produce filtered tidal signals. Using the filtered C-Nav outputs, LSSA is performed using two separate programs to calculate the tidal components. When applicable, comments on data quality are given. These results are compared to constituent data previously collected by the Canadian Hydrographic Service (CHS), and the National Oceanic and Atmospheric Administration (NOAA).

During the 1980's, David Wells, Petr Vanicek, and Spiro Pagiatakis of the University of New Brunswick produced an updated version of LSSA software, along with an accompanying technical paper, published as Wells et al. [1985]. Updates to this software were made by Mike Craymer of Natural Resources Canada's (NRCan) Geodetic Survey Division (GSD) as recently as 1999 [Craymer, 2003]. The updates include the

use of a command file to input data into the program. An example of a command file, and a sample output file from this research are found in Appendix II. This FORTRAN based software calculates amplitude and phase values of operator defined harmonics within an input time series. Statistical values such as parameter variance and co-variances are also calculated. This software is designed for spectral analysis of any time series data set.

Mike Foreman of the Canadian Department of Fisheries and Oceans (DFO) Institute of Ocean Sciences (IOS) in Sydney, British Columbia, developed a similar LSSA software package in the late 1970's specifically for spectral analysis of tidal time series. The software manual was published as Foreman [1977]. The PC executable was created using FORTRAN, and was last updated in October 1992. The manual has been updated several times, the last of which was via postscript file attachment in 1996 [http://www-sci.pac.dfo-mpo.gc.ca/osap/projects/tidpack/tidpack_e.htm, 2004]. Although there is no means to obtain statistical information on the results using this program, it is pre-designed to employ 45 main constituents, and 24 shallow water constituents [Foreman, 1977], as well as identifying inference between closely correlated frequencies. This reduces the error caused by interference of closely linked constituents. An explanation of the program and data sets, as well as the constituent data file, is included in Foreman [1977].

Chapter 7 Results and Analysis

This chapter outlines the significant results, gained using the analysis algorithms described in Chapter 5, that contribute to the realization of, or conversely the discounting of, the C-Nav GcGPS in achieving the operational capability statements as outlined in Section 1.1. These results are grouped into three relevant sections: the raw performance of C-Nav in three dimensional positioning in the Canadian Arctic, the coarse detection of tidal signals for the purpose of hydrographic surveying, and lastly, the sampling and decomposition of the Franklin Bay tidal signal using harmonic analysis. The first of these sections will answer the questions regarding the validity of previous C-Nav research with respect to operations in the Canadian North. The second portion of this chapter, similar to the static evaluations, illustrates attempts to filter the C-Nav vertical solution to a usable tidal reference upon which hydrographic soundings can be based. In addition to the Arctic data, results from data collected in Shippagan, New Brunswick, in the summer of 2003 are presented. The final section of this chapter compares the results of the harmonic analysis techniques with previous tidal constituent determinations for the Franklin Bay region.

7.1 C-Nav Arctic Observations

C-Nav GPS operations aboard the Amundsen commenced 19 February 2004, day of year (DOY) 50. However, due to the requirement for firmware upgrades, hardware configuration, and other problems in data management, continuous logging at a data rate of 1 Hz was not started until DOY 57.

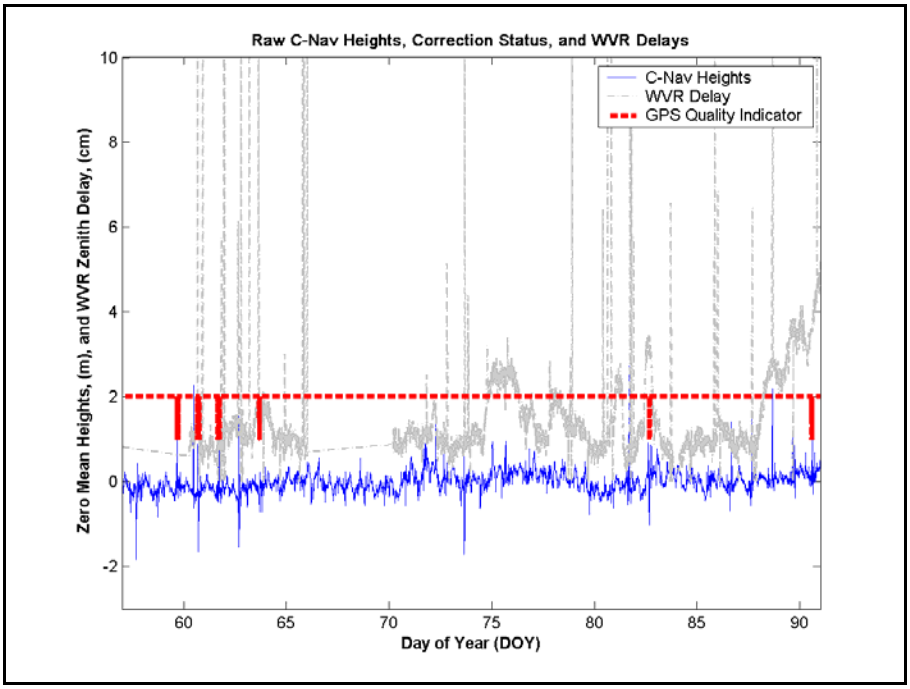

Figure 7.1: Raw Observations

In Figure 7.1, the C-Nav NMEA vertical solutions are plotted along with the GPS quality indicator. The quality indicator for an uncorrected GPS fix is '1', and for a differential fix, '2'. What this means is that for periods where the C-Nav correction message was not received via Inmarsat, or was deemed corrupt and therefore not used, the indicator gives a value of '1'. When the correction message was received, decoded, and used in position

determination without apparent error, the quality indicator reads '2'. As previously mentioned, Inmarsat reception degrades in the Polar Regions, as elevation angles decrease. In this research, the C-Nav correction message was received 99.82% of the time. It must be noted however that as the vessel was frozen into the ice, there were no pitch or roll effects to account for in Inmarsat reception. With an underway vessel, low elevation angles can be further reduced by vessel movements. For example, a 5º elevation angle can be reduced to horizontal with respect to the antenna if the vessel rolls 5º away from the incoming signal, as seen in Figure 7.2.

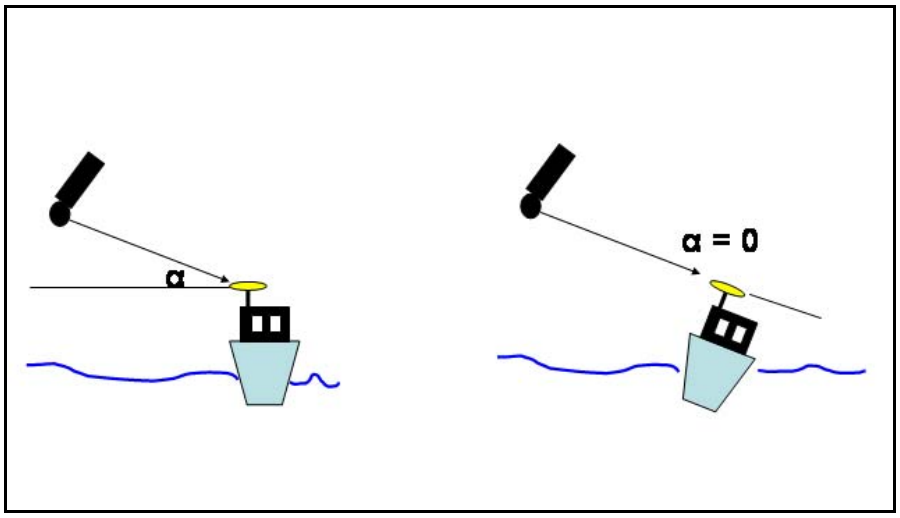

Figure 7.2: Effects of Pitch and Roll on Elevation Angle

The effects of pitch and roll have been reduced with the constant gain design of the Inmarsat antenna. The antenna reception pattern provides constant gain from nadir to below horizontal [Kleiner, 2003]. The low elevation effects on Inmarsat reception in this research are suspected to be a result of meteorological activity. Looking at Figure 7.1, most of the incidences of corrective signal loss occur during periods of increased tropospheric delay, caused by heightened weather conditions. The effects of increased

storm activity are amplified at low elevations as the incoming signal must pass through substantially more atmosphere en-route to the antenna. Increased attenuation of the incoming signal from the ionosphere could produce correction message corruption and rejection, thus reducing the system to stand alone positioning. The effect of GcGPS correction loss on the vertical solution is considerable, as shown in Figure 7.3.

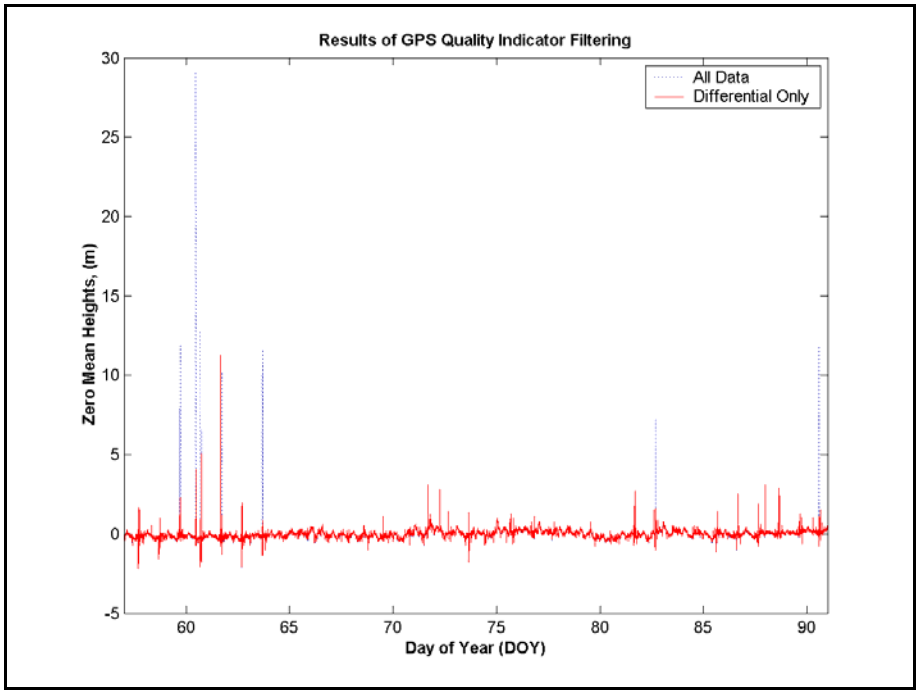

Figure 7.3: Quality Indicator Filter Results

In Figure 7.3, the 'Differential Only' line shows all vertical solutions calculated using differential information. The 'All Data' line spikes illustrate some heights determined without the GcGPS correction message information. The effect of correction signal loss is an immediate degradation of vertical solution in the order of 10's of metres.

Figure 7.4 gives a closer look at the observables over the last 11 days of data collection. Note the loss of differential signal during the periods of increased tropospheric activity.

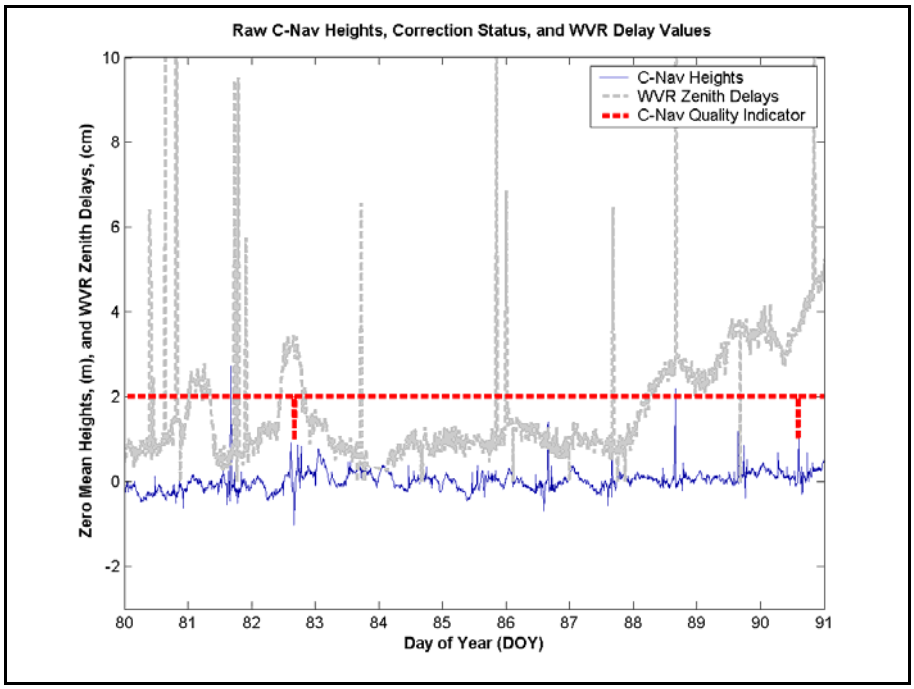

Figure 7.4: Raw Observations, DOY 80-91

The spikes in the WVR delay values are noise in the measurement process, as opposed to ultra short duration weather effects. Visually, the raw C-Nav height determinations remain for the most part within 50 cm of the mean altitude, although several 2-3 metre spikes do exist. During periods of correction loss, height departures of ~7 and >10 metres exist.

In tide retrieval analysis (Section 7.2), the C-Nav heights are compared to the Knudsen K320 sub-bottom profiling sonar as a vertical reference. For this methodology to be employed, the vessel must be horizontally stationary, or at least in an area of flat sea

bottom, so that all changes in depth soundings are the result of tidal influences, or other long wavelength motion. There is some movement expected due to ice motion during the 6 week period onboard. The width of the K320 sonar beam is 30º. Therefore, small horizontal movements will not have a large influence on the mean 225 m depth measurements over the relatively smooth continental shelf floor of Franklin Bay. Figure 7.5 compares three days' horizontal solutions; DOY 65, 75, and 90.

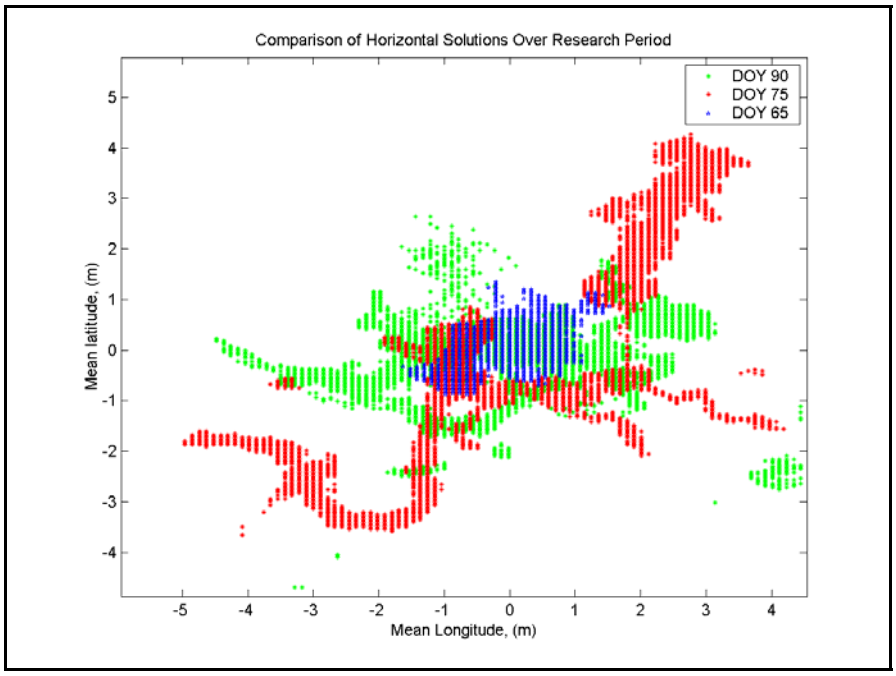

Figure 7.5: Comparison of C-Nav Horizontal Solutions

These three days illustrate the differences in horizontal motion due to the surrounding sea ice (1.5 – 2 metres thick). This ice is land-fast (solidly connected to shore), and therefore does not exhibit the same lateral movement as open sea ice floes. Significant horizontal motions were evident on DOY 75, though the generally stable mean position permits the K320 depths to be used as a 'true' vertical reference without concern of horizontal biases.

7.2 C-Nav Tidal Detection for Hydrographic Surveying

From the results of Section 7.1, we learn that the C-Nav system is capable of operating in the Canadian Arctic and that the methodology of the experiment as outlined in Chapters 5 and 6 is sound. To further improve our C-Nav solutions, brief instances of high DOP value (>1.2) NMEA sentences are filtered from the data. After this cleaning technique, 97.37% of the original NMEA sentences remain, with no breaks exceeding 20 epochs (20 seconds). The parsing techniques described in Section 5.1.2 were used to extract the relevant data, and the vertical solutions were initially smoothed to a mean value for each 60 second epoch. Similar to the sampling rate used by CHS tide gauges, the minute samples were further decimated to 6 minute intervals in order to speed and simplify processing. A low-pass filter, similar to that used in the static evaluation, was employed to eliminate the high frequency noise and the result is shown in Figure 7.6.

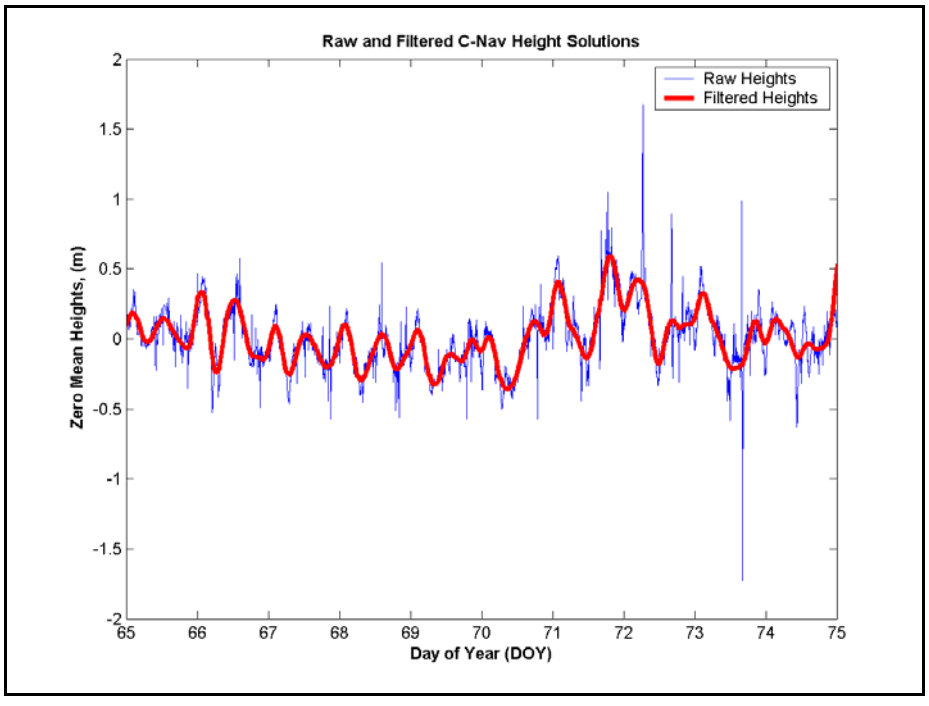

Figure 7.6: Raw and Filtered GPS Heights, DOY 65-75

The cut-off period of the filter was set at six hours. This setting enabled maximum elimination of expectant short period noise (<1 hr), while minimizing attenuation for the desired diurnal and semi-diurnal periods. Longer period filters (7-10 hrs) excessively dampened the C-Nav signal, eliminating tidal amplitude, while shorter periods (1-4 hrs) allowed unwanted noise into the filtered signal. There appears to be a clear semi-diurnal signal present in the filtered C-Nav data. The important question is how well will it match up with sub-bottom depth profile. The Knudsen K320 sonar data also exhibited noise characteristics. This is due to water column turbulence and the nature of sub-bottom refraction, and is easily filtered using a low-pass filter with a moderate cut-off period (~1 hr). The Knudsen exhibited a depth accuracy of 2.7 cm at 1σ.

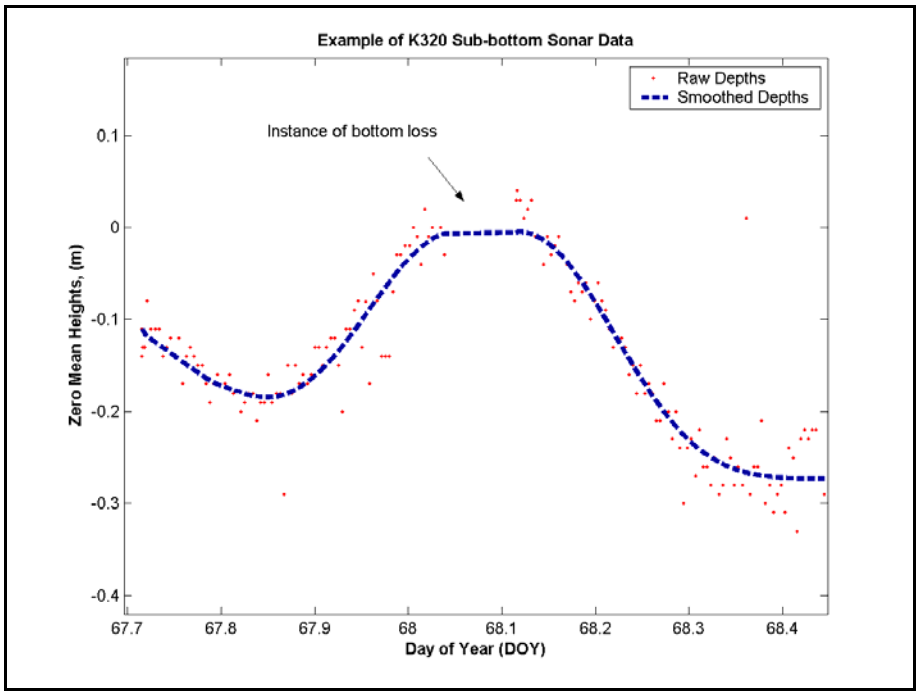

Figure 7.7: Example of K320 Sonar Depth Tracking

As previously mentioned, due to other scientific activities occurring onboard the vessel, there were significant periods of sonar bottom tracking loss. The following comparisons and analysis use some of the cleanest data periods during the field study, and display both raw and filtered versions of the C-Nav and K320 tidal signatures.

7.2.1 Measured Tidal Height Comparisons

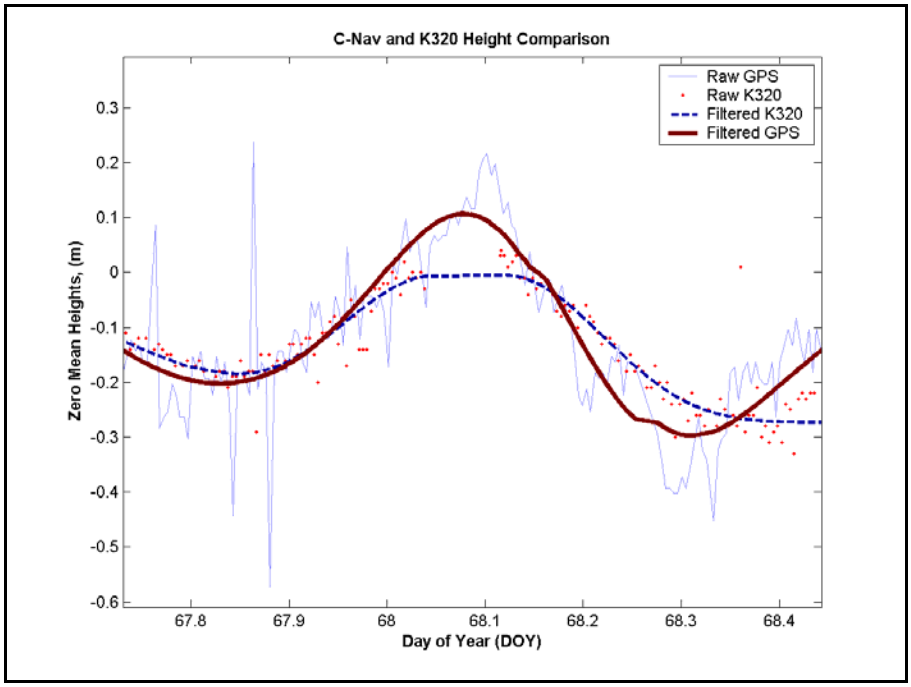

Figure 7.8: DOY 67-68

Figure 7.8 gives a clear indication of C-Nav performance. Save for the tidal peak near DOY 68.1, the C-Nav filtered line maps the true tide as given by the K320 very well. The separation beginning at DOY 68 is a result of K320 data loss and filter interpolation,

rather than C-Nav solution divergence. The C-Nav divergence from the K320 signature at 1σ is 4.8 cm over the 16 hour period shown.

One effect that filtering is unable to handle is tropospheric delays. Although the C-Nav does use an advanced tropospheric delay model (UNB3), in periods of intense short duration tropospheric activity, the residuals unaccounted for by the model can contaminate the positioning solution. These tropospheric events can last from hours to days and thus are difficult to eliminate with simple filtering techniques. Their effects can be seen in Figure 7.9 below.

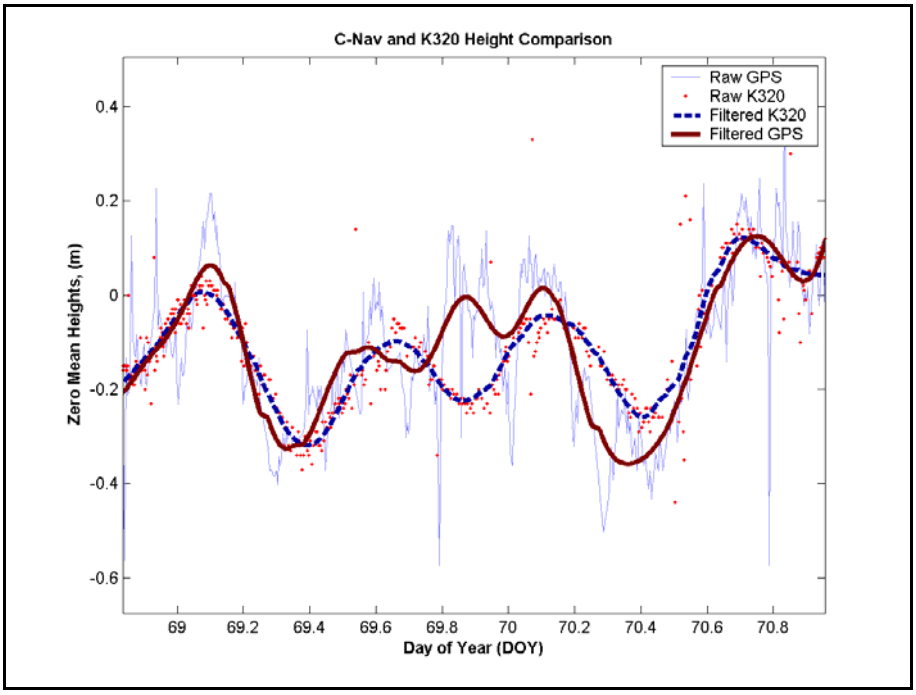

Figure 7.9: Example of Possible Tropospheric Effects

Between DOY 69.8 and 70 in Figure 7.9, there is a local maximum of the C-Nav height signature, while the sonar signature displays a tidal minimum. The duration of the departure is nearly 6 hours (DOY 69.75 to DOY 70), and therefore could easily be

weather effects. Unfortunately, the WVR was not installed over this time period, so confirmation of atmospheric activity is unavailable.

Figures 7.10 through 7.13 on the following pages illustrate various periods of K320 and C-Nav tidal signature comparison.

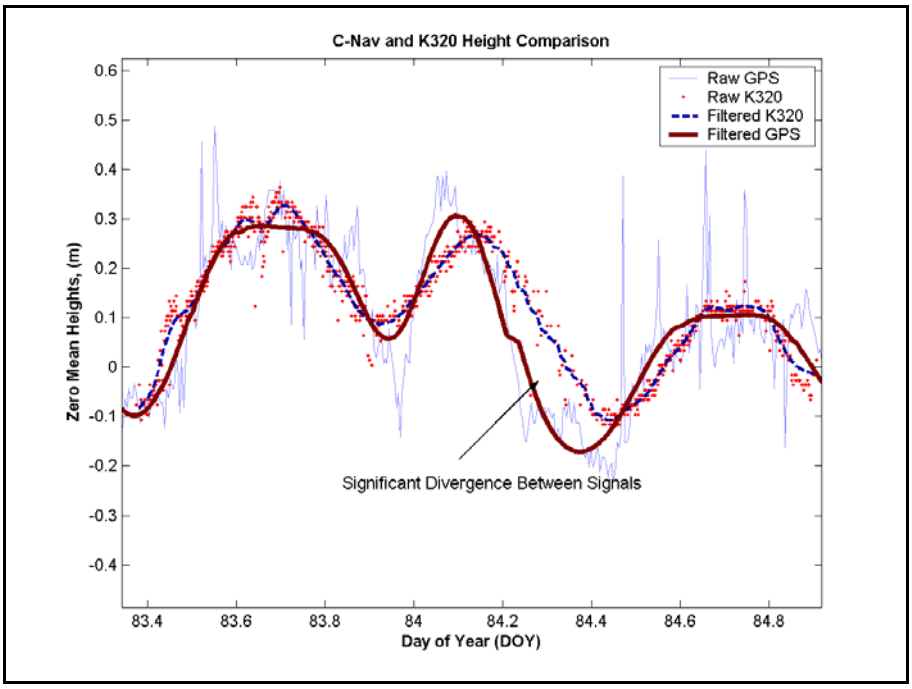

Figure 7.10: DOY 83-84

Over this 36 hour period, the C-Nav signature is very good approximation to the true tides as given by the K320 depth profile. However, following the tidal maximum prior to DOY 84.2, there is some departure from the true signal. Over the course of this period, the standard deviation of the C-Nav heights from the actual tides is 2.9 cm.

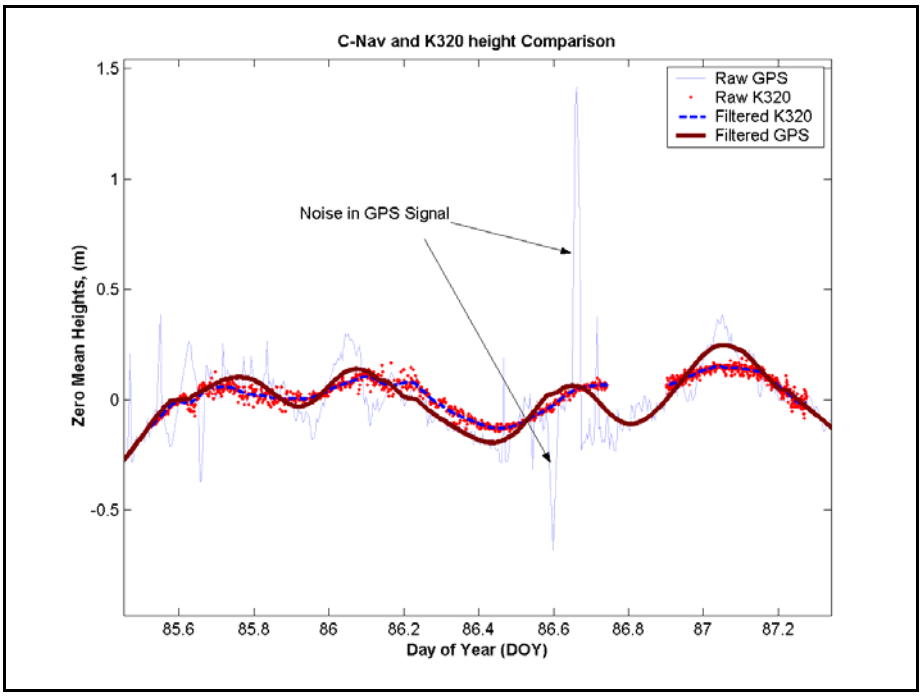

Figure 7.11: DOY 85-87

Figure 7.11 displays the results for another 40 hour period. This period displayed some high amplitude noise as seen by the fluctuations in the raw GPS heights at DOY 86.6. This period does not coincide with heightened levels of tropospheric activity. There is also a break in the sub-bottom data over DOY 86.8. This was caused by deep water column sampling by other members onboard the Amundsen; the submergence of a steel-framed sampling rosette within the K320 beam causes a complete washout of the sonar signal. Even with the 10 cm divergence witnessed with the tidal maximum at DOY 87, the standard deviation of the C-Nav from the true tide is only 4.4 cm.

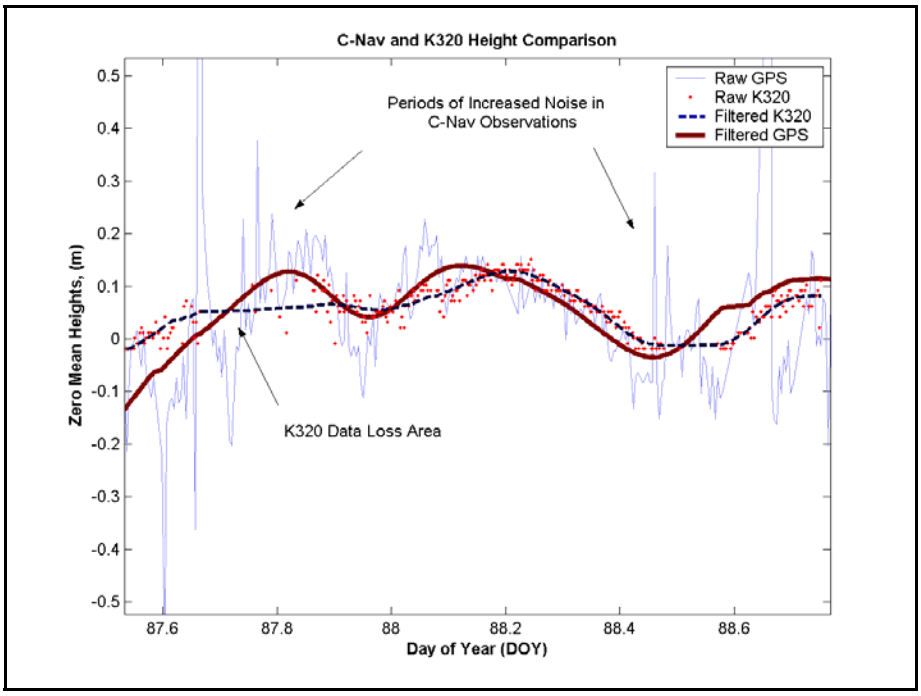

Figure 7.12: DOY 87-88

DOY 87 marks the beginning of the most significant weather activity during the sampling period. Reviewing Figure 7.1 shows a significant increase in the zenith tropospheric delay values. This fact manifests itself in a very noisy GPS vertical solution over the final days of the research. This is also the case in Figure 7.13. Due to the higher levels of noise, there is a greater uncertainty in the performance of the filter. With a standard deviation of 4.7 cm, the filtered GPS signal does however retain its precision.

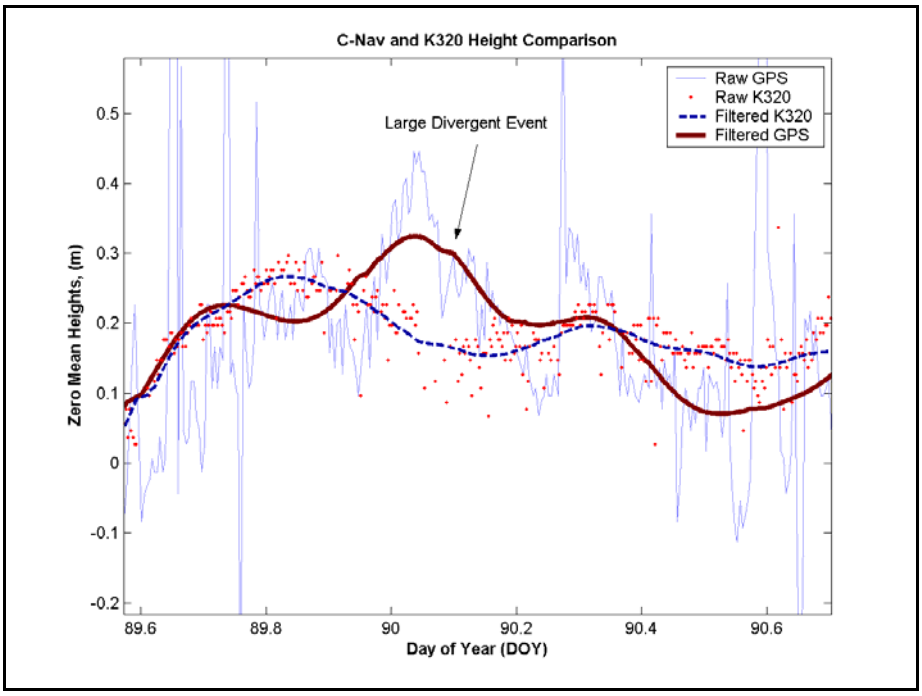

Figure 7.13: DOY 89-90

In Figure 7.13, it must again be noted that this period coincided with greatest levels of tropospheric delays measured by the WVR over the entire research period. This significant event may be the cause of the 14 cm divergent heave in the C-Nav tide signal at DOY 90. Even with this artefact, the standard deviation over the 26 hour period is 6.8 cm.

Over the entire data series, the filtered C-Nav signal exhibited a standard deviation of 4.3 cm from the smoothed K320 depth signal. This is a remarkable level of precision for a differential positioning system.

7.2.2 Comparison of C-Nav Solutions with Predicted Tides

The previous section has shown the C-Nav height solutions to be remarkably consistent with the 'true' tides measured in Franklin Bay. In the following figures, comparisons between the 'true', C-Nav derived, and predicted tides will be made in order to illustrate the requirement for a high precision stand alone vertical positioning system in the Canadian Arctic.

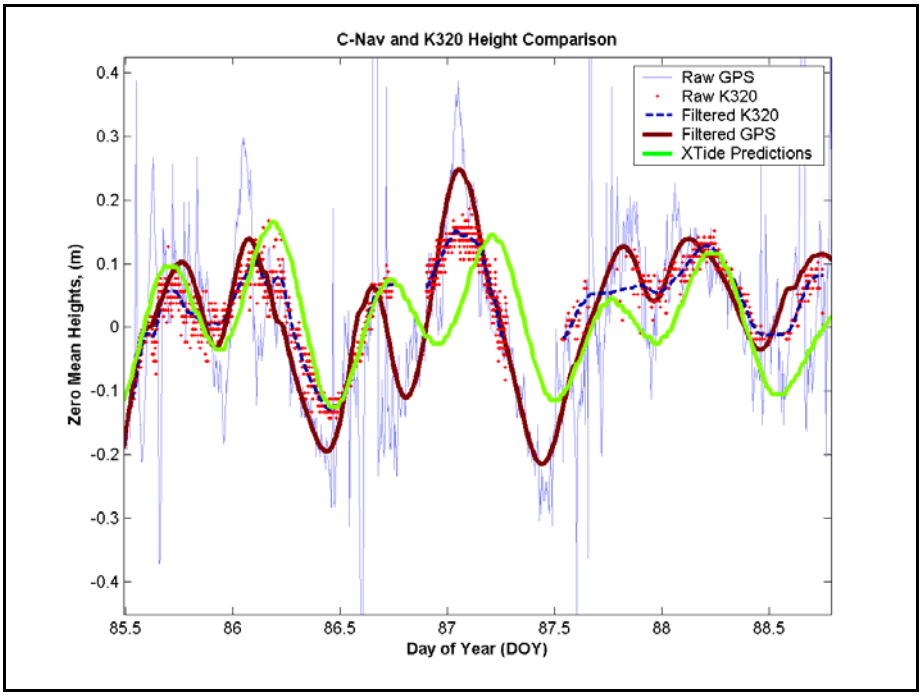

Figure 7.14: Comparison of Measured and Predicted Tidal Signals

Over the entire data set, the standard deviation of the XTide predicted tides from the measured K320 signal is 5.3 cm, slightly larger than the 4.3 cm value for the filtered GPS solutions presented in Section 7.2.1. In Figure 7.14, there are obvious occasions of divergence at DOY 87, DOY 88, and DOY 88.5. It should also be noted that these predictions result from an ideal scenario, i.e., the tidal constituents in Franklin Bay are

known, and the predictions given are for this location, so no co-tidal modelling was required to transfer the constituents from the prediction location to the vessel. There are few other areas in the Arctic with known constituents. In most cases, Arctic predictions are based upon weak constituents, and on-site values are further degraded as the predictions must be employed at areas far from the actual location of constituent analysis. This brings us to the second stage of operational capabilities. Can the smoothed C-Nav signal be used for harmonic analysis of the Arctic Tides in Franklin Bay?

7.3 Harmonic Analysis Results

Section 7.2 indicates that the filtered C-Nav vertical solution is comparable if not better than using predicted tides even immediately at a tidal station. Is this filtered solution capable of accurately measuring the tides so that harmonic analysis can be conducted on the resultant time series in hopes of refining, in the case of Franklin Bay, or defining, in many areas of the Arctic, tidal constituents at a given station? In an attempt to answer this question, several comparisons were made, employing LSSA, between the filtered GPS NMEA data, filtered post-processed GPS data, the filtered K320 data, and currently defined constituent values in Franklin Bay.

7.3.1 Least Squares Spectral Analysis

LSSA is a mathematical technique that allows us to break down the tidal time series into a composite signal of known frequency components with varying amplitude and phase constants, as explained in section 3.2.2. Two LSSA programs were used in this research as outlined in Chapter 6. The Wells et al. [1985] version is more suitable to this study as it allows us to statistically compare the results. Although Foreman's [1977] software is more suited for ocean tide analysis, it is limited in that it does not produce statistical information on the results.

Dave Flater's XTide is generally considered the best tidal prediction software available [Wells, 2003], as it uses all historical data collected by CHS and NOAA gauges. Therefore his harmonic values for Franklin Bay (69.95° N, 126 .92° W), shown in Table 7.1, are used for the comparison in this section.

Table 7.1: XTide Harmonic File for Franklin Bay, NWT [from XTide, 2003]

Constituent	Period (hrs)	Amplitude (cm)	Phase (°)	Min. Record Length (days)
M2	12.421	9.8	170.0	0.54
K1	23.934	4.2	16.1	1
O1	25.819	3.7	42.4	13.7
S2	12.000	3.2	205.4	14.8
MSF	177.184	2.6	87.2	14.8
N2	12.658	1.9	144.3	27.6
P1	24.066	1.1	12.4	182.6
K2	11.967	0.9	198.0	182.6
Q1	26.868	0.7	55.4	27.6

(Minimum record values from Godin, [1972])

Table 7.1 lists the relevant components in order of amplitude. When conducting tidal analysis, these should be the easiest to extract from the signal. However, we must also consider the Rayleigh criterion for each component as we move down the list of importance. Remember the Rayleigh criterion is used to measure the minimum sample length required for component inclusion in the harmonic analysis. The minimum record lengths required for each constituent are given in Table 7.1 as well.

The only significant contributors to the amplitude not permissible in the sample analysis are the diurnal basic solar component P1, and the luni-solar declinational K2. These constituents require a sampling record of 182.6 days to properly observe without bias from nearby frequencies. Therefore, in the analysis of the time series, only the remaining seven of the nine significant constituents will be investigated.

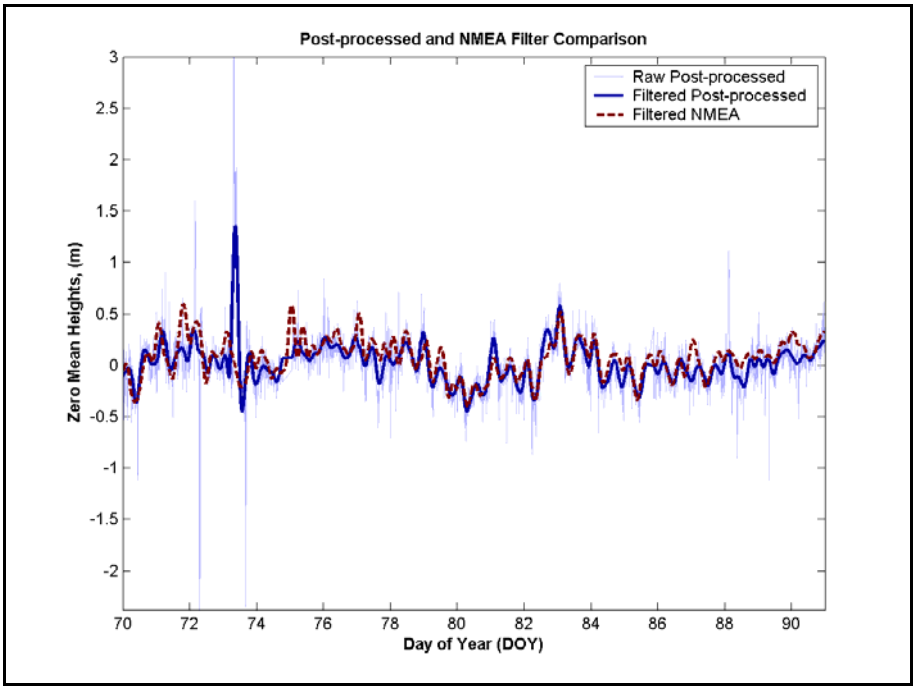

Figure 7.15: Post Processed C-Nav Height Solutions

As tidal constituents are not required in real-time, the opportunity to use more accurate post-processed C-Nav height solutions is available. Using the NRCan CSRS PPP online program mentioned previously in Section 6.3.2, C-Nav RINEX files were processed (as per Appendix III), smoothed using a 6 hour period low-pass filter, and analysed with the LSSA software packages. The results are shown in Figure 7.15. There does not appear to be a significant improvement in the filtered signal with the post-processed data. This post processed data is computed a stand alone, without a reference station. The standard deviation of the post-processed data noise (16.5 cm) is in fact greater than when using the NMEA GPGGA strings (13.6 cm). The residuals of the two raw data series (NMEA and post-processed) from their respective filtered signals are plotted in Figure 7.16.

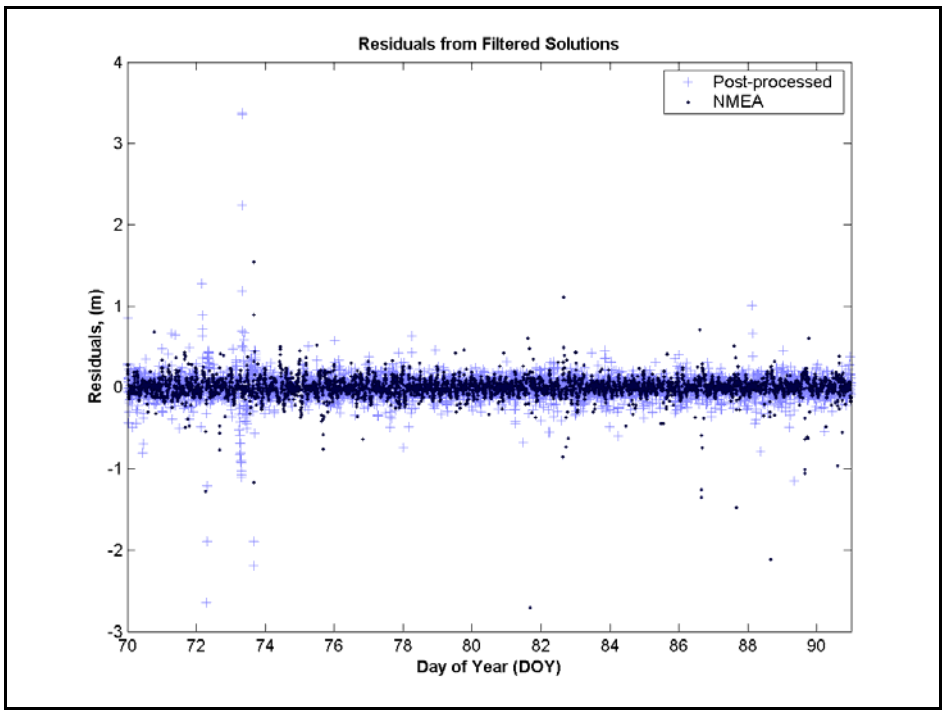

Figure 7.16: Raw Data Set Residuals

There is no apparent advantage in using the post-processed, stand-alone solutions. In the next section, both the NMEA and post-processed time series will be analysed using LSSA, and compared to both the historical Franklin Bay constituents and the K320 solutions.

7.3.2 LSSA Using Wells et al.

Table 7.2 outlines the results from the LSSA (using Wells et al., [1985]).

Table 7.2: LSSA Results – Wells et al. [1985]

Const.	Period (hrs)	XTide		C-Nav NMEA		C-Nav Post-Processed		Knudsen K320	
		Amp / 1σ (cm)	Phase / 1σ (°)	Amp / 1σ (cm)	Phase / 1σ (°)	Amp / 1σ (cm)	Phase / 1σ (°)	Amp / 1σ (cm)	Phase / 1σ (°)
M2	12.421	9.8	170.0	7.8 / 0.7	66.0 / 7.3	10.7 / 0.8	224.1 / 4.3	8.1 / 0.8	237.7 / 5.9
K1	23.934	4.2	16.1	4.7 / 0.7	78.8 / 6.2	3.7 / 0.8	80.6 / 12.4	4.1 / 0.6	23.9 / 11.4
O1	25.819	3.7	42.4	2.6 / 0.7	321.1 / 5.9	2.6 / 0.8	11.1 / 17.5	3.0 / 0.8	311.8 / 5.0
S2	12.000	3.2	205.4	5.7 / 0.7	66.0 / 7.3	3.3 / 0.8	58.2 / 13.9	4.4 / 0.7	62.1 / 5.3
MSF	177.184	2.6	87.2	2.7 / 0.7	139.0 / 15.1	5.1 / 0.7	113.8 / 8.9	2.7 / 0.5	62.9 / 6.4
N2	12.658	1.9	144.3	2.1 / 0.7	23.9 / 19.3	1.6 / 0.8	357.1 / 28.4	2.7 / 0.6	20.3 / 13.9
Q1	26.868	0.7	55.4	2.6 / 0.7	78.1 / 16.2	1.2 / 0.8	199.8 / 36.8	3.2 / 0.6	353.83 / 11.7

There were no correlations greater than ±0.50 found between the C-Nav NMEA constituents. This indicates that the Rayleigh criterion was achieved for each harmonic and there should be no significant contamination due to frequency interference effects. The same was the case for post-processed data. The K320 data however, exhibited

correlation between M2 and S2, with a correlation factor of -0.61, and between K1 and O1, with a correlation of -0.55.

In this comparison, we are using the K320 data as the true measured tide. Looking only at the amplitude, the performance of the C-Nav NMEA data appears to be quite acceptable. The filtered NMEA amplitudes of each constituent are statistically compatible with the K320 amplitudes at 95% (2σ). The same cannot be said for the post processed data. The post-processed heights were similarly filtered for high DOP epochs. Solutions of poor geometry therefore should have been removed form the input time series. As the underlying theme of this research in general is to develop basic but efficient algorithms that can be used to measure tidal signals, rigorous processing techniques were avoided.

The phase values calculated for each constituent do not agree amongst the three data series. This could be the result of a phase bias, though this would affect each harmonic similarly. Phase values are the tidal constant most difficult to calculate. In this research, the phase of the XTide harmonics cannot be relied upon as the ice will induce phase lag into the signal. There should however be a stronger agreement between the two C-Nav signals, and the K320 measure tide. Ultimately, tidal analysis cannot be relied upon unless a very long time series is used. When harmonics are defined by organizations such as the CHS, they utilise years of continuous observation to determine constituent values. This is required to capture the very long wavelength harmonics, but it also has the effect of creating redundancy as more cycles of the shorter wavelengths are observed, thus strengthening the geometry of the least squares problem, and improving the results. As a side evaluation of the LSSA algorithm, a test was conducted using a 30

day data set from Saint John, New Brunswick, where the tides are very well determined. A comparison of XTide harmonics for Saint John, and some derived using LSSA on a historical data set from CHS are presented as Table 7.3.

Table 7.3: Saint John, New Brunswick LSSA Tide Determinations

Name	Saint John Harmonics		LSSA Determination		Difference	
	Amplitude (cm)	Phase (º)	Amplitude (cm)	Phase (º)	Amplitude (cm)	Phase (º)
M2	301.4	0	299.0	0	-2.4	0.0
N2	59.6	341.8	61.8	335.1	+2.2	-6.4
S2	48.5	35.5	49.2	35.9	+0.7	+0.4
K1	15.7	154.2	19.7	157.4	+4.0	+3.2

To avoid phase bias due to inconsistent time origins, the dominant M2 tides were assigned the same phase value, so that the differential phase could be better evaluated. The phase agreements are much better for this separate evaluation. This indicates that the LSSA algorithm is sound, and that any phase discrepancies are inherent to the data.

7.3.3 LSSA Using Foreman

The Foreman [1992] version of the LSSA software has several disadvantages in this research. It is designed for long term analysis of a tidal signal, and is pre-designed to include 69 components. There are only 9 components in Franklin Bay that significantly contribute to the tidal signal (> 5mm) and only 7 of those could be examined due to the Rayleigh criterion. Due to its design for long term analysis, it suffers somewhat over this brief sampling period. Significant output for the C-Nav NMEA data is shown below.

Table 7.4: LSSA Results – Foreman [1992]

Name	Frequency (cycles/hour)	Amplitude (cm)	Phase (°)
MSF	0.00282193	1.0	300.42
Q1	0.0372185	2.4	59.37
O1	0.03873065	0.3	88.82
NO1	0.04026859	1.3	114.67
K1	0.04178075	1	209.34
J1	0.0432929	1.5	157.96
001	0.04483084	1.7	323.04
UPS1	0.04634299	1.0	198.82
N2	0.07899925	0.5	257.22
M2	0.0805114	1.6	176.41
S2	0.08333334	1.6	293.40
ETA2	0.08507364	1.0	110.52
MO3	0.11924206	1.9	161.27
M3	0.1207671	1.4	115.38
MK3	0.12229215	1.4	66.17
SK3	0.12511408	1.8	201.82
MN4	0.15951064	0.6	1.87
M4	0.1610228	1.3	115.16
MS4	0.16384473	1.3	125.05
S4	0.16666667	0.6	93.46
2SK5	0.20844743	0.7	307.39

There are some obvious problems in the results. By including the tertiary and shallow water constituents (denoted with 3 and 4), much of the spectral value of the signal is absorbed in the high frequency components, which reduces the amplitude of the known prevalent constituents such as M2, K2, S1, and O1. By this analysis, the tertiary and shallow constituents account for 42.5% of the spectral amplitude. In reality, this is not the case. As mentioned, this program is designed for analysis of a much longer time series, thereby allowing the relatively longer harmonics (diurnal and semi-diurnal) to build more weight through repetition and redundancy. Similar effects were seen in the analysis of the K320 data. Given a longer research period, this program may have proven functional. However, given the positive results and greater statistical insight provided by

the Wells et al. [1985] LSSA program, it was therefore concluded that this version of LSSA software was not suitable for this research project.

Chapter 8 Conclusions and Recommendations

The purpose of this research was stated to be the determination of the suitability of the C&C Technologies C-Nav Globally Corrected GPS receiver as an instrument in tidal retrieval in an area of micro-tidal influence, the Canadian Arctic. To achieve this goal, a C-Nav receiver was installed on the CCGS Amundsen during her 14 month over-wintering scientific expedition through the Northwest Passage of Canada's Arctic. The first challenge of the receiver was to operate outside its specified environmental envelope, limited for cold weather operations to -20° Celsius. The C-Nav operated continuously from early September 2003, to the time of writing of this report (July 2004), with no apparent deficiencies due to temperature or other environmental effects.

8.1 Operational Capability Statements

In defining the suitability of the C-Nav for tidal retrieval, two questions were asked. Can the C-Nav kinematic solution be used as a stand alone positioning instrument for hydrographic surveys? Can it be used as a sampling device for tidal data? To refine the purpose of this research as put forth through these two questions, four operational capability objectives were stated. These four statements, defined in Section 1.1, are now considered.

Statement 1

The vertical positioning precision possible with raw NMEA data string outputs is of an order commensurate with IHO 1st Order survey standards.

Revisiting Table 3.5, the vertical sounding accuracy (at 95%) required for 1st Order surveys in metres is $\pm\sqrt{[.5^2 + (0.13*d)^2]}$, where d is water depth. If we assume that both terms of this error equation contribute equally, and that the errors incurred as a result of propagation and other transmit related noise are manifested in the depth dependent term, then we equate the first squared term as the allowable uncertainty in vertical control. Within this term, in addition to errors in positioning, we include errors in the vessel altitude caused by heave, draft, squat, tides, and other long wavelength factors. Heave is mitigated with inertial sensors, so the bulk of the 50 cm error budget remains for positioning and long wavelength effects. An accurate GPS position delivered at 1 Hz can come well within this allowance. The easiest determination of the quality of the raw NMEA sentence C-Nav outputs comes from the static evaluation. During the evaluation carried out in Chapter 5, the standard deviation of the C-Nav signal compared to earth tides was determined to be 6.2 cm. Expanding this to 2σ, ~95%, the accuracy delivered is just over 12 cm. This more than accomplishes the goal of operational capability statement 1.

Statement 2

Simple processing methods exist that enable a smoothed vertical solution to be delivered in real or near-real time, and this smoothed solution can provide accuracies commensurate with IHO Special Order survey standards.

In static testing at Fredericton, New Brunswick (46º N), the standard deviation of the raw NMEA elevation outputs was 6.2 cm. This uncertainty value swelled to 13.6 cm during the Arctic observations. Still, this decimetre level makes the C-Nav solution relatively high precision. The first goal of the objective statement is to produce a smoothed height signal with quick but efficient algorithms so that the resultant values can be used in real or near real-time. This was accomplished with a basic low-pass filter design, with cut-off frequency selected so that high frequency noise and desired signal attenuation were limited. The resultant tidal signal yielded a standard deviation of 4.3 cm from the K320 observed tide. The smoothing algorithm runs continuously and can be routed to output filtered NMEA sentences.

To ascertain the suitability of this performance, we again revisit Table 3.5, and using the same processes as outlined in Statement 1 above, the tolerance on vertical control for Special Order surveys is determined to be 25 cm. In fact, this number should be reduced as the second term adds only 7.5 cm per 10 metres of depth. Considering an extreme scenario of survey in ~10 m of water, the total allowable budget for positioning and propagation would only be 32.5 cm. In this extreme case, the positioning tolerance could be assumed to be ~15 cm. Therefore, we will investigate the C-Nav performance under these most restrictive circumstances. In Chapter 7, the filtered C-Nav standard deviation from the K320 signal throughout the entire data series was shown to be 4.3 cm.

At 95%, this would give ~ 9 cm of uncertainty. Even under the extreme scenario described above, the C-Nav performance is acceptable at a 95% confidence interval.

Statement 3

The smoothed vertical solution provides a tidal time series signal that can be decomposed with LSSA techniques for harmonic tidal analysis.

The filtered C-Nav signal was analysed using LSSA in attempts to decompose the tidal harmonics. The results in this section are somewhat mixed. Although amplitude values derived were statistically consistent with the true tides as measured by the Knudsen K320 sonar, the phase values did not exhibit the same level of agreement. The K320 was also in disagreement with previously determined values. As mentioned, the phase values are difficult to accurately predict with a short time series. The lack of concurrence may be attributable to the short time series as opposed to a deficiency in the C-Nav height determinations.

Statement 4

GcGPS is capable of surmounting the obstacles normally inherent to Arctic operations.

When using GPS in the Polar Regions, system performance is often degraded because the constellation is designed for optimum performance at lower latitudes. Instances of high DOP values, and possible 'holes' in the constellation can make some

stand alone systems unreliable in the Arctic. As well, since the C-Nav corrections are received via a geo-stationary satellite, correction reception is a factor. During the operations aboard the Amundsen, the Inmarsat reception level was 99.82%. Even when high DOP value epochs were removed from this solution, 97.37% of the original time series remained. Within this reduced data set, other than the occasional brief 1-2 m spike in the vertical signature, it appears that the C-Nav surmounted the obstacles inherent to Arctic GPS operations.

8.2 Conclusions

The implementation of the C-Nav GcGPS receiver aboard the CCGS Amundsen as an instrument for the retrieval of tidal data was a success. The unit proved itself worthy of operations in the harshness of the Canadian Arctic in terms of both the physical and the GPS related environment. Under those trying circumstances, the receiver was able to detect and accurately measure the 40 cm tidal range to a precision of 4.3 cm. This was done using several efficient data handling and processing techniques, most importantly including low-pass filtering.

The filtered C-Nav tidal signal was also able to give accurate determinations of constituent amplitudes. These values are within centimetres of the true amplitudes as determined with the K320 sub-bottom profiler. The only noted deficiency was in constituent phase determination. This may have been a result of insufficient data, as opposed to a C-Nav performance shortcoming.

8.3 Recommendations for Future Work

The only objective not met was accurate determinations of constituent phase values. This has been thought to be a result of insufficient data period as opposed to a C-Nav performance fault. To answer this question, deployment of a C-Nav system should be carried out in a region of moderate to high tidal influence for an extended period of time (~ 1 year). A region of high tidal influence will make it easier to visualize if there are inconsistencies in the phase values as observed, or if this situation was simply the result of extracting the micro-tidal signature present in Franklin Bay from the noisy GPS heights.

Other possible avenues for research include a robust analysis of the performance of the C-Nav while underway in survey operations, or using more rigorous processing techniques, and perhaps a base station. Although this was partially carried out by Osbourne et al., [2004], by not accounting for the pitch and roll of the vessel, they induced biases in the C-Nav height signal. Further investigation in this area is also required.

The C-Nav system, including the Inmarsat correction link, performed well in this research. However, between Franklin Bay and the North Pole, there still exists nearly 1200 nautical miles of occasionally navigable waters. Further investigation is required into accurately defining the C-Nav/Inmarsat envelope in the Arctic. Although the Arctic area is of primary concern for those of us in Canada, there is also a need to investigate this technology in the Antarctic region.

References

Bisnath, S., D. E. Wells, and D. Dodd (2003). "Evaluation of commercial carrier phase-based WADGPS services for marine applications." *Proceedings of the Institute of Navigation GPS/GNSS 200.* Portland, Oregon, U.S.A.

C&C Technologies, 2003. *C-Nav 2000 RM Product Brochure.* ftp://ftp.cctechnol.com/pub/C-Nav/CNav_2000_RM.pdf, accessed on: 14 November 2003.

C&C Technologies, 2003. *C-Nav GPS System Operations Manual.* ftp://ftp.cctechnol.com/pub/C-Nav/C-Nav%20Manual.pdf, accessed on: 23 October 2003.

Chance, J., J. M. Gravley, J. Roscoe-Hudson, and A. Kleiner. (2003). "GPS for Global Tidal Measurements." *Hydro INTERNATIONAL.* Vol. 7, No. 8.

Corvallis Microtechnology Inc., 2004. *Introduction to GPS.* http://www.cmtinc.com/gpsbook , accessed May 2004.

Craymer, M. (2003). Personal Communication. Natural Resources Canada. Ottawa, Ontario, Canada.

DeLoach, S.R., (1996). "GPS Tides: A Project to Determine Tidal Datums with the Global Positioning System." Department of Geodesy and Geomatics Engineering Technical Report No. 181. University of New Brunswick, Fredericton, N.B., Canada.

Dixon, K. (2003). "Decimetre accuracy – without base stations." *Geomatics World*, Vol.11, No. 4,pp. 32-34.

Flater, D. (2003). *Harmonic Tide Clock and Tide Predictor* http://www.flaterco.com/xtide/index.html, accessed on: 17 September 2003.

Forrester, W.D. (1983). *Canadian Tide Manual*. Department of Fisheries and Oceans, Canadian Hydrographic Service, Ottawa.

Foreman, M.G.G. (1977). "Manual for Tidal Heights Analysis and Prediction." Pacific Marine Science Report 77-10, Institute of Ocean Sciences, Sidney, British Columbia, Canada.

Foreman, M.G.G. (1992). Updates to software originally presented as Pacific Marine Science Report 77-10, Institute of Ocean Sciences, Sidney, British Columbia, Canada.

Godin, G. (1972). *The Analysis of Tides.* University of Toronto Press, Toronto.

Gregorius, T. (1996). "GIPSY-OASIS II, How It Works." Department of Geomatics Report, University of Newcastle upon Tyne, Newcastle upon Tyne, U.K.

Hatch, R., T. Sharpre, and P. Galyean. (2001). *StarFire: A Global High Accuracy Differential GPS System.* Accessed on-line in September 2003 at www.cctechnol.com/papers/StarFireAGlobalHighAccuracySystem.pdf

Hofmann-Wellenhof, B., H. Lichtenegger, and J. Collins. (2001). *GPS Theory and Practice.* 5th ed., SpringerWien, New York.

Hughes Clarke, J., (2003). "Imaging and Mapping III." Department of Geodesy and Geomatics Engineering Lecture Notes for Course No. GGE 3353., University of New Brunswick, Fredericton, N.B., Canada.

Hughes Clarke, J., (2003). Personal Communication. Department of Geodesy and Geomatics Engineering, University of New Brunswick, Fredericton, New Brunswick, Canada.

Kleiner, A. (2003) Personal Communication. C&C Technologies, Lafayette, Louisiana, USA.

Lachapelle, G., C.Liu, G. Lu, Q. Weignen, and R. Hare. (1993). "Water Level Profiling with GPS." *Proceedings of the Institute of Navigation GPS '93,* Salt Lake City, Utah, U.S.A.

Langley, R.B. (2004) Personal Communication. Department of Geodesy and Geomatics Engineering, University of New Brunswick, Fredericton, New Brunswick, Canada.

Legree, P. (2004) Personal Communication. Geodetic Survey Division, Natural Resources Canada, Ottawa, Ontario, Canada.

Leick, A. (1995). *GPS Satellite Surveying.* John Wiley & Sons, Inc., New York.

Linux, (2004). *Advanced Bash Scripting Guide.* http://howtos.linux.com/guides/abs-guide/awk.shtml, accessed on: 21 April 2004.

Marchuk, G.I., and B.A. Kagan. (1984). *Ocean Tides, Mathematical Models and Numerical Experiments.* Pergamon Press, New York.

Mendes, V.B. (1999). "Modeling the Neutral-Atmosphere Propagation Delay in Radiometric Space Techniques." Department of Geodesy and Geomatics Engineering Technical Report No. 199, University of New Brunswick, Fredericton, N.B., Canada.

Misra, P., and P. Enge (2001). *Global Positioning System, Signals, Measurements, and Performance.* Ganga-Jamuna Press, Lincoln.

Osbourne, A., and L. K. Wing. (2004). "GcGPS for Offshore Tide Measurement." *Geomatics World.* Vol.12, No. 3, pp. 22-23.

Roscoe Hudson, J., and T. Sharp (2001) "Globally Corrected GPS (GcGPS): C-Nav GPS System." *Proceedings of the Dynamic Positioning Conference*, Houston, Texas, U.S.A.

Sanders, P. (2003). "RTK Tide Basics." *Hydro INTERNATIONAL*. Vol. 7, No. 10, pp. 26-29.

Wells, D.E., and E.J. Krakiwsky. (1971). "The Method of Least Squares." Department of Geodesy and Geomatics Engineering Lecture Notes No. 18, University of New Brunswick, Fredericton, N.B., Canada.

Wells, D.E., (Ed.) (1986). *Guide to GPS Positioning*. Canadian GPS Associates. Reprinted as Department of Geodesy and Geomatics Engineering Lecture Notes No. 58, University of New Brunswick, Fredericton, N.B., Canada.

Wells, D. E., P. Vanicek, and S. Pagiatakis (1985). "Least Squares Spectral Analysis Revisited." Department of Geodesy and Geomatics Engineering Technical Report No. 84, University of New Brunswick, Fredericton, N.B., Canada.

Wells, D.E. (2003). Personal Communication. Department of Geodesy and Geomatics Engineering, University of New Brunswick, Fredericton, New Brunswick, Canada.

Appendix I

GREP and AWK Script Descriptions

GREP (*grep*) is Linux command used to search a file for a pattern. Newer versions of *grep* have been developed to give the user enhanced capabilities (*egrep*) or limited expressions that provide for faster search times (*fgrep*). The basic syntax of the grep command is:

grep *(search argument) (search file) (options)*

There are numerous options, the most common output related options being:

null	- no options declared will print the results to screen
> *outfile*	- outputs results to output file *outfile*
| (pipe)	- pipes output to follow on command series

AWK (*awk*) is a command line programming language built by A.V. Aho, P.J. Weinberger, and B.W. Kernighan. It is based on *C* syntax. It is a combination of the regular expression search capabilities of *grep* and the advanced string and array handling features of the *C* language. Basic command syntax is:

awk –F "*delimiter*" 'BEGIN {*initial arguments*} {*line arguments*}
END {*terminating arguments*}' *infile (options)*

The –F switch defines the field delimiting character. If no –F switch is used; white space (space or tab) is the default. The options are similar to those used above with GREP. The combined command used to parse the NMEA GPGGA sentences to text files is shown on the next page.

fgrep 00.00 doy80.txt |

This initial command searches the file doy70.txt for lines containing the string '00.00'. These lines are piped to a following command.

awk -F "," 'BEGIN {} {time = $2; diff = $7; num = $8; dop = $9; height = $10; printf("%2.2f.%2.2f.%d.%1.1f\n",time/10000,height,diff,num,dop)} END {}' |

This *awk* command first delimits the incoming lines by comma. In the line argument section, variable names (*time*) are assigned to each column number (*$2*). Each argument is separated by a semi-colon. The *printf* C command prints the designated data as per the argument. There are no terminating arguments and the output is piped again to following command.

awk -F "." 'BEGIN {} {h = $1; m = $2; d1 = $3; d2 = $4; diff = $5; num =$6; dop1 = $7; dop2 = $8; printf("%2.4f \t%2.2f \t%d \t%d.\t%d.%d\n",h + m/60, d1 + 2/100, diff, num, dop1, dop2)} END {}' |

This command uses period delimiters to manipulate the data into files containing time in decimal hours.

awk 'BEGIN {} {hr=$1; h=$2; diff=$3; num =$4 dop=$5; printf("%2.5f \t%2.2f \t%d \t%d \t%1.1f\n",70+(hr/24),h,diff,num, dop)} END {}' > doy80_strip.txt

Another *awk* iteration uses white space delimiters and changes the time of each epoch into Day of year (DOY). The output data is sent to file doy80_strip.txt. An example of a line from the initial input file and a line from the output file are given below.

Input

```
$GPGGA,000000.00,7002.73621,N,12618.08905,W,2,10,1.1,25.63,M,-8.99,M,8,0108*66
```

Output

```
80.0000     25.63       2           10          1.1

DOY         Height      GPS         #           DOP
                        Quality     SV's
                        Indicator
```

Appendix II

Filter Selection

The ideal filter for this research is one that optimizes for flat amplitude response, and has zero phase distortion. Flat amplitude response is important so as to prohibit any contaminating effects (attenuation ripple) from entering the filtered tidal series. Zero phase is important so that there is no delay or phase offsets that would create errors in both the hydrographic height determinations, and the oceanographic constituent analysis. For a real-time application, filter design is restricted to causal filters. In this thesis, the focus is on the ability of C-Nav heights to be effectively filtered, with efficient processing, in order to extract the tidal signature. Once this is achieved, future design of a causal filter will be capable of delivering in real time.

A digital Butterworth was selected as it has a maximally flat amplitude response and uses minimal processing resources in minimal time. Butterworth filters have a standard pass band attenuation of –3 dB (50% of amplitude). The filter was implemented using the Matlab® **filtfilt** function to create the desired zero phase model.

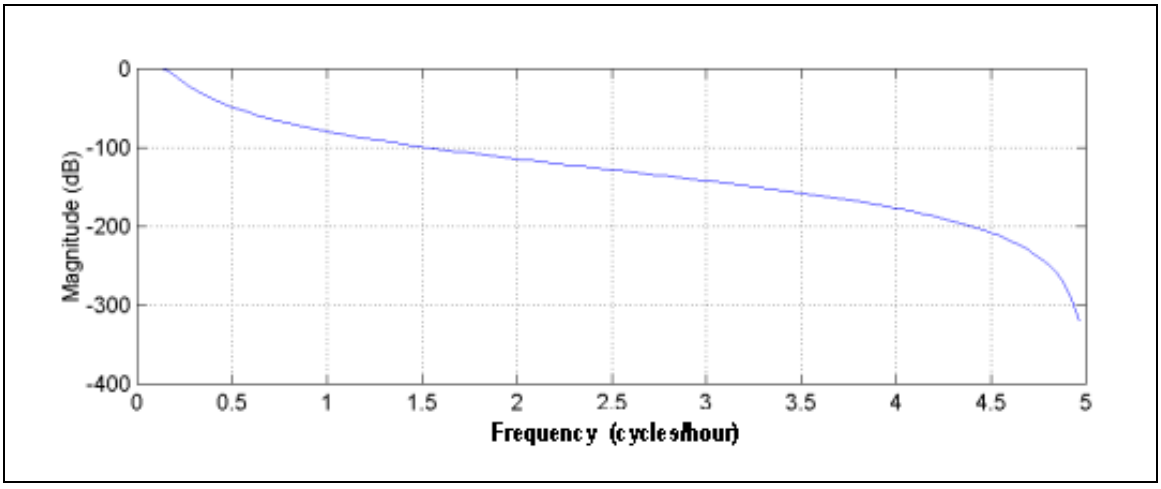

The above image displays the magnitude of the 5th order Butterworth low pass filter. The highest desired tidal frequencies (~12 hr periods) are less than 0.085 cycles/hour. Much of the GPS noise occurs near the sampling frequency (in this case, 10 cycles per hour).

Appendix III

CSRS PPP Processing Options

The Geodetic Survey Division (GSD) of Natural Resources Canada (NRCan) has produced an online, GPS precise point positioning service, called CSRS-PPP. It can be found through the NRCan website at:

http://www.geod.nrcan.gc.ca/index_e/products_e/services_e/ppp_e.html

The service allows for the upload of RINEX files with options for static or kinematic mode, and NAD83 (CSRS) or WGS84 solutions. While not available to the public, there is an advanced version of the service, still in beta test phase. The full online service is expected to be available Spring 2005 [Legree, 2004]. This version allows the user to make selections in order to optimize the processing depending on certain options. For this research, the following options were selected:

Dynamics:	kinematic
Observations:	code and phase
Frequency:	L3 (L1 and L2)
Satellite ephemeris:	SP3 (precise orbits)
Precise satellite clock input:	yes
Satellite clock interpolation:	yes
Ionospheric grid input:	no
Solve station coordinates:	yes
Tropospheric delay:	model
Backward substitution:	yes
Reference System:	NAD83
Coordinate System:	ellipsoidal

Appendix IV

Sample LSSA Files

Sample LSSA Command File

TESTT.CMD

DCNAV.DAT	Input data file name
DCNAV.OUT	Output listing file name
DCNAV.PLT	Output plot data file name
BATCH	Mode (BATCH or SQNTL)
UN	EQual or UNequal time series
Y	Plot time series? (Y or N)
0	Datum biases (#,times of biases)
1	Linear trend switch (0=off,1=on)
7 0.5 0.5175 0.5274 0.9973 1.0758 1.1195 7.3827	Forced periods (#,periods)
0	User function switch (0=no,1=yes)
25.00 0.5000	Cut-off for listing std.dev. and corr.
1 .25 .0001 50	Band #, longest, shortest, # periods

The first three records of this file denote the input, output, and time series output filenames. The method of processing is denoted as batch or sequential, with allowances for equal or unequal time series, datum biases, and linear trends. Note that the periods of concern are entered in days, as this was the unit of time in the data series. The last two records deal with the allowable spectrum of noise, in this case limited from 1 minute to 4 hours.

Sample LSSA Output File

DCNAV.OUT

```
-----------------------------------------------------
 LSSA:  Least Squares Spectral Analysis
       Version 3.2 (14 Jan 99)
 Copyright (c) 1989-99 University of New Brunswick
-----------------------------------------------------

  5.7032600e+001 -9.2000000e-002

Input command file                : TESTT.CMD
Input data file                   : DCNAV.DAT
Output listing file               : DCNAV.OUT
Output plot data file             : DCNAV.PLT

Processing mode                 : BATCH
Time series spacing             : UN
Plot time series ?              : Y

Datum biases                    :         0
Linear trend switch (0=off,1=on)  :         1
Forced periods                  :         7
  0.500000000000000       0.517500000000000       0.527400000000000
  0.997300000000000       1.07580000000000        1.11950000000000
   7.38270000000000
User-defined function (0=off,1=on)  :         0
Limit for listing st.dev. (%)     :   25.0000000000000
Limit for listing correlations    :   0.500000000000000

Spectral band label             :         1
Longest period                  :   0.250000000000000
Shortest period                 :   0.100000000000000D-003
No. of periods                  :        50


 SOLUTION FOR KNOWN CONSTITUENTS


        DATUM   LINEAR   FORCED   COSINE     SINE      USER
         BIAS    TREND   PERIOD    TERM      TERM    DEFINED AMPLITUDE   (SIGMA)    PHASE  (SIGMA)

 NUMBER      0       0       7       7       7       0


   1- 2                0.500  0.231E-01  0.520E-01        0.569E-01 ( 0.720E-02)  66.04 (  7.26)
   3- 4                0.517 -0.639E-01 -0.453E-01       0.784E-01 ( 0.729E-02) 215.34 (  5.31)
   5- 6                0.527  0.197E-01  0.874E-02        0.206E-01 ( 0.725E-02)  23.89 ( 19.29)
   7- 8                0.997  0.129E-01  0.656E-01        0.469E-01 ( 0.716E-02)  78.84 (  6.23)
   9- 10               1.076  0.550E-01 -0.444E-01        0.257E-01 ( 0.729E-02) 321.08 (  5.91)
  11- 12               1.119  0.531E-02  0.252E-01        0.257E-01 ( 0.723E-02)  78.09 ( 16.19)
  13- 14               7.383 -0.205E-01  0.178E-01        0.272E-01 ( 0.712E-02) 138.98 ( 15.11)


   OUTSTANDING STANDARD DEVIATIONS OF KNOWN CONSTITUENTS
   (LARGER THAN  25.0 % OF ESTIMATED MAGNITUDE)

   NUMBER  STANDARD DEVIATION

     1       0.722E-02
     5       0.725E-02
     6       0.727E-02
     7       0.722E-02
    11       0.726E-02
    12       0.723E-02
```

```
 13       0.720E-02
 14       0.708E-02
OUTSTANDING CORRELATIONS BETWEEN KNOWN CONSTITUENTS
(LARGER IN ABSOLUTE VALUE THAN 0.50)

 NUMBER     CORRELATION

    NONE WAS FOUND




   RESIDUAL TIME SERIES QUADRATIC NORM    0.22646E+02
   RESIDUAL TIME SERIES VARIANCE          0.24195E-01
   RESIDUAL TIME SERIES STANDARD DEV.     0.15555E+00
```

The most important record in the output file is of course the Solution for Known Constituents. This record lists each harmonic solution as period, cosine term, sine term, and then amplitude (amplitude std. dev.) and phase (phase std. dev.). Any standard deviation or component correlation exceeding the operator input levels defined in the command file are listed as well. The residual time series is output as well but has been removed in this example for the sake of clarity. Statistical qualities of the residuals are also computed, including the quadratic norm, variance, and standard deviation.